

Lawrence Berkeley National Laboratory

LBL Publications

Title

Power corrections for N-jettiness subtractions at O α s

Permalink

<https://escholarship.org/uc/item/2wn5k0kx>

Journal

Journal of High Energy Physics, 2018(12)

ISSN

1126-6708

Authors

Ebert, Markus A
Moult, Ian
Stewart, Iain W
[et al.](#)

Publication Date

2018-12-01

DOI

10.1007/jhep12(2018)084

Peer reviewed

Power corrections for N -jettiness subtractions at $\mathcal{O}(\alpha_s)$

Markus A. Ebert,^a Ian Mould,^{b,c} Iain W. Stewart,^a Frank J. Tackmann,^d Gherardo Vita^a and Hua Xing Zhu^e

^aCenter for Theoretical Physics, Massachusetts Institute of Technology, 77 Massachusetts Ave, Cambridge, MA 02139, U.S.A.

^bBerkeley Center for Theoretical Physics, University of California, 336 Le Conte Hall, Berkeley, CA 94720, U.S.A.

^cTheory Group, Lawrence Berkeley National Laboratory, 1 Cyclotron Road, Berkeley, CA 94720, U.S.A.

^dTheory Group, Deutsches Elektronen-Synchrotron (DESY), Notkestraße 85, D-22607 Hamburg, Germany

^eDepartment of Physics, Zhejiang University, 38 Zheda Road, Hangzhou, Zhejiang 310027, China

E-mail: ebert@mit.edu, ianmould@lbl.gov, iains@mit.edu, frank.tackmann@desy.de, vita@mit.edu, zhuhx@zju.edu.cn

ABSTRACT: We continue the study of power corrections for N -jettiness subtractions by analytically computing the complete next-to-leading power corrections at $\mathcal{O}(\alpha_s)$ for color-singlet production. This includes all nonlogarithmic terms and all partonic channels for Drell-Yan and gluon-fusion Higgs production. These terms are important to further improve the numerical performance of the subtractions, and to better understand the structure of power corrections beyond their leading logarithms, in particular their universality. We emphasize the importance of computing the power corrections differential in both the invariant mass, Q , and rapidity, Y , of the color-singlet system, which is necessary to account for the rapidity dependence in the subtractions. This also clarifies apparent disagreements in the literature. Performing a detailed numerical study, we find excellent agreement of our analytic results with a previous numerical extraction.

KEYWORDS: QCD Phenomenology

ARXIV EPRINT: [1807.10764](https://arxiv.org/abs/1807.10764)

Contents

1	Introduction	1
2	N-jettiness subtractions, definitions and notation	2
3	Born measurements at subleading power	5
3.1	General setup and notation	5
3.2	Power expansion in soft and collinear limits	6
4	Master formula for power corrections to next-to-leading power	7
4.1	General setup for color-singlet SCET _I observables	7
4.2	Collinear master formula for 0-jettiness	10
4.3	Soft master formula for 0-jettiness	11
4.4	Universality of power corrections for 0-jettiness	12
4.4.1	Universality of collinear limit	13
4.4.2	Universality of soft limit	14
5	Power corrections at NLO for color singlet production	15
5.1	Gluon-fusion Higgs production	15
5.1.1	$gg \rightarrow Hg$	16
5.1.2	$gq \rightarrow Hq$	18
5.1.3	$q\bar{q} \rightarrow Hq$	20
5.1.4	$q\bar{q} \rightarrow Hg$	20
5.2	Drell-Yan production	20
5.2.1	$q\bar{q} \rightarrow Vg$	21
5.2.2	$gq \rightarrow Vq$	22
5.2.3	$gq \rightarrow Vq$	23
6	Comparison with integrated results in the literature	23
6.1	Treatment of the NLO phase space	24
6.2	Explicit comparison to results in the literature for $gg \rightarrow Hg$	26
6.2.1	Comparison at LL	28
6.2.2	Comparison at NLL	30
7	Numerical results	31
7.1	Drell-Yan production	32
7.2	Gluon-fusion Higgs production	34
8	Conclusions	43
A	Derivation of NLO leading power results	44
A.1	Leading-power expansion of matrix elements	45
A.2	NLO soft function	46
A.3	NLO beam function	47
B	Comparison of NLP contributions for $gg \rightarrow Hg$ at NLO	49

1 Introduction

The precision study of the Standard Model at the LHC, as well as increasingly sophisticated searches for physics beyond the Standard Model, require precision predictions for processes in a complicated hadron collider environment. When calculating higher-order QCD corrections, the presence of infrared divergences require techniques to isolate and cancel all divergences. Completely analytic calculations are only possible for some of the simplest cases, e.g. [1–3], while for more complicated processes, in particular those involving jets in the final state, numerical techniques are typically required.

At next-to-leading order (NLO) the FKS [4, 5] and CS [6–8] subtraction schemes provide generic subtractions for arbitrary processes, and have been used to great success. At next-to-next-to-leading order (NNLO), due to the more complicated structure of infrared singularities, the development of general subtraction schemes has proven more difficult. While subtraction schemes have been demonstrated both for color-singlet production [9–15], as well as for several processes involving jets in the final state [16–22], significant work is still required before efficient NNLO subtractions can be achieved for arbitrary colored final states.

N -jettiness subtractions [20, 22] are based on the N -jettiness resolution variable \mathcal{T}_N [23, 24], and are applicable to generic N -jet final states. They have successfully been applied to NNLO calculations for a variety of color-singlet final states [25–29], as well as final states involving a single jet [20, 21, 30–33]. They are also a key ingredient in one of the first methods for combining NNLO calculations with parton showers [34, 35]. The leading-power subtraction terms are given by an all-orders factorization formula derived in refs. [23, 24] using soft-collinear effective theory (SCET) [36–40]. Required ingredients are explicitly known to NNLO with up to a single jet in the final state [41–55].

An important feature of N -jettiness subtractions is that power corrections in the resolution variable can be calculated in an expansion about the soft and collinear limits, allowing the numerical performance of the subtractions to be systematically improved. Recently there has been significant interest in understanding subleading power corrections to collider cross sections [56–71]. Advances in the understanding of subleading power limits using SCET [65, 66] have allowed the leading logarithmic (LL) next-to-leading power (NLP) corrections to be computed at NLO and NNLO [62, 64], with independent calculations of the same terms done by a second group in refs. [63, 70]. The leading logarithms have also been resummed to all orders for pure glue QCD for 2-jettiness in $H \rightarrow gg$ [72].

The inclusion of the leading logarithms was found to improve the numerical accuracy, and thereby the computational efficiency, of N -jettiness subtractions for color-singlet production by up to an order of magnitude [62, 64]. The analytic calculation of the next-to-leading logarithmic (NLL) power corrections is important for several reasons. Theoretically, it greatly furthers our understanding of the power corrections, since the perturbative structure becomes significantly more nontrivial at NLL as compared to at LL. From a practical perspective, they provide further substantial improvements in the numerical performance of the subtractions. In particular, they make the subtractions much more robust in cases where there are accidental cancellations between different channels or where the NLL terms are numerically enhanced relative to the LL terms.

In this paper, we compute the full NLP corrections at $\mathcal{O}(\alpha_s)$ for both Drell-Yan and gluon-fusion Higgs production in all partonic channels, including the nonlogarithmic terms (which are the NLL terms at $\mathcal{O}(\alpha_s)$). One focus of this paper is to derive a master formula for the NLP corrections to 0-jettiness at $\mathcal{O}(\alpha_s)$ and to discuss in detail the subleading-power calculation, in particular the treatment of measurements at subleading power, which in our case are the invariant mass Q and rapidity Y of the color-singlet system. More generally, one can consider measuring any observable that does not vanish for the partonic process at lowest order in perturbation theory, which we refer to as Born measurements. Our analysis lays the ground for extending the calculation of the NLP corrections to higher powers, higher orders in α_s , and to more complicated processes.

We also perform a detailed numerical study comparing our analytic results with the full nonsingular result extracted numerically from MCFM8 [27, 73–75], which allows us both to verify our analytic calculation and to probe the typical size of the higher-power corrections in various different partonic channels. We find that the NLL power corrections can exhibit a much more pronounced Y dependence from PDF effects than is the case at LL, which demonstrates the importance of calculating the power corrections fully differential in the Born phase space.

Our discussion of the Born measurements also allows us to clarify an apparent disagreement in the recent literature regarding the LL power corrections. As we discuss in more detail in section 6, since the calculations in refs. [63, 70] are not differential in the color-singlet rapidity Y , their results can only be used fully integrated over Y .¹ In contrast, the results computed here, which agree with those previously derived by a subset of the present authors in refs. [62, 64], are differential in Y . When integrating over all Y , integration by parts is used to explicitly show that these LL results are equivalent to those of refs. [63, 70]. In section 6 we also compare our new differential NLL results with the integrated results of ref. [70].

The outline of this paper is as follows: in section 2, we briefly review N -jettiness subtractions for color-singlet production and define our notation. In section 3, we discuss in some detail the treatment of Born measurements at subleading power. In section 4, we derive a formula to NLP for the soft and collinear power corrections for 0-jettiness. Although our primary focus is on NLO, the general strategy is valid to higher orders as well. In section 5, we use our master formula to derive explicit results for the NLP power corrections at NLO for both Drell-Yan and gluon-fusion Higgs production. In section 6, we provide a detailed comparison with the literature for those partonic channels where results are available. In section 7, we present a detailed numerical study, and compare our analytic results with a previous numerical extraction. We conclude in section 8.

2 N-jettiness subtractions, definitions and notation

In this section we briefly review N -jettiness subtractions [20, 22] in the context of color-singlet production, and discuss the structure of the power corrections to the subtraction

¹We thank the authors of refs. [63, 70] for discussions and confirmation of this point.

scheme. This also allows us to define the notation that will be used in the rest of this paper. For a detailed discussion, we refer the reader to ref. [22].

To compute a cross section for color-singlet production $\sigma(X)$, where X denotes some set of cuts on the Born phase space, we write the cross section as an integral over the differential cross section in the resolution variable \mathcal{T}_0

$$\sigma(X) = \sigma(X, \mathcal{T}_{\text{cut}}) + \int_{\mathcal{T}_{\text{cut}}} d\mathcal{T}_0 \frac{d\sigma(X)}{d\mathcal{T}_0}, \quad (2.1)$$

where

$$\sigma(X, \mathcal{T}_{\text{cut}}) \equiv \int^{\mathcal{T}_{\text{cut}}} d\mathcal{T}_0 \frac{d\sigma(X)}{d\mathcal{T}_0}. \quad (2.2)$$

For a general measure, the 0-jettiness \mathcal{T}_0 can be defined as [45, 76]

$$\mathcal{T}_0 = \sum_i \min \left\{ \frac{2q_a \cdot k_i}{Q_a}, \frac{2q_b \cdot k_i}{Q_b} \right\}, \quad (2.3)$$

where the sum runs over all hadronic momenta k_i in the final state. Here, $q_{a,b}$ are projected Born momenta (referred to as label momenta in SCET), which are given in terms of the total leptonic invariant mass Q and rapidity Y as

$$q_a^\mu = x_a E_{\text{cm}} \frac{n^\mu}{2} = Q e^Y \frac{n^\mu}{2}, \quad q_b^\mu = x_b E_{\text{cm}} \frac{\bar{n}^\mu}{2} = Q e^{-Y} \frac{\bar{n}^\mu}{2}, \quad (2.4)$$

where

$$n^\mu = (1, 0, 0, 1), \quad \bar{n}^\mu = (1, 0, 0, -1) \quad (2.5)$$

are lightlike vectors along the beam directions. The choice in eq. (2.4) corresponds to parameterizing the Born phase space in terms of Q and Y , and this choice already enters in the leading-power factorization theorem, where the beam functions are evaluated at $x_{a,b} = Q e^{\pm Y}$.

The $Q_{a,b}$ measures in eq. (2.3) determine the different definitions of 0-jettiness. Two different definitions, originally introduced in refs. [23, 44] as beam thrust, are the leptonic and hadronic definitions given by

$$\begin{aligned} \text{leptonic:} \quad Q_a = Q_b = Q, \quad \mathcal{T}_0^{\text{lep}} &= \sum_i \min \left\{ \frac{x_a E_{\text{cm}}}{Q} n \cdot k_i, \frac{x_b E_{\text{cm}}}{Q} \bar{n} \cdot k_i \right\} \\ &= \sum_i \min \left\{ e^Y n \cdot k_i, e^{-Y} \bar{n} \cdot k_i \right\} \\ \text{hadronic:} \quad Q_{a,b} = x_{a,b} E_{\text{cm}}, \quad \mathcal{T}_0^{\text{cm}} &= \sum_i \min \left\{ n \cdot k_i, \bar{n} \cdot k_i \right\}. \end{aligned} \quad (2.6)$$

It has been shown [62] that the power corrections for the hadronic definition are poorly behaved, and grow exponentially with rapidity, while the $e^{\pm Y}$ factor in the measure for the leptonic definition exactly avoids this effect.

For later convenience, we write the dimensionful and dimensionless 0-jettiness resolution variables in terms of a Y -dependent parameter $\rho(Y)$ as

$$\mathcal{T}_0^x = \sum_i \min\{\rho_x k_i^+, \rho_x^{-1} k_i^-\}, \quad \tau^x \equiv \frac{\mathcal{T}_0^x}{Q}, \quad (2.7)$$

with

$$\begin{aligned} \text{leptonic:} \quad & \rho_{\text{lep}} = e^Y, \quad \tau^{\text{lep}} = \frac{\mathcal{T}_0^{\text{lep}}}{Q}, \\ \text{hadronic:} \quad & \rho_{\text{cm}} = 1, \quad \tau^{\text{cm}} = \frac{\mathcal{T}_0^{\text{cm}}}{Q}. \end{aligned} \quad (2.8)$$

In the following, we will mostly drop the subscript 0 on \mathcal{T}_0 , since there should be no cause for confusion that our results are for 0-jettiness. For generic results that apply to both the leptonic and hadronic definitions we also drop the superscript and simply use \mathcal{T} and τ , keeping a generic parameter ρ when necessary.

To implement the N -jettiness subtractions, we now add and subtract a subtraction term to the cross section (suppressing the dependence on the Born measurements X for simplicity)

$$\begin{aligned} \sigma &= \sigma^{\text{sub}}(\mathcal{T}_{\text{cut}}) + \int_{\mathcal{T}_{\text{cut}}} d\mathcal{T}_0 \frac{d\sigma}{d\mathcal{T}_0} + [\sigma(\mathcal{T}_{\text{cut}}) - \sigma^{\text{sub}}(\mathcal{T}_{\text{cut}})] \\ &\equiv \sigma^{\text{sub}}(\mathcal{T}_{\text{cut}}) + \int_{\mathcal{T}_{\text{cut}}} d\mathcal{T}_0 \frac{d\sigma}{d\mathcal{T}_0} + \Delta\sigma(\mathcal{T}_{\text{cut}}). \end{aligned} \quad (2.9)$$

Since \mathcal{T}_0 is a zero jet resolution variable, for $\tau = \mathcal{T}_0/Q \rightarrow 0$ we can expand the differential cross section $d\sigma/d\tau$ and its cumulative $\sigma(\tau_{\text{cut}})$ about the soft and collinear limits from $\tau \rightarrow 0$ and $\tau_{\text{cut}} \rightarrow 0$ as

$$\begin{aligned} \frac{d\sigma}{d\tau} &= \frac{d\sigma^{(0)}}{d\tau} + \frac{d\sigma^{(2)}}{d\tau} + \frac{d\sigma^{(4)}}{d\tau} + \dots, \\ \sigma(\tau_{\text{cut}}) &= \sigma^{(0)}(\tau_{\text{cut}}) + \sigma^{(2)}(\tau_{\text{cut}}) + \sigma^{(4)}(\tau_{\text{cut}}) + \dots. \end{aligned} \quad (2.10)$$

Here $d\sigma^{(0)}/d\tau$ and $\sigma^{(0)}(\tau_{\text{cut}})$ contain all leading-power terms,

$$\frac{d\sigma^{(0)}}{d\tau} \sim \delta(\tau) + \left[\frac{\ln^j \tau}{\tau} \right]_+, \quad \sigma^{(0)}(\tau_{\text{cut}}) \sim \ln^j \tau_{\text{cut}}. \quad (2.11)$$

These terms must be included in the subtraction term to obtain a finite result, namely

$$\sigma^{\text{sub}}(\mathcal{T}_{\text{cut}}) = \sigma^{(0)}(\tau_{\text{cut}} = \mathcal{T}_{\text{cut}}/Q) [1 + \mathcal{O}(\tau_{\text{cut}})]. \quad (2.12)$$

The further terms in the series expansion in eq. (2.10) are suppressed by powers of τ

$$\tau \frac{d\sigma^{(2k)}}{d\tau} \sim \mathcal{O}(\tau^k \ln^j \tau), \quad \sigma^{(2k)}(\tau_{\text{cut}}) \sim \mathcal{O}(\tau_{\text{cut}}^k \ln^j \tau_{\text{cut}}). \quad (2.13)$$

While these terms with $k \geq 1$ do not need to be included in the subtraction term, the size of the neglected term, $\Delta\sigma(\tau_{\text{cut}})$ is determined by the leading-power corrections that are left out

of σ^{sub} . Therefore, including additional power corrections in σ^{sub} can significantly improve the performance of the subtraction. Indeed, general scaling arguments imply that up to an order of magnitude in performance can be gained for each subleading power logarithm that is included in the subtractions [22]. For the leading logarithms, this was explicitly confirmed for most partonic channels in the numerical studies in refs. [62, 64]. Here, we extend the calculation to the NLL terms at $\mathcal{O}(\alpha_s)$, which yields the nonlogarithmic terms, hence giving the complete NLP result. The remaining NLO power corrections then scale at worst as $\alpha_s \tau_{\text{cut}}^2 \log \tau_{\text{cut}}$, and will be very small, as we will see in our numerical studies.

3 Born measurements at subleading power

We begin by discussing in some detail the treatment of the Born measurements, Q^2 and Y , which plays an important role at subleading powers. We will use the soft and collinear expansions from SCET, which provide a convenient language when discussing the power expansion of QCD amplitudes at fixed order. We will not need to employ any of the field theory technology from SCET for our analysis here.

3.1 General setup and notation

Consider the production of a color-singlet final state L of fixed invariant mass Q and rapidity Y , together with an arbitrary measurement \mathcal{T} that only acts on hadronic radiation and gives $\mathcal{T} = 0$ at Born level. Since the observable \mathcal{T} resolves soft and collinear emissions it will induce large logarithms $\ln(\mathcal{T}/Q)$. Our goal is to expand the cross section in \mathcal{T} (or $\tau = \mathcal{T}/Q$) in order to systematically understand its logarithmic structure.

Consider proton-proton scattering with the underlying partonic process

$$a(p_a) + b(p_b) \rightarrow L(p_1, \dots) + X(k_1, \dots), \quad (3.1)$$

where L is the leptonic (color-singlet) final state and X denotes additional QCD radiation. Its cross section reads

$$\begin{aligned} \frac{d\sigma}{dQ^2 dY d\mathcal{T}} &= \int_0^1 d\zeta_a d\zeta_b \frac{f_a(\zeta_a) f_b(\zeta_b)}{2\zeta_a \zeta_b E_{\text{cm}}^2} \int \left(\prod_i \frac{d^d k_i}{(2\pi)^d} (2\pi) \delta_+(k_i^2) \right) \int \frac{d^d q}{(2\pi)^d} |\mathcal{M}(p_a, p_b; \{k_i\}, q)|^2 \\ &\times (2\pi)^d \delta^{(d)}(p_a + p_b - k - q) \delta(Q^2 - q^2) \delta\left(Y - \frac{1}{2} \ln \frac{q^-}{q^+}\right) \delta[\mathcal{T} - \hat{\mathcal{T}}(\{k_i\})]. \end{aligned} \quad (3.2)$$

Here, the incoming momenta are given by

$$p_a^\mu = \zeta_a E_{\text{cm}} \frac{n^\mu}{2}, \quad p_b^\mu = \zeta_b E_{\text{cm}} \frac{\bar{n}^\mu}{2}, \quad (3.3)$$

$k = \sum_i k_i$ is the total outgoing hadronic momentum, and q is the total leptonic momentum. Since our measurements are not sensitive to the details of the leptonic final state, we have absorbed the leptonic phase space integral into the matrix element,

$$\begin{aligned} |\mathcal{M}(p_a, p_b; \{k_i\}, q)|^2 &= \int d\Phi_L(q) |\mathcal{M}(p_a, p_b; \{k_i\}, \{p_j\})|^2, \\ d\Phi_L(q) &= \prod_j \frac{d^d p_j}{(2\pi)^d} (2\pi) \delta_+(p_j^2 - m_j^2) (2\pi)^d \delta^{(d)}\left(q - \sum_j p_j\right). \end{aligned} \quad (3.4)$$

The matrix element \mathcal{M} contains the renormalization scale $\mu^{2\epsilon}$, which as always is associated with the renormalized coupling $\alpha_s(\mu)$, and may also contain virtual corrections. For now the measurement function $\hat{\mathcal{T}}(\{k_i\})$ is kept arbitrary.

We can now solve the Q^2 and Y measurements to fix the incoming momenta as

$$\begin{aligned}\zeta_a(k) &= \frac{1}{E_{\text{cm}}} \left(k^- + e^{+Y} \sqrt{Q^2 + k_T^2} \right), \\ \zeta_b(k) &= \frac{1}{E_{\text{cm}}} \left(k^+ + e^{-Y} \sqrt{Q^2 + k_T^2} \right).\end{aligned}\tag{3.5}$$

Taking the Jacobian factors from solving the δ functions into account, eq. (3.2) becomes

$$\frac{d\sigma}{dQ^2 dY d\mathcal{T}} = \int \left(\prod_i \frac{d^d k_i}{(2\pi)^d} (2\pi) \delta_+(k_i^2) \right) \frac{f_a(\zeta_a) f_b(\zeta_b)}{2\zeta_a \zeta_b E_{\text{cm}}^4} A(Q, Y; \{k_i\}) \delta[\mathcal{T} - \hat{\mathcal{T}}(\{k_i\})],\tag{3.6}$$

where we defined

$$A(Q, Y; \{k_i\}) \equiv |\mathcal{M}(p_a, p_b, \{k_i\}, q = p_a + p_b - k)|^2\tag{3.7}$$

to stress that the squared matrix element only depends on the Born measurements Q and Y , which fix the incoming momenta through eqs. (3.3) and (3.5), and the emission momenta k_i . Note that we have left implicit in our notation in eq. (3.6) the dependence of $\zeta_{a,b}$ on k through eq. (3.5). They are restricted to $\zeta_{a,b} \in [0, 1]$, which is implicit in the support of the proton PDFs.

3.2 Power expansion in soft and collinear limits

Instead of solving the \mathcal{T} measurement function to express (some of the) k_i in terms of \mathcal{T} , we find that a convenient strategy to organize the expansion in \mathcal{T} is to multipole expand the final state momenta. At this stage we need only assume that \mathcal{T} is a SCET_I observable, which is true for many definitions of N -jettiness. For such observables, it is known from SCET_I that we can organize the cross section in terms of a power counting parameter $\lambda \sim \sqrt{\tau}$. All momenta k_i can then be categorized as either collinear or soft modes (since we work in SCET_I these are often called ultrasoft, although we will not make this distinction), whose momenta scale as

$$\begin{aligned}n\text{-collinear} &: k_n \sim Q(\lambda^2, 1, \lambda), \\ \bar{n}\text{-collinear} &: k_{\bar{n}} \sim Q(1, \lambda^2, \lambda), \\ \text{soft} &: k_s \sim Q(\lambda^2, \lambda^2, \lambda^2),\end{aligned}\tag{3.8}$$

where we decomposed each momentum into lightcone coordinates

$$k^\mu = k^- \frac{n^\mu}{2} + k^+ \frac{\bar{n}^\mu}{2} + k_\perp^\mu \equiv (k^+, k^-, k_\perp).\tag{3.9}$$

Here n and \bar{n} are lightlike vectors satisfying $n \cdot \bar{n} = 2$. The components of the momenta that scale like λ^2 are referred to as residual momenta. The soft momenta are homogeneous,

and have purely residual scaling. Overlap between the soft and collinear modes occurring in integrals over final state momenta is removed by the zero-bin subtraction procedure [77].

The benefit of this decomposition is that it allows one to expand eq. (3.6) in λ , agnostic of the actual measurement \mathcal{T} . The LP result is then simply obtained by expanding the cross section through λ^0 , the NLP result by expanding through λ^2 , etc. Note that when performing this expansion, all other factors, such as $Q, E_{\text{cm}} \sim \lambda^0$.

While the expansion of the matrix element is of course process dependent, we can give general expressions for the incoming momentum fractions eq. (3.5), independent of the process and observable \mathcal{T} . If k is a soft momentum, then the expansion required at NLP is given by

$$\begin{aligned}\zeta_a(k) &= x_a \left(1 + \frac{k^- e^{-Y}}{Q} \right) + \mathcal{O}(\lambda^4), \\ \zeta_b(k) &= x_b \left(1 + \frac{k^+ e^{+Y}}{Q} \right) + \mathcal{O}(\lambda^4),\end{aligned}\tag{3.10}$$

where we factored out the Born momentum fractions

$$x_a = \frac{Q e^{+Y}}{E_{\text{cm}}}, \quad x_b = \frac{Q e^{-Y}}{E_{\text{cm}}}.\tag{3.11}$$

In the n -collinear limit, we obtain

$$\begin{aligned}\zeta_a(k) &= x_a \left[\left(1 + \frac{k^- e^{-Y}}{Q} \right) + \frac{k_T^2}{2Q^2} \right] + \mathcal{O}(\lambda^4), \\ \zeta_b(k) &= x_b \left[1 + \left(\frac{k^+ e^{+Y}}{Q} + \frac{k_T^2}{2Q^2} \right) \right] + \mathcal{O}(\lambda^4).\end{aligned}\tag{3.12}$$

For clarity, we have grouped terms of the same power counting in round brackets. Similarly, one can obtain the \bar{n} -collinear limit, or any combination as might appear when combining multiple emissions.

4 Master formula for power corrections to next-to-leading power

In this section we derive a master formula for the NLP corrections. This formula applies to any SCET_I observable in color-singlet production. In section 5, we will apply it to derive explicit results for Drell-Yan and gluon-fusion Higgs production.

4.1 General setup for color-singlet SCET_I observables

For reference, we start with the LO cross section for the production of a color-singlet final state L of invariant mass Q^2 and rapidity Y , together with an (up to now arbitrary) measurement \mathcal{T} acting only on hadronic radiation,

$$\frac{d\sigma^{\text{LO}}}{dQ^2 dY d\mathcal{T}} = \frac{f_a(x_a) f_b(x_b)}{2x_a x_b E_{\text{cm}}^4} A^{\text{LO}}(Q, Y) \delta(\mathcal{T}),\tag{4.1}$$

where $x_{a,b} = \frac{Q}{E_{\text{cm}}} e^{\pm Y}$ and A^{LO} is the squared matrix element in the Born kinematics, see eq. (3.7). For future reference, we also define the LO partonic cross section, $\hat{\sigma}^{\text{LO}}(Q, Y)$, by

$$\frac{d\sigma^{\text{LO}}}{dQ^2 dY d\mathcal{T}} = \hat{\sigma}^{\text{LO}}(Q, Y) f_a(x_a) f_b(x_b) \delta(\mathcal{T}), \quad \hat{\sigma}^{\text{LO}}(Q, Y) = \frac{A^{\text{LO}}(Q, Y)}{2x_a x_b E_{\text{cm}}^4}. \quad (4.2)$$

Next, consider an additional real emission to the Born process. Eq. (3.6) yields

$$\frac{d\sigma}{dQ^2 dY d\mathcal{T}} = \int \frac{d^d k}{(2\pi)^d} (2\pi) \delta_+(k^2) \frac{f_a(\zeta_a) f_b(\zeta_b)}{2\zeta_a \zeta_b E_{\text{cm}}^4} A(Q, Y; \{k\}) \delta[\mathcal{T} - \hat{\mathcal{T}}(\{k\})], \quad (4.3)$$

where we remind the reader that the incoming momenta $p_{a,b}$ are given by eq. (3.5),

$$\begin{aligned} p_a^\mu &= \zeta_a(k) E_{\text{cm}} \frac{n^\mu}{2} = \left(k^- + e^{+Y} \sqrt{Q^2 + k_T^2} \right) \frac{n^\mu}{2}, \\ p_b^\mu &= \zeta_b(k) E_{\text{cm}} \frac{\bar{n}^\mu}{2} = \left(k^+ + e^{-Y} \sqrt{Q^2 + k_T^2} \right) \frac{\bar{n}^\mu}{2}. \end{aligned} \quad (4.4)$$

From these solutions, we see the interesting feature that at subleading power, regardless of the type of final-state emission, the momenta entering both PDFs are modified.

Since we do not measure the azimuthal angle of k , it can be integrated over,

$$\int \frac{d^d k}{(2\pi)^d} (2\pi) \delta_+(k^2) = \frac{\Omega_{2-2\epsilon}}{4(2\pi)^{d-1}} \int_0^\infty \frac{dk^+ dk^-}{(k^+ k^-)^\epsilon} = \frac{(4\pi)^{-2+\epsilon}}{\Gamma(1-\epsilon)} \int_0^\infty \frac{dk^+ dk^-}{(k^+ k^-)^\epsilon}. \quad (4.5)$$

Eq. (4.3) simplifies to

$$\frac{d\sigma}{dQ^2 dY d\mathcal{T}} = \int_0^\infty \frac{dk^+ dk^-}{(k^+ k^-)^\epsilon} \frac{f_a(\zeta_a) f_b(\zeta_b)}{(4\pi)^2 2\zeta_a \zeta_b E_{\text{cm}}^4} \frac{(4\pi)^\epsilon}{\Gamma(1-\epsilon)} A(Q, Y; \{k\}) \delta[\mathcal{T} - \hat{\mathcal{T}}(\{k\})]. \quad (4.6)$$

So far, this expression is still exact. In the next step, we wish to expand the NLO cross section in $\lambda \sim \mathcal{T}/Q$. When \mathcal{T} is a SCET_I observable, we can use the EFT knowledge from SCET_I to expand the momentum k in both collinear and soft limits, as discussed in section 3.

At NLP, we need to expand eq. (4.6) consistently through $\mathcal{O}(\lambda^2)$. The $\mathcal{O}(\lambda^2)$ power corrections arise from the following sources:

- The incoming momenta $\zeta_{a,b}$. While collinear and soft limits yield quite different power expansions, both give a well-defined expansion in λ . We thus simply define the expansion

$$\zeta_{a,b} = x_{a,b} \left[\frac{1}{z_{a,b}} + \Delta_{a,b}^{(2)} + \mathcal{O}(\lambda^4) \right], \quad (4.7)$$

where $z_{a,b} \sim \lambda^0$ and $\Delta_{a,b}^{(2)} \sim \lambda^2$. We have pulled out the Born momentum fractions $x_{a,b}$ and written $1/z_{a,b}$ as a fraction for later convenience. Explicit expressions can be obtained from eqs. (3.10) and (3.12), and will be given below.

- PDFs. Since the momenta $\zeta_{a,b}$ enter the PDFs, these also have to be power expanded,

$$\begin{aligned} f_{a,b}(\zeta_{a,b}) &= f_{a,b}\left(\frac{x_{a,b}}{z_{a,b}}\right) + x_{a,b}\Delta_{a,b}^{(2)} f'_{a,b}\left(\frac{x_{a,b}}{z_{a,b}}\right) + \mathcal{O}(\lambda^4) \\ &\equiv f_{a,b} + x_{a,b}\Delta_{a,b}^{(2)} f'_{a,b} + \mathcal{O}(\lambda^4). \end{aligned} \quad (4.8)$$

- Flux factor. Similar to the PDFs, we have to expand the flux factor

$$\frac{1}{\zeta_a \zeta_b} = \frac{z_a z_b}{x_a x_b} \left[1 - z_a \Delta_a^{(2)} - z_b \Delta_b^{(2)} \right]. \quad (4.9)$$

- Matrix element. The expansion of the matrix element depends both on the process and the considered limit. Here, we define the LP and NLP expansions by

$$A(Q, Y; \{k\}) = A^{(0)}(Q, Y; \{k\}) + A^{(2)}(Q, Y; \{k\}) + \dots \quad (4.10)$$

In the soft limit $A^{(0)} \sim \lambda^{-4}$ and $A^{(2)} \sim \lambda^{-2}$, while in the collinear limit $A^{(0)} \sim \lambda^{-2}$ and $A^{(2)} \sim \lambda^0$. In both cases we have the scaling $\int dk^+ dk^- A^{(2j)} \sim \lambda^{2j}$, which is why the soft and collinear corrections enter at the same order.

For example, for a $2 \rightarrow 2$ process, the matrix element can be written in terms of the Mandelstam variables

$$\begin{aligned} s_{ab} &= 2p_a \cdot p_b = \frac{Q^2}{z_a z_b} \left[1 + z_a \Delta_a^{(2)} + z_b \Delta_b^{(2)} + \mathcal{O}(\lambda^4) \right], \\ s_{ak} &= -2p_a \cdot k = -k^+ Q e^{+Y} \left(\frac{1}{z_a} + \Delta_a^{(2)} + \mathcal{O}(\lambda^4) \right), \\ s_{bk} &= -2p_b \cdot k = -k^- Q e^{-Y} \left(\frac{1}{z_b} + \Delta_b^{(2)} + \mathcal{O}(\lambda^4) \right). \end{aligned} \quad (4.11)$$

Since these terms now have a definite power counting, one can simply insert eq. (4.11) into $A(Q, Y; \{k\})$ and expand to the required order in λ .

- Measurement. Depending on the observable, the measurement function $\hat{\mathcal{T}}$ may also receive power corrections. Since 0-jettiness is defined in terms of n, \bar{n}, Q and Y , none of which receive power corrections in our approach, we do not have such corrections, and will therefore not write them explicitly in the following formulae. More generally, these could be obtained from expanding $\delta[\mathcal{T} - \hat{\mathcal{T}}(\{k\})]$.

Inserting all these expansions into eq. (4.6) and expanding consistently to $\mathcal{O}(\lambda^2)$, we obtain the LP result

$$\frac{d\sigma^{(0)}}{dQ^2 dY d\mathcal{T}} = \int_0^\infty \frac{dk^+ dk^-}{(k^+ k^-)^\epsilon} \frac{z_a z_b f_a f_b}{(4\pi)^2 2x_a x_b E_{\text{cm}}^4} \frac{(4\pi)^\epsilon}{\Gamma(1-\epsilon)} A^{(0)}(Q, Y; \{k\}) \delta[\mathcal{T} - \hat{\mathcal{T}}(\{k\})] \quad (4.12)$$

and the NLP master formula

$$\begin{aligned} \frac{d\sigma^{(2)}}{dQ^2 dY d\mathcal{T}} &= \int_0^\infty \frac{dk^+ dk^-}{(k^+ k^-)^\epsilon} \frac{z_a z_b}{(4\pi)^2 2x_a x_b E_{\text{cm}}^4} \frac{(4\pi)^\epsilon}{\Gamma(1-\epsilon)} \delta[\mathcal{T} - \hat{\mathcal{T}}(\{k\})] \\ &\times \left\{ A^{(0)}(Q, Y; \{k\}) \left[f_a f_b \left(-z_a \Delta_a^{(2)} - z_b \Delta_b^{(2)} \right) + x_a \Delta_a^{(2)} f'_a f_b + x_b \Delta_b^{(2)} f_a f'_b \right] \right. \\ &\quad \left. + f_a f_b A^{(2)}(Q, Y; \{k\}) \right\}, \end{aligned} \quad (4.13)$$

where $z_{a,b} \equiv z_{a,b}(k)$ and $\Delta_{a,b}^{(2)} \equiv \Delta_{a,b}^{(2)}(k)$ are defined by eq. (4.7). Note that the LP limits of the matrix elements are universal, and hence eq. (4.12) holds independently of the process, i.e. it only depends on the observable \mathcal{T} . Although the focus of this paper is on the power corrections, in appendix A we provide a brief derivation of the leading-power terms. Likewise, the $A^{(0)}$ term together with the square bracketed factor on the second line of eq. (4.13) is universal, such that all the process dependence arises from the last $A^{(2)}$ term. We will discuss this in more detail in section 4.4.

In the following, we will evaluate eq. (4.13) in both the soft and collinear limit for 0-jettiness, eq. (2.7), whose measurement function for one emission is given by

$$\delta[\mathcal{T} - \hat{\mathcal{T}}(k)] = \Theta(\rho k^+ - \rho^{-1} k^-) \delta(\mathcal{T} - \rho^{-1} k^-) + \Theta(\rho^{-1} k^- - \rho k^+) \delta(\mathcal{T} - \rho k^+). \quad (4.14)$$

The value of ρ depends on the specific definition of \mathcal{T} , as given in eq. (2.8).

4.2 Collinear master formula for 0-jettiness

The expansion of the incoming momenta $\zeta_{a,b}$ for an n -collinear emission $k \sim (\lambda^2, 1, \lambda)$ has been given in eq. (3.12),

$$\begin{aligned} \zeta_a(k) &= x_a \left[\left(1 + \frac{k^- e^{-Y}}{Q} \right) + \frac{k_T^2}{2Q^2} \right] + \mathcal{O}(\lambda^4), \\ \zeta_b(k) &= x_b \left[1 + \left(\frac{k^+ e^{+Y}}{Q} + \frac{k_T^2}{2Q^2} \right) \right] + \mathcal{O}(\lambda^4), \end{aligned} \quad (4.15)$$

so the explicit expressions for the expansion eq. (4.7) are

$$\begin{aligned} z_a &= \left(1 + \frac{k^- e^{-Y}}{Q} \right)^{-1}, & \Delta_a^{(2)} &= \frac{k_T^2}{2Q^2}, \\ z_b &= 1, & \Delta_b^{(2)} &= \left(\frac{k^+ e^{+Y}}{Q} + \frac{k_T^2}{2Q^2} \right). \end{aligned} \quad (4.16)$$

Since an n -collinear emission satisfies $k^- \gg k^+$, the 0-jettiness measurement eq. (4.14) simplifies to

$$\delta[\mathcal{T} - \hat{\mathcal{T}}(k)] = \delta(\mathcal{T} - \rho k^+). \quad (4.17)$$

Note that the integration in eq. (4.13) also includes the region $k^- \rightarrow 0$, where the assumption $k^- \gg k^+$ is invalid. Indeed, this region corresponds to the soft expansion. It is guaranteed by the zero-bin subtraction procedure that this overlap regime between the soft and collinear limits is not double counted [77]. An important benefit of 0-jettiness and our setup here is that the zero-bin contribution that removes the overlap is scaleless and vanishes in pure dimensional regularization, such that we do not need to consider it further.

Eq. (4.17) fixes the k^+ integral in eq. (4.13). It is also useful to write the remaining k^- integration in terms of z_a using eq. (4.16), giving

$$k^- = Q e^Y \frac{1 - z_a}{z_a}, \quad \int_0^\infty dk^- = \int_{x_a}^1 \frac{dz_a}{z_a^2} Q e^Y. \quad (4.18)$$

Here the lower bound on the integration follows from the physical support of the PDF $f_a(x_a/z_a)$. Plugging back into eq. (4.13), we obtain the n -collinear master formula

$$\begin{aligned} \frac{d\sigma_n^{(2)}}{dQ^2 dY d\mathcal{T}} &= \int_{x_a}^1 \frac{dz_a}{z_a} \frac{1}{2x_a x_b E_{\text{cm}}^4} \frac{Q e^Y}{\rho} \left(\frac{Q\mathcal{T} e^Y}{\rho} \right)^{-\epsilon} \frac{z_a^\epsilon}{(1-z_a)^\epsilon} \frac{(4\pi)^\epsilon}{(4\pi)^2 \Gamma(1-\epsilon)} \\ &\times \left\{ \frac{\mathcal{T} e^Y}{Q\rho} A^{(0)}(Q, Y, \{k\}) \left[f_a f_b \frac{(1-z_a)^2 - 2}{2z_a} + \frac{1-z_a}{2z_a} x_a f'_a f_b + \frac{1+z_a}{2z_a} f_a x_b f'_b \right] \right. \\ &\quad \left. + f_a f_b A^{(2)}(Q, Y, \{k\}) \right\}, \end{aligned} \quad (4.19)$$

where k is given by

$$k^\mu = Q e^Y \frac{1-z_a}{z_a} \frac{n^\mu}{2} + \frac{\mathcal{T} \bar{n}^\mu}{\rho} \frac{1}{2} + \sqrt{Q\mathcal{T} \frac{e^Y}{\rho} \frac{1-z_a}{z_a}} n_\perp^\mu. \quad (4.20)$$

It only remains to plug in the expansions of the matrix element $A^{(0)}$ and $A^{(2)}$ and to expand in ϵ . Note that even in the n -collinear case considered here, both the n and \bar{n} -collinear incoming momenta receive power corrections, see eq. (4.4), leading to derivatives of both PDFs in eq. (4.19).

The analogous results for the \bar{n} -collinear limit are obtained in the same manner, giving

$$\begin{aligned} \frac{d\sigma_{\bar{n}}^{(2)}}{dQ^2 dY d\mathcal{T}} &= \int_{x_b}^1 \frac{dz_b}{z_b} \frac{1}{2x_a x_b E_{\text{cm}}^4} \frac{Q\rho}{e^Y} \left(\frac{Q\mathcal{T}\rho}{e^Y} \right)^{-\epsilon} \frac{z_b^\epsilon}{(1-z_b)^\epsilon} \frac{(4\pi)^\epsilon}{(4\pi)^2 \Gamma(1-\epsilon)} \\ &\times \left\{ \frac{\mathcal{T}\rho}{Q e^Y} A^{(0)}(Q, Y, \{k\}) \left[f_a f_b \frac{(1-z_b)^2 - 2}{2z_b} + \frac{1+z_b}{2z_b} x_a f'_a f_b + \frac{1-z_b}{2z_b} f_a x_b f'_b \right] \right. \\ &\quad \left. + f_a f_b A^{(2)}(Q, Y, \{k\}) \right\}, \end{aligned} \quad (4.21)$$

where k is given by

$$k^\mu = \mathcal{T}\rho \frac{n^\mu}{2} + \frac{Q}{e^Y} \frac{1-z_b}{z_b} \frac{\bar{n}^\mu}{2} + \sqrt{Q\mathcal{T} \frac{\rho}{e^Y} \frac{1-z_b}{z_b}} n_\perp^\mu. \quad (4.22)$$

4.3 Soft master formula for 0-jettiness

The expansion of the incoming momenta $\zeta_{a,b}$ for a soft emission $k \sim (\lambda^2, \lambda^2, \lambda^2)$ has been given in eq. (3.10),

$$\begin{aligned} \zeta_a(k) &= x_a \left(1 + \frac{k^- e^{-Y}}{Q} \right) + \mathcal{O}(\lambda^4), \\ \zeta_b(k) &= x_b \left(1 + \frac{k^+ e^{+Y}}{Q} \right) + \mathcal{O}(\lambda^4), \end{aligned} \quad (4.23)$$

so the explicit expressions for the expansion eq. (4.7) are

$$\begin{aligned} z_a &= 1, & \Delta_a^{(2)} &= \frac{k^- e^{-Y}}{Q}, \\ z_b &= 1, & \Delta_b^{(2)} &= \frac{k^+ e^{+Y}}{Q}. \end{aligned} \quad (4.24)$$

Plugging back into eq. (4.13), we get

$$\begin{aligned} \frac{d\sigma_s^{(2)}}{dQ^2 dY d\mathcal{T}} &= \int_0^\infty \frac{dk^+ dk^-}{(k^+ k^-)^\epsilon} \frac{1}{(4\pi)^2 2x_a x_b E_{\text{cm}}^4} \frac{(4\pi)^\epsilon}{\Gamma(1-\epsilon)} \delta[\mathcal{T} - \hat{\mathcal{T}}(\{k\})] \left\{ \frac{1}{Q} A^{(0)}(Q, Y, \{k\}) \right. \\ &\quad \times \left[f_a f_b (-k^- e^{-Y} - k^+ e^{+Y}) + k^- e^{-Y} x_a f'_a f_b + k^+ e^{+Y} f_a x_b f'_b \right] \\ &\quad \left. + f_a f_b A^{(2)}(Q, Y, \{k\}) \right\}. \end{aligned} \quad (4.25)$$

Here, the measurement is given by eq. (4.14),

$$\delta[\mathcal{T} - \hat{\mathcal{T}}(k)] = \Theta(\rho k^+ - \rho^{-1} k^-) \delta(\mathcal{T} - \rho^{-1} k^-) + \Theta(\rho^{-1} k^- - \rho k^+) \delta(\mathcal{T} - \rho k^+). \quad (4.26)$$

We can further simplify eq. (4.25) by utilizing the fact that $A^{(0)}$ and $A^{(2)}$ have a well defined dependence on k^+ or k^- because of power counting and mass dimension,

$$A^{(0)}(Q, Y, \{k\}) = \frac{\bar{A}^{(0)}(Q, Y)}{k^+ k^-}, \quad A^{(2)}(Q, Y, \{k\}) = \frac{\bar{A}_+^{(2)}(Q, Y)}{k^+} + \frac{\bar{A}_-^{(2)}(Q, Y)}{k^-}. \quad (4.27)$$

Here the \bar{A} 's are process-dependent expressions that depend on the Born measurements Q and Y , but are independent of both k^+ and k^- . This implies that the k^\pm integrals in eq. (4.25) have the generic structure

$$\int_0^\infty \frac{dk^+ dk^-}{(k^+ k^-)^\epsilon} \frac{\delta[\mathcal{T} - \hat{\mathcal{T}}(k)]}{(k^+)^\alpha (k^-)^\beta} = \rho^{\alpha-\beta} \mathcal{T}^{1-\alpha-\beta-2\epsilon} \left(\frac{1}{\epsilon + \alpha - 1} + \frac{1}{\epsilon + \beta - 1} \right). \quad (4.28)$$

We then find the soft NLP master formula

$$\begin{aligned} \frac{d\sigma_s^{(2)}}{dQ^2 dY d\mathcal{T}} &= \frac{1}{(4\pi)^2 2x_a x_b E_{\text{cm}}^4} \frac{(4\pi)^\epsilon}{\Gamma(1-\epsilon)} \frac{1}{\epsilon} \frac{\mathcal{T}^{-2\epsilon}}{Q} \frac{1-2\epsilon}{1-\epsilon} \left\{ \bar{A}^{(0)}(Q, Y) \right. \\ &\quad \times \left[f_a(x_a) f_b(x_b) \left(-\frac{\rho}{e^Y} - \frac{e^Y}{\rho} \right) + \frac{\rho}{e^Y} x_a f'_a(x_a) f_b(x_b) + \frac{e^Y}{\rho} f_a(x_a) x_b f'_b(x_b) \right] \\ &\quad \left. + f_a(x_a) f_b(x_b) \left[\rho Q \bar{A}_+^{(2)}(Q, Y) + \frac{Q}{\rho} \bar{A}_-^{(2)}(Q, Y) \right] \right\}. \end{aligned} \quad (4.29)$$

4.4 Universality of power corrections for 0-jettiness

Having derived our master formulas, in this section we comment on the universality of the power corrections. In both the collinear and soft limits the power corrections arising from the derivatives of the PDFs and from the expansion of the flux factor are proportional to the LP matrix element $A^{(0)}(Q, Y)$, see eqs. (4.19) and (4.29). Since the factorization properties of $A^{(0)}(Q, Y)$ are universal, most of the NLP corrections are universal as well, in the sense that they essentially reduce to the LO cross section times a universal factor, as we will make explicit below. The only process-dependent piece arises from the NLP expansion $A^{(2)}(Q, Y)$ of the matrix element. We stress that this limit is defined in our particular choice of Born measurements Q^2 and Y . Using different observables, e.g. q^\pm , the NLP corrections to $\zeta_{a,b}$ in eq. (3.5) would change, inducing also a change of the NLP matrix element.

4.4.1 Universality of collinear limit

We begin by considering the n -collinear limit of a real emission amplitude in detail. We consider the Born process

$$\kappa_a(q_a) + \kappa_b(q_b) \rightarrow L(q_a + q_b), \quad (4.30)$$

where κ_i denotes all quantum numbers, including flavor, of the incoming partons, and L is the leptonic final state of momentum $q = q_a + q_b$. The incoming momenta for the hard collision are given by

$$q_a^\mu = x_a E_{\text{cm}} \frac{n^\mu}{2} = Q e^{+Y} \frac{n^\mu}{2}, \quad q_b^\mu = x_b E_{\text{cm}} \frac{\bar{n}^\mu}{2} = Q e^{-Y} \frac{\bar{n}^\mu}{2}. \quad (4.31)$$

Now consider that parton a arises from an n -collinear splitting of a parton with flavor a' ,

$$\kappa'_a(q'_a) + \kappa_b(q_b) \rightarrow L(q'_a + q_b - k) + \kappa_1(k). \quad (4.32)$$

To describe this at leading power, we only need the $\mathcal{O}(\lambda^0)$ relations for the momenta of the incoming partons, which can be read off from eqs. (4.15) and (4.16),

$$q'^\mu_a = \frac{q_a^\mu}{z_a} + \mathcal{O}(\lambda^2) = \frac{Q e^Y}{z_a} \frac{n^\mu}{2} + \mathcal{O}(\lambda^2). \quad (4.33)$$

The n -collinear emission is given by eq. (4.20),

$$k^\mu = Q e^Y \frac{1 - z_a}{z_a} \frac{n^\mu}{2} + \frac{\mathcal{T}}{\rho} \frac{\bar{n}^\mu}{2} + \sqrt{Q \mathcal{T} \frac{e^Y}{\rho} \frac{1 - z_a}{z_a}} n^\mu_\perp. \quad (4.34)$$

It follows that the leptonic momentum $q' = q'_a + q_b - k = q + \mathcal{O}(\lambda^2)$ is equal to the Born momentum $q = q_a + q_b$, and hence the collinear splitting does not affect the leptonic phase space at LP.

The LP limit only exists if the splitting $\kappa'_a \rightarrow \kappa_a + \kappa_1$ is allowed, in which case it is given by the $\mathcal{O}(\lambda^{-2})$ piece of the squared amplitude,

$$A_{a'b \rightarrow Lk}(Q, Y, \{k\}) = \frac{8\pi\alpha_s \mu_{\text{MS}}^{2\epsilon}}{Q e^Y k^+} P_{aa'}(z_a, \epsilon) A_{ab \rightarrow L}^{\text{LO}}(Q, Y) + \mathcal{O}(\lambda^0), \quad (4.35)$$

where the $1/k^+$ gives rise to the λ^{-2} behavior of the amplitude. Here the $P_{aa'}$ are the ϵ -dimensional splitting functions which are summarized in appendix A.

Recall that in our case, the measurement fixes $k^+ = \mathcal{T}/\rho$. In the notation of eq. (4.10), we hence have for the LP matrix element

$$A_{a'b \rightarrow Lk}^{(0)}(Q, Y, \{k\}) = 8\pi\alpha_s \mu_{\text{MS}}^{2\epsilon} \frac{\rho}{Q \mathcal{T} e^Y} P_{aa'}(z_a, \epsilon) A_{ab \rightarrow L}^{\text{LO}}(Q, Y). \quad (4.36)$$

These results enable us to explicitly give the universal part of the NLP result in the collinear limit. Inserting into the collinear master formula eq. (4.19) and converting to the

$\overline{\text{MS}}$ scheme, we find

$$\begin{aligned}
 & \frac{d\sigma_n^{(2)}}{dQ^2 dY d\mathcal{T}} \\
 &= \hat{\sigma}^{\text{LO}}(Q, Y) \frac{\alpha_s e^Y}{4\pi Q \rho} \times \left(\frac{Q\mathcal{T} e^Y}{\mu^2 \rho} \right)^{-\epsilon} \frac{e^{\epsilon\gamma_E}}{\Gamma(1-\epsilon)} \int_{x_a}^1 \frac{dz_a}{z_a} \frac{z_a^\epsilon}{(1-z_a)^\epsilon} P_{aa'}(z_a, \epsilon) \\
 & \times \left[f_{a'}\left(\frac{x_a}{z_a}\right) f_b(x_b) \frac{(1-z_a)^2 - 2}{z_a} + \frac{1-z_a}{z_a} x_a f_{a'}'\left(\frac{x_a}{z_a}\right) f_b(x_b) + \frac{1+z_a}{z_a} f_{a'}\left(\frac{x_a}{z_a}\right) x_b f_b'(x_b) \right] \\
 & + \int_{x_a}^1 \frac{dz_a}{z_a} \frac{f_a(x_a/z_a) f_b(x_b)}{2x_a x_b E_{\text{cm}}^4} \frac{Q e^Y}{\rho} \left(\frac{Q\mathcal{T} e^Y}{\rho} \right)^{-\epsilon} \frac{z_a^\epsilon}{(1-z_a)^\epsilon} \frac{(4\pi)^\epsilon}{(4\pi)^2 \Gamma(1-\epsilon)} A^{(2)}(Q, Y, \{k\}).
 \end{aligned} \tag{4.37}$$

Here, we factored out the LO partonic cross section eq. (4.2), which is only possible because the collinear splitting leaves the leptonic momentum invariant at LP. We have made explicit the universal piece and nonuniversal components. As already discussed, the full nonuniversal structure arises from the NLP matrix element $A^{(2)}(Q, Y, \{k\})$ in the last line.

It would also be interesting to understand if there is a universal structure to $A^{(2)}(Q, Y)$. This has recently been studied in ref. [78] for pure n gluon scattering amplitudes at the level of the Cachazo-He-Yuan scattering equations [79, 80], where it was proven that in the subleading power collinear limits the tree-level amplitude factorizes into a convolution of the $n - 1$ gluon integrand and a universal collinear kernel. It would be interesting to understand this at the level of the amplitude itself, as well as for fermions. Unlike at leading power, we do not expect that there are universal subleading power splitting functions that are simply functions of z , but there may exist splitting functions that involve differential or integral operators, as occurs in the soft limit at subleading power [81, 82]. Understanding this will be particularly important for generalizing the calculation of the power corrections to more complicated processes.

4.4.2 Universality of soft limit

As for the collinear case, the LP soft limit of the matrix element is universal. Following similar steps as in section 4.4.1, one can express the LP soft limit by

$$A_{ab \rightarrow Lk}^{(0)}(Q, Y; \{k\}) = \frac{16\pi\alpha_s\mu_{\overline{\text{MS}}}^{2\epsilon}\mathbf{C}}{k^+k^-} \times A_{ab \rightarrow L}^{\text{LO}}(Q, Y), \tag{4.38}$$

which only exists for $ab = gg, q\bar{q}$ and where $\mathbf{C} = C_A, C_F$ is the appropriate Casimir constant. We thus obtain

$$\begin{aligned}
 \frac{d\sigma_s^{(2)}}{dQ^2 dY d\mathcal{T}} &= \frac{\hat{\sigma}^{\text{LO}} \alpha_s \mathbf{C}}{Q \pi} \left[\frac{1}{\epsilon} - \ln \frac{\mathcal{T}^2}{\mu^2} - 1 \right] \\
 & \times \left[f_a(x_a) f_b(x_b) \left(-\frac{\rho}{e^Y} - \frac{e^Y}{\rho} \right) + \frac{\rho}{e^Y} x_a f_a'(x_a) f_b(x_b) + \frac{e^Y}{\rho} f_a(x_a) x_b f_b'(x_b) \right] \\
 & + \frac{f_a(x_a) f_b(x_b)}{(4\pi)^2 2x_a x_b E_{\text{cm}}^4} \frac{(4\pi)^\epsilon}{\Gamma(1-\epsilon)} \frac{1}{\epsilon} \mathcal{T}^{-2\epsilon} \frac{1-2\epsilon}{1-\epsilon} \left[\rho |\overline{A}_+^{(2)}(Q, Y)|^2 + \frac{1}{\rho} |\overline{A}_-^{(2)}(Q, Y)|^2 \right].
 \end{aligned} \tag{4.39}$$

As for the collinear case, this emphasizes that the terms arising from the expansion of the PDFs and flux factor are universal, in the sense that they only depend on the universal LP soft limit of the amplitude. The only nonuniversal contributions are $|\overline{A}_{\pm}^{(2)}|^2$. However, these terms can in fact be derived from universal formulae [81–83] involving differential operators. This has been recently studied in the threshold limit, where one only requires soft contributions [67]. However, when one is away from the threshold limit as considered here, one in general requires collinear contributions, which as discussed above, are not (yet) known to be universal.

5 Power corrections at NLO for color singlet production

In this section we give explicit results for the full NLP correction for 0-jettiness at NLO for Higgs and Drell-Yan production in all partonic channels. Since we only consider cases that are s -channel processes at Born level, the LO matrix element only depends on Q and one can factor out the LO partonic cross section $\hat{\sigma}^{\text{LO}}(Q)$. We write the NLP cross section as

$$\begin{aligned} \frac{d\sigma^{(2,n)}}{dQ^2 dY d\mathcal{T}} = & \hat{\sigma}^{\text{LO}}(Q) \left(\frac{\alpha_s}{4\pi}\right)^n \int_{x_a}^1 \frac{dz_a}{z_a} \int_{x_b}^1 \frac{dz_b}{z_b} \left[f_i\left(\frac{x_a}{z_a}\right) f_j\left(\frac{x_b}{z_b}\right) C_{f_i f_j}^{(2,n)}(z_a, z_b, \mathcal{T}) \right. \\ & \left. + \frac{x_a}{z_a} f'_i\left(\frac{x_a}{z_a}\right) f_j\left(\frac{x_b}{z_b}\right) C_{f'_i f_j}^{(2,n)}(z_a, z_b, \mathcal{T}) + f_i\left(\frac{x_a}{z_a}\right) \frac{x_b}{z_b} f'_j\left(\frac{x_b}{z_b}\right) C_{f_i f'_j}^{(2,n)}(z_a, z_b, \mathcal{T}) \right], \end{aligned} \quad (5.1)$$

where as always

$$x_a = \frac{Qe^Y}{E_{\text{cm}}}, \quad x_b = \frac{Qe^{-Y}}{E_{\text{cm}}}. \quad (5.2)$$

We will always express the real emission amplitudes in terms of the Mandelstam variables

$$s_{ab} = 2p_a \cdot p_b, \quad s_{ak} = -2p_a \cdot k, \quad s_{bk} = -2p_b \cdot k. \quad (5.3)$$

This allows us to straightforwardly obtain the LP and NLP expansion using eq. (4.11). We will give an explicit example of the derivation of the soft and collinear master formulas for the $gg \rightarrow Hg$ channel, and only summarize the results in the other channels.

5.1 Gluon-fusion Higgs production

We begin by considering Higgs production in gluon fusion in the $m_t \rightarrow \infty$ limit. At NLP, there are three different partonic channels, $gg \rightarrow Hg$, $q\bar{q} \rightarrow Hg$ and $qg \rightarrow Hq$, which we consider separately. The calculation for $gg \rightarrow Hg$ is shown in full detail as an illustration of our master formulae. The LL power corrections were computed in [63, 64]. Ref. [64] also computed the $q\bar{q} \rightarrow Hg$ NLL power corrections. The NLL power corrections for all partonic channels for gluon fusion Higgs were computed in [70]. We will compare with these results in section 6.

Throughout this section we consider on-shell Higgs production, for which the partonic cross section is given by

$$\hat{\sigma}^{\text{LO}}(Q, Y) = \frac{A^{\text{LO}}(Q, Y)}{2x_a x_b E_{\text{cm}}^4} = 2\pi\delta(Q^2 - m_H^2) \frac{|\mathcal{M}_{gg \rightarrow H}^{\text{LO}}(Q)|^2}{2Q^2 E_{\text{cm}}^2}. \quad (5.4)$$

The LO matrix element in $d = 4 - 2\epsilon$ dimensions is given by [84, 85]

$$|\mathcal{M}_{gg \rightarrow H}^{\text{LO}}(Q)|^2 = \frac{\alpha_s^2 Q^4}{576\pi^2 v^2} \left(\frac{4\pi\mu_{\overline{\text{MS}}}^2}{m_t^2} \right)^{2\epsilon} \frac{\Gamma^2(1+\epsilon)}{1-\epsilon}. \quad (5.5)$$

5.1.1 $gg \rightarrow Hg$

The spin- and color-averaged squared amplitude for $g(p_a) + g(p_b) \rightarrow H(q) + g(k)$ is given by [84]

$$\begin{aligned} A_{gg \rightarrow Hg}(Q, Y, \{k\}) &= A_{gg \rightarrow H}^{\text{LO}}(Q) \times \frac{8\pi\alpha_s C_A \mu_{\overline{\text{MS}}}^{2\epsilon}}{Q^4(1-\epsilon)} \\ &\times \left[(1-2\epsilon) \frac{Q^8 + s_{ab}^4 + s_{ak}^4 + s_{bk}^4}{s_{ab}s_{ak}s_{bk}} + \frac{\epsilon}{2} \frac{(Q^4 + s_{ab}^2 + s_{ak}^2 + s_{bk}^2)^2}{s_{ab}s_{ak}s_{bk}} \right]. \end{aligned} \quad (5.6)$$

n -collinear limit. Expanding eq. (5.6) using eqs. (4.11) and (4.16), the LP and NLP limits of the matrix element are obtained as

$$\begin{aligned} A_{gg \rightarrow Hg}^{(0)}(Q, Y; \{k\}) &= 16\pi\alpha_s C_A \mu_{\overline{\text{MS}}}^{2\epsilon} A_{gg \rightarrow H}^{\text{LO}}(Q) \frac{(1-z_a + z_a^2)^2}{(1-z_a)z_a} \frac{\rho e^{-Y}}{Q\mathcal{T}}, \\ A_{gg \rightarrow Hg}^{(2)}(Q, Y; \{k\}) &= 16\pi\alpha_s C_A \mu_{\overline{\text{MS}}}^{2\epsilon} A_{gg \rightarrow H}^{\text{LO}}(Q) \frac{1}{Q^2 z_a^2} \left[1 + 5z_a^2 - z_a^3 + 2z_a^4 - z_a^5 - 2z_a^2 \frac{1}{1-\epsilon} \right]. \end{aligned} \quad (5.7)$$

Since our scaling variable is $\lambda \sim \sqrt{\mathcal{T}/Q}$, we clearly see that $A^{(0)} \sim \lambda^{-2}$ and $A^{(2)} \sim \lambda^0$, as required at LP and NLP.

Inserting these expansions into eq. (4.19) and converting to the $\overline{\text{MS}}$ scheme yields

$$\begin{aligned} \frac{d\sigma_n^{(2)}}{dQ^2 dY d\mathcal{T}} &= \hat{\sigma}_{gg \rightarrow H}^{\text{LO}}(Q) \times \frac{\alpha_s C_A}{\pi} \int_{x_a}^1 \frac{dz_a}{z_a} \frac{1}{Q} \frac{e^Y}{\rho} \left(\frac{\mathcal{T}Q}{\mu^2} \frac{e^Y}{\rho} \right)^{-\epsilon} \frac{z_a^\epsilon}{(1-z_a)^\epsilon} \frac{e^{\epsilon\gamma_E}}{\Gamma(1-\epsilon)} \\ &\times \left\{ \frac{(1-z_a + z_a^2)^2}{(1-z_a)z_a} \left[f_a f_b \frac{(1-z_a)^2 - 2}{2z_a} + x_a f'_a f_b \frac{1-z_a}{2z_a} + f_a x_b f'_b \frac{1+z_a}{2z_a} \right] \right. \\ &\left. + f_a f_b \frac{1}{z_a^2} \left[1 + 5z_a^2 - z_a^3 + 2z_a^4 - z_a^5 - 2z_a^2 \frac{1}{1-\epsilon} \right] \right\}. \end{aligned} \quad (5.8)$$

To expand this in ϵ , we collect all powers of $(1-z_a)$ and then use the distributional identity

$$(1-z_a)^{-1-\epsilon} = -\frac{\delta(1-z_a)}{\epsilon} + \mathcal{L}_0(1-z_a) + \mathcal{O}(\epsilon), \quad (5.9)$$

where $\mathcal{L}_0(1-z) = 1/(1-z)_+$ is the usual plus distribution. We also combine the two separate $f_a f_b$ pieces, as at this level there is no use to further distinguish the universal and

process dependent pieces. This yields

$$\begin{aligned}
 \frac{d\sigma_n^{(2)}}{dQ^2 dY d\mathcal{T}} &= \hat{\sigma}_{gg \rightarrow H}^{\text{LO}}(Q) \times \frac{\alpha_s}{4\pi} 4C_A \frac{e^Y}{Q\rho} \int_{x_a}^1 \frac{dz_a}{z_a} \\
 &\times \left\{ f_g\left(\frac{x_a}{z_a}\right) f_g(x_b) \left[\left(\frac{1}{\epsilon} - \ln \frac{Q\mathcal{T}e^Y}{\mu^2\rho} \right) \delta(1-z_a) \right. \right. \\
 &\quad \left. \left. + \frac{1-2z_a+8z_a^2-14z_a^3+12z_a^4-10z_a^5+3z_a^6}{2z_a^2} \mathcal{L}_0(1-z_a) \right] \right. \\
 &\quad \left. + \frac{x_a}{z_a} f_g'\left(\frac{x_a}{z_a}\right) f_g(x_b) \frac{(1-z_a+z_a^2)^2}{2z_a} \right. \\
 &\quad \left. + f_g\left(\frac{x_a}{z_a}\right) x_b f_g'(x_b) \left[\left(-\frac{1}{\epsilon} + \ln \frac{Q\mathcal{T}e^Y}{\mu^2\rho} \right) \delta(1-z_a) \right. \right. \\
 &\quad \left. \left. + \frac{(1+z_a)(1-z_a+z_a^2)^2}{2z_a^2} \mathcal{L}_0(1-z_a) \right] \right\}. \quad (5.10)
 \end{aligned}$$

Comparing to eq. (5.1), we can read off the n -collinear kernels,

$$\begin{aligned}
 C_{f_g f_g, n}^{(2,1)}(z_a, z_b, \mathcal{T}) &= 4C_A \frac{e^Y}{Q\rho} \left[\left(\frac{1}{\epsilon} - \ln \frac{Q\mathcal{T}e^Y}{\mu^2\rho} \right) \delta(1-z_a) \right. \\
 &\quad \left. + \frac{1-2z_a+8z_a^2-14z_a^3+12z_a^4-10z_a^5+3z_a^6}{2z_a^2} \mathcal{L}_0(1-z_a) \right] \delta(1-z_b), \\
 C_{f_g' f_g, n}^{(2,1)}(z_a, z_b, \mathcal{T}) &= 4C_A \frac{e^Y}{Q\rho} \frac{(1-z_a+z_a^2)^2}{2z_a} \delta(1-z_b), \\
 C_{f_g f_g', n}^{(2,1)}(z_a, z_b, \mathcal{T}) &= 4C_A \frac{e^Y}{Q\rho} \left[\left(-\frac{1}{\epsilon} + \ln \frac{Q\mathcal{T}e^Y}{\mu^2\rho} \right) \delta(1-z_a) \right. \\
 &\quad \left. + \frac{(1+z_a)(1-z_a+z_a^2)^2}{2z_a^2} \mathcal{L}_0(1-z_a) \right] \delta(1-z_b). \quad (5.11)
 \end{aligned}$$

Soft limit. To expand the matrix element in the soft limit, we use eqs. (4.11) and (4.24) to obtain

$$A_{gg \rightarrow Hg}(Q, Y, \{k\}) = A_{gg \rightarrow H}^{\text{LO}}(Q) \times 16\pi\alpha_s C_A \frac{\mu_{\overline{\text{MS}}}^{2\epsilon}}{k^+ k^-} + \mathcal{O}(\lambda^0). \quad (5.12)$$

Note that the first term scales as $(k^+ k^-)^{-1} \sim \lambda^{-4}$, while there is no $\mathcal{O}(\lambda^{-2})$ component. The NLP term in the expansion of the amplitude thus vanishes, and in the notation of eq. (4.27) we have

$$\overline{A}_{gg \rightarrow Hg}^{(0)}(Q) = A_{gg \rightarrow H}^{\text{LO}}(Q) \times 16\pi\alpha_s C_A \mu_{\overline{\text{MS}}}^{2\epsilon}, \quad \overline{A}_{gg \rightarrow Hg}^{(2)}(Q) = 0. \quad (5.13)$$

Inserting into eq. (4.29) and converting to the $\overline{\text{MS}}$ scheme yields

$$\begin{aligned}
 \frac{d\sigma_s^{(2)}}{dQ^2 dY d\mathcal{T}} &= \hat{\sigma}_{gg \rightarrow H}^{\text{LO}}(Q) \frac{\alpha_s}{4\pi} \times 4C_A \frac{1}{Q} \left(\frac{1}{\epsilon} - \ln \frac{\mathcal{T}^2}{\mu^2} - 1 \right) \\
 &\times \left[f_g(x_a) f_g(x_b) \left(-\frac{\rho}{e^Y} - \frac{e^Y}{\rho} \right) + \frac{\rho}{e^Y} x_a f_g'(x_a) f_g(x_b) + \frac{e^Y}{\rho} f_g(x_a) x_b f_g'(x_b) \right]. \quad (5.14)
 \end{aligned}$$

Since there is no NLP matrix element, one can also obtain this from the universal expression for the soft limit in eq. (4.39). Comparing to eq. (5.1), we can read off the soft kernel,

$$\begin{aligned}
 C_{f_g f_g, s}^{(2,1)}(z_a, z_b, \mathcal{T}) &= 4C_A \frac{1}{Q} \left(-\frac{e^Y}{\rho} - \frac{\rho}{e^Y} \right) \left(\frac{1}{\epsilon} - \ln \frac{\mathcal{T}^2}{\mu^2} - 1 \right) \delta(1-z_a) \delta(1-z_b), \\
 C_{f'_g f'_g, s}^{(2,1)}(z_a, z_b, \mathcal{T}) &= 4C_A \frac{1}{Q} \frac{\rho}{e^Y} \left(\frac{1}{\epsilon} - \ln \frac{\mathcal{T}^2}{\mu^2} - 1 \right) \delta(1-z_a) \delta(1-z_b), \\
 C_{f_g f'_g, s}^{(2,1)}(z_a, z_b, \mathcal{T}) &= 4C_A \frac{1}{Q} \frac{e^Y}{\rho} \left(\frac{1}{\epsilon} - \ln \frac{\mathcal{T}^2}{\mu^2} - 1 \right) \delta(1-z_a) \delta(1-z_b). \tag{5.15}
 \end{aligned}$$

Final result. Adding the n -collinear kernel eq. (5.11), the \bar{n} -collinear kernel which follows from symmetry, and the soft kernel eq. (5.15), all poles in ϵ cancel as expected, and we obtain

$$\begin{aligned}
 C_{f_g f_g}^{(2,1)}(z_a, z_b, \mathcal{T}) &= 4C_A \frac{e^Y}{Q\rho} \left[\left(\ln \frac{\mathcal{T}\rho}{Qe^Y} + 1 \right) \delta(1-z_a) \right. \\
 &\quad \left. + \frac{1-2z_a+8z_a^2-14z_a^3+12z_a^4-10z_a^5+3z_a^6}{2z_a^2} \mathcal{L}_0(1-z_a) \right] \delta(1-z_b) \\
 &\quad + \left(a \leftrightarrow b, \frac{\rho}{e^Y} \rightarrow \frac{e^Y}{\rho} \right), \\
 C_{f'_g f'_g}^{(2,1)}(z_a, z_b, \mathcal{T}) &= 4C_A \frac{\rho}{Qe^Y} \delta(1-z_a) \left[\left(-\ln \frac{\mathcal{T}e^Y}{Q\rho} - 1 \right) \delta(1-z_b) \right. \\
 &\quad \left. + \frac{(1+z_b)(1-z_b+z_b^2)^2}{2z_b^2} \mathcal{L}_0(1-z_b) \right] \\
 &\quad + 4C_A \frac{e^Y}{Q\rho} \frac{(1-z_a+z_a^2)^2}{2z_a} \delta(1-z_b), \\
 C_{f_g f'_g}^{(2,1)}(z_a, z_b, \mathcal{T}) &= 4C_A \frac{e^Y}{Q\rho} \left[\left(-\ln \frac{\mathcal{T}\rho}{Qe^Y} - 1 \right) \delta(1-z_a) \right. \\
 &\quad \left. + \frac{(1+z_a)(1-z_a+z_a^2)^2}{2z_a^2} \mathcal{L}_0(1-z_a) \right] \delta(1-z_b) \\
 &\quad + 4C_A \frac{\rho}{Qe^Y} \delta(1-z_a) \frac{(1-z_b+z_b^2)^2}{2z_b}. \tag{5.16}
 \end{aligned}$$

Substituting these results into eq. (5.1) yields the NLP cross section for $gg \rightarrow Hg$ at NLO.

5.1.2 $gq \rightarrow Hq$

The $gq \rightarrow Hq$ channel has power corrections at both LL and NLL. The spin- and color-averaged squared amplitude for $g(p_a) + q(p_b) \rightarrow H(q) + q(k)$ is given by [84]

$$A_{gq \rightarrow Hq}(Q, Y, \{k\}) = -A_{gg \rightarrow H}^{\text{LO}}(Q) \times 8\pi\alpha_s C_F \mu_{\text{MS}}^{2\epsilon} \frac{1}{Q^4 s_{bk}} \left[s_{ab}^2 + s_{ak}^2 - \epsilon(s_{ab} + s_{ak})^2 \right]. \tag{5.17}$$

Soft limit. The LP soft limit vanishes, since a leading-power soft interaction (which is eikonal) cannot change a n -collinear quark into a n -collinear gluon and soft quark. However

this does occur at NLP in the soft expansion and yields

$$A_{gq \rightarrow Hq}^{(2)}(Q, Y, \{k\}) = A_{gg \rightarrow H}^{\text{LO}}(Q) \times 8\pi\alpha_s C_F \mu_{\text{MS}}^{2\epsilon} \frac{1-\epsilon}{Q k^- e^{-Y}}, \quad (5.18)$$

and the soft kernel is given by

$$C_{f_g f_q, s}^{(1,2)}(z_a, z_b, \mathcal{T}) = 2C_F \frac{e^Y}{Q\rho} \left(\frac{1}{\epsilon} - \ln \frac{\mathcal{T}^2}{\mu^2} - 2 \right) \delta(1-z_a) \delta(1-z_b). \quad (5.19)$$

\bar{n} -collinear limit. The \bar{n} -collinear limit has both a LP and NLP contribution, given by

$$\begin{aligned} A_{gq \rightarrow Hq}^{(0)}(Q, Y, \{k\}) &= A_{gg \rightarrow H}^{\text{LO}}(Q) \times 8\pi\alpha_s C_F \frac{e^Y}{\rho} \frac{1 + (1-z_b)^2 - \epsilon z_b^2}{Q\mathcal{T}z_b}, \\ A_{gq \rightarrow Hq}^{(2)}(Q, Y, \{k\}) &= A_{gg \rightarrow H}^{\text{LO}}(Q) \times 4\pi\alpha_s C_F \mu_{\text{MS}}^{2\epsilon} \frac{4 - z_b^3 + z_b^4 - \epsilon z_b^2(4 - z_b + z_b^2)}{Q^2 z_b^2}. \end{aligned} \quad (5.20)$$

The \bar{n} -collinear kernel is obtained as

$$\begin{aligned} C_{f_g f_q, \bar{n}}^{(1,2)}(z_a, z_b, \mathcal{T}) &= C_F \frac{\rho}{Q e^Y} \delta(1-z_a) \frac{2 - 2z_b + 5z_b^2 - 5z_b^3 + 2z_b^4}{z_b^2}, \\ C_{f'_g f_q, \bar{n}}^{(1,2)}(z_a, z_b, \mathcal{T}) &= C_F \frac{\rho}{Q e^Y} \delta(1-z_a) \frac{(1+z_b)[1 + (1-z_b)^2]}{z_b^2}, \\ C_{f_g f'_q, \bar{n}}^{(1,2)}(z_a, z_b, \mathcal{T}) &= C_F \frac{\rho}{Q e^Y} \delta(1-z_a) \frac{(1-z_b)[1 + (1-z_b)^2]}{z_b}. \end{aligned} \quad (5.21)$$

n -collinear limit. The n -collinear limit vanishes at LP. The NLP expansion of the matrix element gives

$$A_{gq \rightarrow Hq}^{(2)}(Q, Y, \{k\}) = A_{gg \rightarrow H}^{\text{LO}}(Q) \times \frac{8\pi\alpha_s C_F \mu_{\text{MS}}^{2\epsilon} (1-\epsilon)}{Q^2 (1-z_a) z_a}. \quad (5.22)$$

The only nonvanishing kernel is

$$C_{f_g f_q, n}^{(1,2)}(z_a, z_b, \mathcal{T}) = 2C_F \frac{e^Y}{Q\rho} \left[\left(\frac{-1}{\epsilon} + \ln \frac{Q\mathcal{T}e^Y}{\mu^2 \rho} + 1 \right) \delta(1-z_a) + \frac{\mathcal{L}_0(1-z_a)}{z_a} \right] \delta(1-z_b). \quad (5.23)$$

Final result. Combining the n -collinear, \bar{n} -collinear, and soft kernels, the $1/\epsilon$ pole vanishes, and we obtain the final results,

$$\begin{aligned} C_{f_g f_q}^{(1,2)}(z_a, z_b, \mathcal{T}) &= 2C_F \frac{e^Y}{Q\rho} \left[\left(-\ln \frac{\mathcal{T}\rho}{Q e^Y} - 1 \right) \delta(1-z_a) + \frac{\mathcal{L}_0(1-z_a)}{z_a} \right] \delta(1-z_b) \\ &\quad + C_F \frac{\rho}{Q e^Y} \delta(1-z_a) \frac{2 - 2z_b + 5z_b^2 - 5z_b^3 + 2z_b^4}{z_b^2}, \\ C_{f'_g f_q}^{(1,2)}(z_a, z_b, \mathcal{T}) &= C_F \frac{\rho}{Q e^Y} \delta(1-z_a) \frac{(1+z_b)[1 + (1-z_b)^2]}{z_b^2}, \\ C_{f_g f'_q}^{(1,2)}(z_a, z_b, \mathcal{T}) &= C_F \frac{\rho}{Q e^Y} \delta(1-z_a) \frac{(1-z_b)[1 + (1-z_b)^2]}{z_b}. \end{aligned} \quad (5.24)$$

Substituting these results into eq. (5.1) yields the NLP cross section for $gq \rightarrow Hq$ at NLO.

5.1.3 $qg \rightarrow Hq$

The final results needed in eq. (5.1) for $qg \rightarrow Hq$ follow from eq. (5.24) by flipping $a \leftrightarrow b$, $e^Y/\rho \leftrightarrow \rho/e^Y$ and $f_g \leftrightarrow f_q$,

$$\begin{aligned}
C_{f_q f_g}^{(1,2)}(z_a, z_b, \mathcal{T}) &= 2C_F \frac{\rho}{Qe^Y} \delta(1-z_a) \left[\left(-\ln \frac{\mathcal{T}e^Y}{Q\rho} - 1 \right) \delta(1-z_b) + \frac{\mathcal{L}_0(1-z_b)}{z_b} \right] \\
&\quad + C_F \frac{e^Y}{Q\rho} \frac{2-2z_a+5z_a^2-5z_a^3+2z_a^4}{z_a^2} \delta(1-z_b), \\
C_{f'_q f'_g}^{(1,2)}(z_a, z_b, \mathcal{T}) &= C_F \frac{e^Y}{Q\rho} \frac{(1-z_a)[1+(1-z_a)^2]}{z_a} \delta(1-z_b), \\
C_{f_q f'_g}^{(1,2)}(z_a, z_b, \mathcal{T}) &= C_F \frac{e^Y}{Q\rho} \frac{(1+z_a)[1+(1-z_a)^2]}{z_a^2} \delta(1-z_b). \tag{5.25}
\end{aligned}$$

5.1.4 $q\bar{q} \rightarrow Hg$

The $q\bar{q} \rightarrow Hg$ channel first contributes at NLL. It was first given in [64] and then in [70], which agreed, but we reproduce it here for completeness. The squared matrix element, including the average on the initial state spin and colors, is given by [84]

$$A_{q\bar{q} \rightarrow Hg}(Q, Y, \{k\}) = A_{gg \rightarrow H}^{\text{LO}}(Q) \times \frac{64\pi}{3} \alpha_s C_F \mu_{\text{MS}}^{2\epsilon} \frac{1-\epsilon}{Q^4 s_{ab}} [s_{ak}^2 + s_{bk}^2 - \epsilon(s_{ak} + s_{bk})^2]. \tag{5.26}$$

With our choice of Born measurements, the soft limit vanishes both at LP and NLP, leaving only the collinear NLP correction. The LP collinear limit also vanishes, leaving only the NLP n -collinear limit

$$A_{q\bar{q} \rightarrow Hg}^{(2)}(Q, Y, \{k\}) = A_{gg \rightarrow H}^{\text{LO}}(Q) \times \frac{64\pi}{3} \alpha_s C_F \mu_{\text{MS}}^{2\epsilon} (1-\epsilon)^2 \frac{(1-z_a)^2}{Q^2 z_a}, \tag{5.27}$$

and the \bar{n} -collinear result is obtained by replacing $z_a \leftrightarrow z_b$. Combining both, we obtain the kernel for eq. (5.1)

$$C_{f_q f_{\bar{q}}}^{(2,1)}(z_a, z_b, \mathcal{T}) = \frac{16C_F}{3} \frac{1}{Q} \left[\frac{e^Y}{\rho} \frac{(1-z_a)^2}{z_a} \delta(1-z_b) + \frac{\rho}{e^Y} \delta(1-z_a) \frac{(1-z_b)^2}{z_b} \right]. \tag{5.28}$$

5.2 Drell-Yan production

We now consider the Drell-Yan process $pp \rightarrow Z/\gamma^* \rightarrow l^+l^-$, and for brevity denote it as $pp \rightarrow V$. At NLO we have the partonic channels $q\bar{q} \rightarrow Vg$ and $qg \rightarrow Vq$. The LL power corrections for these channels were calculated to NNLO in [62, 63].

For Drell-Yan, it is important to be able to include off-shell effects. The LO partonic cross section as a function of the leptonic invariant mass Q is given by

$$\hat{\sigma}^{\text{LO}}(Q) = \frac{4\pi\alpha_{em}^2}{3N_c Q^2 E_{\text{cm}}^2} \left[Q_q^2 + \frac{(v_q^2 + a_q^2)(v_l^2 + a_l^2) - 2Q_q v_q v_l (1 - m_Z^2/Q^2)}{(1 - m_Z^2/Q^2)^2 + m_Z^2 \Gamma_Z^2/Q^4} \right]. \tag{5.29}$$

Here, $v_{l,q}$ and $a_{l,q}$ are the standard vector and axial couplings of the leptons and quarks to the Z boson, and we have integrated over the l^+l^- phase space.

5.2.1 $q\bar{q} \rightarrow Vg$

We first consider the partonic channel $q\bar{q} \rightarrow Vg$. The squared amplitude is given by [86]

$$|\mathcal{M}_{q\bar{q} \rightarrow Vg}|^2 = |\mathcal{M}_{q\bar{q} \rightarrow V}|^2 \times \frac{8\pi\alpha_s C_F \mu_{\text{MS}}^{2\epsilon}}{Q^2} \left[(1 - \epsilon) \left(\frac{s_{ak}}{s_{bk}} + \frac{s_{bk}}{s_{ak}} \right) + \frac{2s_{ab}Q^2}{s_{ak}s_{bk}} - 2\epsilon \right]. \quad (5.30)$$

Soft limit. With our setup, the soft limit of the matrix element has no NLP correction,

$$A_{q\bar{q} \rightarrow Vg}(Q, Y, \{k\}) = A_{q\bar{q} \rightarrow V}^{\text{LO}}(Q) \times \frac{16\pi\alpha_s C_F \mu_{\text{MS}}^{2\epsilon}}{k^+ k^-} + \mathcal{O}(\lambda^0), \quad (5.31)$$

and the soft kernels are given by

$$\begin{aligned} C_{f_q f_{\bar{q}},s}^{(2,1)}(z_a, z_b, \mathcal{T}) &= 4C_F \left(-\frac{e^Y}{Q\rho} - \frac{\rho}{Qe^Y} \right) \left(\frac{1}{\epsilon} - \ln \frac{\mathcal{T}^2}{\mu^2} - 1 \right) \delta(1 - z_a) \delta(1 - z_b), \\ C_{f'_q f_{\bar{q}},s}^{(2,1)}(z_a, z_b, \mathcal{T}) &= 4C_F \frac{\rho}{Qe^Y} \left(\frac{1}{\epsilon} - \ln \frac{\mathcal{T}^2}{\mu^2} - 1 \right) \delta(1 - z_a) \delta(1 - z_b), \\ C_{f_q f'_{\bar{q}},s}^{(2,1)}(z_a, z_b, \mathcal{T}) &= 4C_F \frac{e^Y}{Q\rho} \left(\frac{1}{\epsilon} - \ln \frac{\mathcal{T}^2}{\mu^2} - 1 \right) \delta(1 - z_a) \delta(1 - z_b). \end{aligned} \quad (5.32)$$

Collinear limit. The n -collinear expansion of the matrix element yields (at NLP, we only need $\epsilon \rightarrow 0$)

$$A_{q\bar{q} \rightarrow Vg}^{(0)}(Q, Y, \{k\}) = A_{q\bar{q} \rightarrow V}^{\text{LO}}(Q) \times 8\pi\alpha_s C_F \mu_{\text{MS}}^{2\epsilon} \frac{\rho}{e^Y} \frac{1 + z_a^2 - \epsilon(1 - z_a)^2}{Q\mathcal{T}(1 - z_a)}, \quad (5.33)$$

$$A_{q\bar{q} \rightarrow Vg}^{(2)}(Q, Y, \{k\}) = A_{q\bar{q} \rightarrow V}^{\text{LO}}(Q) \times 4\pi\alpha_s C_F \frac{1 - z_a + z_a^2 - z_a^3}{Q^2 z_a}. \quad (5.34)$$

The n -collinear kernel is

$$\begin{aligned} C_{f_q f_{\bar{q}},n}^{(2,1)}(z_a, z_b, \mathcal{T}) &= 4C_F \frac{e^Y}{Q\rho} \left[\left(\frac{1}{\epsilon} - \ln \frac{Q\mathcal{T}e^Y}{\mu^2 \rho} \right) \delta(1 - z_a) \right. \\ &\quad \left. + \frac{1}{2}(z_a - 2)(1 + z_a^2) \mathcal{L}_0(1 - z_a) \right] \delta(1 - z_b), \\ C_{f'_q f_{\bar{q}},n}^{(2,1)}(z_a, z_b, \mathcal{T}) &= 4C_F \frac{e^Y}{Q\rho} \frac{1 + z_a^2}{4} \delta(1 - z_b), \\ C_{f_q f'_{\bar{q}},n}^{(2,1)}(z_a, z_b, \mathcal{T}) &= 4C_F \frac{e^Y}{Q\rho} \left[\left(-\frac{1}{\epsilon} + \ln \frac{Q\mathcal{T}e^Y}{\mu^2 \rho} \right) \delta(1 - z_a) \right. \\ &\quad \left. + \frac{(1 + z_a)(1 + z_a^2)}{4z_a} \mathcal{L}_0(1 - z_a) \right] \delta(1 - z_b). \end{aligned} \quad (5.35)$$

Final result. Adding the n , \bar{n} and s kernel, we get

$$\begin{aligned}
 C_{f_q f_{\bar{q}}}^{(2,1)}(z_a, z_b, \mathcal{T}) &= 4C_F \frac{e^Y}{Q\rho} \left[\left(\ln \frac{\mathcal{T}\rho}{Qe^Y} + 1 \right) \delta(1-z_a) + \frac{1}{2}(z_a-2)(1+z_a^2) \mathcal{L}_0(1-z_a) \right] \delta(1-z_b) \\
 &\quad + \left(\frac{e^Y}{\rho} \rightarrow \frac{\rho}{e^Y}, a \leftrightarrow b \right), \\
 C_{f'_q f'_{\bar{q}}}^{(2,1)}(z_a, z_b, \mathcal{T}) &= 4C_F \frac{\rho}{Qe^Y} \delta(1-z_a) \left[\left(-\ln \frac{\mathcal{T}e^Y}{Q\rho} - 1 \right) \delta(1-z_b) + \frac{(1+z_b)(1+z_b^2)}{4z_b} \mathcal{L}_0(1-z_b) \right] \\
 &\quad + 4C_F \frac{e^Y}{Q\rho} \frac{1+z_a^2}{4} \delta(1-z_b), \\
 C_{f_q f'_{\bar{q}}}^{(2,1)}(z_a, z_b, \mathcal{T}) &= 4C_F \frac{e^Y}{Q\rho} \left[\left(-\ln \frac{\mathcal{T}\rho}{Qe^Y} - 1 \right) \delta(1-z_a) + \frac{(1+z_a)(1+z_a^2)}{4z_a} \mathcal{L}_0(1-z_a) \right] \delta(1-z_b) \\
 &\quad + 4C_F \frac{\rho}{Qe^Y} \delta(1-z_a) \frac{1+z_b^2}{4}. \tag{5.36}
 \end{aligned}$$

Substituting these results into eq. (5.1) yields the NLP cross section for $q\bar{q} \rightarrow Vg$ at NLO.

5.2.2 $qg \rightarrow Vq$

Next we consider the partonic channel $qg \rightarrow Vq$. The squared amplitude is given by [86]

$$A_{qg \rightarrow Vq}(Q, Y, \{k\}) = -A_{q\bar{q} \rightarrow V}^{\text{LO}}(Q) \times \frac{8\pi\alpha_s T_F \mu_{\text{MS}}^{2\epsilon}}{Q^2(1-\epsilon)} \left[(1-\epsilon) \left(\frac{s_{ab}}{s_{bk}} + \frac{s_{bk}}{s_{ab}} \right) + \frac{2s_{ak}Q^2}{s_{ab}s_{bk}} - 2\epsilon \right]. \tag{5.37}$$

Soft limit. The LP soft limit vanishes, and the NLP soft expansion is given by

$$A_{qg \rightarrow Vq}^{(2)}(Q, Y, \{k\}) = A_{q\bar{q} \rightarrow V}^{\text{LO}}(Q) \times 8\pi\alpha_s T_F \mu_{\text{MS}}^{2\epsilon} \frac{e^Y}{Qk^-}. \tag{5.38}$$

The soft kernel is given by

$$C_{f_q f_{g,s}}^{(2,1)} = 2T_F \frac{e^Y}{Q\rho} \left(\frac{1}{\epsilon} - \ln \frac{\mathcal{T}^2}{\mu^2} - 1 \right) \delta(1-z_a) \delta(1-z_b). \tag{5.39}$$

n -collinear limit. The n -collinear limit does not contribute at LP, since the LP interaction can not change the \bar{n} -collinear gluon into a \bar{n} -collinear antiquark. The NLP matrix element is given by

$$A_{qg \rightarrow Vq}^{(2)}(Q, Y, \{k\}) = A_{q\bar{q} \rightarrow V}^{\text{LO}}(Q) \times 8\pi\alpha_s T_F \frac{1 + (1-z_a)^2 - \epsilon z_a^2}{(1-\epsilon)(1-z_a)Q^2}, \tag{5.40}$$

and the collinear kernel is

$$\begin{aligned}
 C_{f_q f_{g,n}}^{(2,1)}(z_a, z_b, \mathcal{T}) &= 2T_F \frac{e^Y}{Q\rho} \left[\left(\frac{-1}{\epsilon} + \ln \frac{Q\mathcal{T}e^Y}{\mu^2\rho} \right) \delta(1-z_a) \right. \\
 &\quad \left. + [1 + (1-z_a)^2] \mathcal{L}_0(1-z_a) \right] \delta(1-z_b). \tag{5.41}
 \end{aligned}$$

\bar{n} -collinear limit. The \bar{n} -collinear limit is IR finite, so we work in $d = 4$,

$$A_{qg \rightarrow Vq}^{(0)}(Q, Y, \{k\}) = A_{q\bar{q} \rightarrow V}^{\text{LO}}(Q) \times 8\pi\alpha_s T_F \frac{e^Y}{\rho} \frac{1 - 2z_b + 2z_b^2}{Q\mathcal{T}}, \quad (5.42)$$

$$A_{qg \rightarrow Vq}^{(2)}(Q, Y, \{k\}) = A_{q\bar{q} \rightarrow V}^{\text{LO}}(Q) \times 4\pi\alpha_s T_F \frac{1 + z_b + 4z_b^2 - 8z_b^3 + 4z_b^4}{Q^2 z_b}. \quad (5.43)$$

The \bar{n} -collinear kernel is given by

$$\begin{aligned} C_{f_q f_g, \bar{n}}^{(2,1)}(z_a, z_b, \mathcal{T}) &= T_F \frac{\rho}{Q e^Y} \delta(1 - z_a) (1 - z_b) (1 + 8z_b - 6z_b^2), \\ C_{f'_q f_g, \bar{n}}^{(2,1)}(z_a, z_b, \mathcal{T}) &= T_F \frac{\rho}{Q e^Y} \delta(1 - z_a) \frac{(1 + z_b)(1 - 2z_b + 2z_b^2)}{z_b}, \\ C_{f_q f'_g, \bar{n}}^{(2,1)}(z_a, z_b, \mathcal{T}) &= T_F \frac{\rho}{Q e^Y} \delta(1 - z_a) (1 - z_b) (1 - 2z_b + 2z_b^2). \end{aligned} \quad (5.44)$$

Final result. Adding the s, n, \bar{n} kernels, the pole in ϵ cancels and we get

$$\begin{aligned} C_{f_q f_g}^{(2,1)}(z_a, z_b, \mathcal{T}) &= 2T_F \frac{e^Y}{Q\rho} \left[\left(-\ln \frac{\mathcal{T}\rho}{Q e^Y} - 1 \right) \delta(1 - z_a) + [1 + (1 - z_a)^2] \mathcal{L}_0(1 - z_a) \right] \delta(1 - z_b) \\ &\quad + T_F \frac{\rho}{Q e^Y} \delta(1 - z_a) (1 - z_b) (1 + 8z_b - 6z_b^2), \\ C_{f'_q f_g}^{(2,1)}(z_a, z_b, \mathcal{T}) &= T_F \frac{\rho}{Q e^Y} \delta(1 - z_a) \frac{(1 + z_b)(1 - 2z_b + 2z_b^2)}{z_b}, \\ C_{f_q f'_g}^{(2,1)}(z_a, z_b, \mathcal{T}) &= T_F \frac{\rho}{Q e^Y} \delta(1 - z_a) (1 - z_b) (1 - 2z_b + 2z_b^2). \end{aligned} \quad (5.45)$$

Substituting these results into eq. (5.1) yields the NLP cross section for $qg \rightarrow Vq$ at NLO.

5.2.3 $gq \rightarrow Vq$

For completeness, we also give the explicit results for the $gq \rightarrow Vq$ channel, which can easily be obtained from eq. (5.45) by flipping $a \leftrightarrow b$, $e^Y/\rho \leftrightarrow \rho/e^Y$ and $f_q \leftrightarrow f_g$,

$$\begin{aligned} C_{f_g f_q}^{(2,1)}(z_a, z_b, \mathcal{T}) &= 2T_F \frac{\rho}{Q e^Y} \delta(1 - z_a) \left[\left(-\ln \frac{\mathcal{T} e^Y}{Q\rho} - 1 \right) \delta(1 - z_b) + [1 + (1 - z_b)^2] \mathcal{L}_0(1 - z_b) \right] \\ &\quad + T_F \frac{e^Y}{Q\rho} (1 - z_a) (1 + 8z_a - 6z_a^2) \delta(1 - z_b), \\ C_{f'_g f_q}^{(2,1)}(z_a, z_b, \mathcal{T}) &= T_F \frac{e^Y}{Q\rho} (1 - z_a) (1 - 2z_a + 2z_a^2) \delta(1 - z_b), \\ C_{f_g f'_q}^{(2,1)}(z_a, z_b, \mathcal{T}) &= T_F \frac{e^Y}{Q\rho} \frac{(1 + z_a)(1 - 2z_a + 2z_a^2)}{z_a} \delta(1 - z_b). \end{aligned} \quad (5.46)$$

6 Comparison with integrated results in the literature

In this section, we compare our NLO results to previous results in the literature. The LL results presented by a subset of the present authors in refs. [62, 64] fully agree with the results obtained in this paper.

The results in refs. [63, 70] are given only integrated over the color-singlet rapidity Y , and hence take quite a different form at the integrand level. To compare to them, we integrate our results over Y , which allows us to use integration by parts to bring our results into the same integrated form as those in refs. [63, 70]. For leptonic \mathcal{T} , whose definition involves Y , we find that ref. [70] uses a different definition, and hence we cannot make a meaningful comparison. For hadronic \mathcal{T} , whose definition is independent of Y , we find explicit agreement for the LL results after integrating over Y .

At NLL, the results obtained here for the power corrections differential in Y , for both the leptonic and hadronic definitions and all partonic channels, are new. After integrating over Y we find almost complete agreement with the hadronic results of ref. [70], up to a relatively simple term.²

Since there are a number of differences in our treatment compared to refs. [63, 70], we provide a detailed comparison in this section. In section 6.1 we discuss our different treatments of the NLO phase space and of the Born measurements, and show that the rapidity dependence cannot be easily reconstructed from the results in refs. [63, 70]. In section 6.2 we provide an explicit comparison of the results for the $gg \rightarrow Hg$ channel integrated over rapidity at LL and NLL, both analytically and numerically.

6.1 Treatment of the NLO phase space

The derivation in ref. [70] differs from ours here (and that in refs. [62, 64]) in that it is not differential in the rapidity Y . To explore the differences arising from this, we give a brief derivation of the NLO phase space following the same steps as ref. [70]. Note that in the following we always work with an on-shell process, in contrast to our more general setup in section 4. We also only consider the case $k^+ < k^-$, since the case $k^+ > k^-$ follows by symmetry.

We start with the expression for the NLO phase space as given in ref. [70],

$$\begin{aligned} \frac{d\text{PS}_{\text{NLO}}}{d\mathcal{T}} &= \frac{\mathcal{T}^{-\epsilon}(4\pi\mu_{\text{MS}}^2)^{-\epsilon}}{8\pi\Gamma(1-\epsilon)} \int d\xi_a d\xi_b \frac{f_g(\xi_a)f_g(\xi_b)}{2\xi_a\xi_b E_{\text{cm}}^2} \left(\frac{Q_a\xi_a}{x_a}\right)^{1-\epsilon} \\ &\times \int dz_a (1-z_a)^{-\epsilon} \delta\left(\xi_a\xi_b z_a E_{\text{cm}}^2 - m_H^2 - \frac{Q_a\xi_a}{x_a}\mathcal{T}\right), \end{aligned} \quad (6.1)$$

where $s = E_{\text{cm}}^2$, Q_a is defined in eq. (2.6) and x_a arises from the \mathcal{T} measurement.

We can derive a similar expression in our notation, including in addition the rapidity measurement as done in our main derivation. Denoting the incoming momenta at NLO by $q'_{a,b}$, we have from eq. (3.2)

$$\begin{aligned} \frac{d\text{PS}_{\text{NLO}}}{dY d\mathcal{T}} &= \int_0^1 d\xi_a d\xi_b \frac{f_a(\xi_a)f_b(\xi_b)}{2\xi_a\xi_b E_{\text{cm}}^2} \mu_{\text{MS}}^{2\epsilon} \int \frac{d^d k}{(2\pi)^d} (2\pi)\delta_+(k^2) \int \frac{d^d q}{(2\pi)^d} (2\pi)\delta_+(q^2 - Q^2) \\ &\times (2\pi)^d \delta(q'_a + q'_b - q - k) \delta\left(Y - \frac{1}{2} \ln \frac{q^-}{q^+}\right) \delta[\mathcal{T} - \hat{\mathcal{T}}(k)] \\ &= \frac{1}{8\pi} \frac{(4\pi\mu_{\text{MS}}^2)^\epsilon}{\Gamma(1-\epsilon)} \int_0^1 d\xi_a d\xi_b \frac{f_a(\xi_a)f_b(\xi_b)}{2\xi_a\xi_b E_{\text{cm}}^2} \int_0^\infty \frac{dk^+ dk^-}{(k^+ k^-)^\epsilon} \delta[\mathcal{T} - \hat{\mathcal{T}}(k)] \\ &\times \delta(\xi_a\xi_b E_{\text{cm}}^2 - \xi_a E_{\text{cm}} k^+ - \xi_b E_{\text{cm}} k^- - Q^2) \delta\left(Y - \frac{1}{2} \ln \frac{\xi_a E_{\text{cm}} - k^-}{\xi_b E_{\text{cm}} - k^+}\right). \end{aligned} \quad (6.2)$$

²This missing term has been confirmed by the authors of ref. [70] and was corrected in their version 2.

As in eq. (6.1), we assume that $k^+ < k^-$ to set $\hat{\mathcal{T}}(k) = \rho k^+$, which gives

$$\frac{d\text{PS}^{\text{NLO}}}{dY d\mathcal{T}} = \frac{1}{8\pi} \frac{(4\pi\mu_{\text{MS}}^2)^\epsilon}{\Gamma(1-\epsilon)} \int_0^1 d\xi_a d\xi_b \frac{f_a(\xi_a) f_b(\xi_b)}{2\xi_a \xi_b E_{\text{cm}}^2} \int_0^\infty \frac{dk^-}{\rho} \left(\frac{\rho}{\mathcal{T}k^-} \right)^\epsilon \quad (6.3)$$

$$\times \delta(\xi_a \xi_b E_{\text{cm}}^2 - Q^2 - \xi_a E_{\text{cm}} \mathcal{T} / \rho - \xi_b E_{\text{cm}} k^-) \delta\left(Y - \frac{1}{2} \ln \frac{\xi_a E_{\text{cm}} - k^-}{\xi_b E_{\text{cm}} - \mathcal{T} / \rho}\right).$$

Following ref. [70], we now change variables via $k^- = \xi_a E_{\text{cm}}(1 - z_a)$,

$$\frac{d\text{PS}^{\text{NLO}}}{dY d\mathcal{T}} = \frac{\mathcal{T}^{-\epsilon} (4\pi\mu_{\text{MS}}^2)^\epsilon}{8\pi \Gamma(1-\epsilon)} \int_0^1 d\xi_a d\xi_b \frac{f_a(\xi_a) f_b(\xi_b)}{2\xi_a \xi_b E_{\text{cm}}^2} \left(\frac{\xi_a E_{\text{cm}}}{\rho} \right)^{1-\epsilon} \int dz_a (1 - z_a)^{-\epsilon}$$

$$\times \delta(z_a \xi_a \xi_b E_{\text{cm}}^2 - \xi_a E_{\text{cm}} \mathcal{T} / \rho - Q^2) \delta\left(Y - \frac{1}{2} \ln \frac{z_a \xi_a}{\xi_b - \frac{\mathcal{T}}{\rho E_{\text{cm}}}}\right). \quad (6.4)$$

Up to the rapidity measurement from the final δ function, we find complete agreement with eq. (6.1) if we identify

$$\rho \equiv \rho(Y) = \frac{x_a E_{\text{cm}}}{Q_a(x_a)}. \quad (6.5)$$

At this step, our treatment differs from the one in ref. [70]. Since we explicitly implement measurement δ functions for both Q and Y , we can uniquely solve for ξ_a and ξ_b in terms of Q and Y or equivalently x_a and x_b ,

$$\xi_a = \frac{e^{+Y}}{2z_a^2 E_{\text{cm}}} \left[\frac{\mathcal{T} e^Y}{\rho} (1 - z_a) + \sqrt{\left(\frac{\mathcal{T} e^Y}{\rho} \right)^2 (1 - z_a)^2 + 4Q^2 z_a^2} \right],$$

$$\xi_b = \frac{e^{-Y}}{2z_a E_{\text{cm}}} \left[\frac{\mathcal{T} e^Y}{\rho} (1 + z_a) + \sqrt{\left(\frac{\mathcal{T} e^Y}{\rho} \right)^2 (1 - z_a)^2 + 4Q^2 z_a^2} \right]. \quad (6.6)$$

This holds for both $\rho = 1$ and $\rho = e^Y$. This is equivalent to eq. (3.5) (where we used the notation $\zeta_{a,b}$ instead of $\xi_{a,b}$ here). The reason this expression looks different is just because in eq. (3.5) we performed this step before fixing k^+ in terms of \mathcal{T} and before changing variables from k^- to z_a via $k^- = \xi_a E_{\text{cm}}(1 - z_a)$.

Following a similar strategy as in section 4, one can now replace $\xi_{a,b}$ in eq. (6.4) by the solution eq. (6.6), take the Jacobian from solving the δ functions into account, and then simply expand in \mathcal{T} . The main difference to the derivation in section 4 is that here, one directly expands the phase space in \mathcal{T} , while in section 4 we expanded in terms of the generic power-counting parameter λ .

In ref. [70], there is only the Q^2 measurement but no rapidity measurement, i.e. Y is implicitly integrated over. Hence, there is only one constraint for the two variables ξ_a, ξ_b , whose solution is not unique. They choose to perform the variable transformation from $\xi_{a,b}$ to new variables $\tilde{x}_{a,b}$ defined by

$$\xi_a = \frac{\tilde{x}_a^2 \tilde{x}_b E_{\text{cm}}^2}{z_a \tilde{x}_a \tilde{x}_b E_{\text{cm}}^2 - Q_a(\tilde{x}_a) \mathcal{T}}, \quad \xi_b = \tilde{x}_b. \quad (6.7)$$

We write $\tilde{x}_{a,b}$ here to distinguish these from the Born variables $x_{a,b} = Qe^{\pm Y}/E_{\text{cm}}$ that appear in the Born-projected momenta in eq. (2.4). While they satisfy $\tilde{x}_a\tilde{x}_b = Q^2/E_{\text{cm}}^2$ due to the Q^2 measurement constraint, $(1/2)\ln(\tilde{x}_a/\tilde{x}_b)$ is not equal to the rapidity Y , which would require the solution in eq. (6.6).

In ref. [70], the $\tilde{x}_{a,b}$ defined by eq. (6.7) also enter in the definition of the 0-jettiness measure in eq. (2.3) in place of $x_{a,b}$. As a result, the nonhadronic \mathcal{T} definition in ref. [70] is not the same as the usual leptonic \mathcal{T} with $\rho = e^Y$ that we use. Their hadronic definition is the same as ours, as it has no $x_{a,b}$ dependence. Therefore in the following we restrict our comparison to the hadronic definition.

We also note that one cannot easily recover the rapidity dependence from the integrands of the final results in ref. [70]. To see this explicitly, consider inserting the rapidity measurement by comparing eqs. (6.1) and (6.4), which gives

$$\delta\left(Y - \frac{1}{2}\ln\frac{z_a\xi_a}{\xi_b - \frac{\mathcal{T}}{\rho E_{\text{cm}}}}\right) = \delta\left(Y - \frac{1}{2}\ln\frac{z_a\xi_a^{(0)}}{\xi_b^{(0)}}\right) + \frac{\mathcal{T}}{2}\delta'\left(Y - \frac{1}{2}\ln\frac{z_a\xi_a^{(0)}}{\xi_b^{(0)}}\right)\left(\frac{\xi_b^{\prime(0)}}{\xi_b^{(0)}} - \frac{\xi_a^{\prime(0)}}{\xi_a^{(0)}} - \frac{1}{\xi_b^{(0)}\rho E_{\text{cm}}}\right) + \mathcal{O}(\mathcal{T}^2). \tag{6.8}$$

On the right-hand side we have carried out the power expansion about $\mathcal{T} \rightarrow 0$ and the superscript (0) denotes the results for these variables at LP, while $\xi_a^{\prime(0)} = d\xi_a/d\mathcal{T}|_{\mathcal{T}\rightarrow 0}$, etc. This accounts for the fact that in general the $\xi_{a,b}$ can depend on \mathcal{T} themselves. Equation (6.8) shows that one cannot use the LP expression $\delta[Y - (1/2)\ln(z_a\xi_a^{(0)}/\xi_b^{(0)})] = \delta[Y - (1/2)\ln(\tilde{x}_a/\tilde{x}_b)]$ to recover the Y dependence from the $\tilde{x}_{a,b}$ dependence of the results in ref. [70], as this does not account for the additional power corrections induced by the Y measurement in the second line of eq. (6.8). This implies that the results in ref. [70] and also those in ref. [63] cannot be used when being differential in rapidity or integrated over bins of rapidity, but only integrated over all Y . This was also confirmed to us by the authors.

6.2 Explicit comparison to results in the literature for $gg \rightarrow Hg$

Our final results take a quite different form than those in refs. [63, 70]. For us, both ξ_a and ξ_b receive power corrections resulting in derivatives for both PDFs. In contrast, the variable transformation in eq. (6.7) for the case of $k^+ < k^-$ does not yield power corrections for ξ_b and hence no derivatives of f_b , while the expansion of ξ_a yields derivatives of f_a (and vice versa for $k^+ > k^-$). Due to this different form, one cannot directly compare the integrands of the two results, but one needs to use integration by parts to bring the results into the same form, as we will now show explicitly. In particular, we will show that the results of refs. [62, 64], obtained also here, do agree with the results of refs. [63, 70] at LL when integrating over all Y .

Integrating our result over Y , and transforming the integration variables to $x_{a,b} = Qe^{\pm Y}/E_{\text{cm}}$, we obtain from eq. (5.1)

$$\begin{aligned} \frac{d\sigma^{(2,1)}}{d\mathcal{T}} &= \frac{\alpha_s}{4\pi} \int_0^1 dx_a dx_b 2\pi\delta(x_a x_b E_{\text{cm}}^2 - m_H^2) \frac{|\mathcal{M}_{gg \rightarrow H}^{\text{LO}}(m_H)|^2}{2x_a x_b E_{\text{cm}}^2} \int_{x_a}^1 \frac{dz_a}{z_a} \int_{x_b}^1 \frac{dz_b}{z_b} \\ &\times \left[f_i\left(\frac{x_a}{z_a}\right) f_j\left(\frac{x_b}{z_b}\right) C_{f_i f_j}^{(2,1)}(z_a, z_b, \mathcal{T}) + \frac{x_a}{z_a} f_i'\left(\frac{x_a}{z_a}\right) f_j\left(\frac{x_b}{z_b}\right) C_{f_i' f_j}^{(2,1)}(z_a, z_b, \mathcal{T}) \right. \\ &\quad \left. + \frac{x_b}{z_b} f_i\left(\frac{x_a}{z_a}\right) f_j'\left(\frac{x_b}{z_b}\right) C_{f_i f_j'}^{(2,1)}(z_a, z_b, \mathcal{T}) \right]. \end{aligned} \quad (6.9)$$

We will show the integration by parts explicitly for the $f_i f_j'$ piece. Let us denote the piece we wish to integrate by parts by $D^{(2,1)}$, which can be chosen freely. To integrate over $Y_1 < Y < Y_2$, we switch the integration variables x_a, x_b back to Q^2 and Y , use that

$$\frac{x_b}{z_b} f_j'\left(\frac{x_b}{z_b}\right) = \frac{Qe^{-Y}}{E_{\text{cm}} z_b} f_j'\left(\frac{Qe^{-Y}}{E_{\text{cm}} z_b}\right) = -\frac{d}{dY} f_j\left(\frac{Qe^{-Y}}{E_{\text{cm}} z_b}\right), \quad (6.10)$$

and integrate by parts with respect to Y . Combining the resulting pieces with those in eq. (6.9), we find

$$\begin{aligned} \frac{d\sigma^{(2,1)}}{d\mathcal{T}} &= \frac{\alpha_s}{4\pi} \int_0^1 dx_a dx_b 2\pi\delta(x_a x_b E_{\text{cm}}^2 - m_H^2) \frac{|\mathcal{M}_{gg \rightarrow H}^{\text{LO}}(m_H)|^2}{2x_a x_b E_{\text{cm}}^2} \int_{x_a}^1 \frac{dz_a}{z_a} \int_{x_b}^1 \frac{dz_b}{z_b} \\ &\times \left\{ f_i\left(\frac{x_a}{z_a}\right) f_j\left(\frac{x_b}{z_b}\right) \left[C_{f_i f_j}^{(2,1)}(z_a, z_b, \mathcal{T}) + \frac{d}{dY} D^{(2,1)}(z_a, z_b, \mathcal{T}) \right] \right. \\ &\quad + \frac{x_a}{z_a} f_i'\left(\frac{x_a}{z_a}\right) f_j\left(\frac{x_b}{z_b}\right) \left[C_{f_i' f_j}^{(2,1)}(z_a, z_b, \mathcal{T}) + D^{(2,1)}(z_a, z_b, \mathcal{T}) \right] \\ &\quad \left. + \frac{x_b}{z_b} f_i\left(\frac{x_a}{z_a}\right) f_j'\left(\frac{x_b}{z_b}\right) \left[C_{f_i f_j'}^{(2,1)}(z_a, z_b, \mathcal{T}) - D^{(2,1)}(z_a, z_b, \mathcal{T}) \right] \right\} \\ &- \frac{\alpha_s}{4\pi} \int dQ^2 2\pi\delta(Q^2 - m_H^2) \frac{|\mathcal{M}_{gg \rightarrow H}^{\text{LO}}(m_H)|^2}{2Q^2 E_{\text{cm}}^2} \int_{\frac{Qe^Y}{E_{\text{cm}}}}^1 \frac{dz_a}{z_a} \int_{\frac{Qe^{-Y}}{E_{\text{cm}}}}^1 \frac{dz_b}{z_b} \\ &\times f_i\left(\frac{Qe^Y}{E_{\text{cm}} z_a}\right) f_j\left(\frac{Qe^{-Y}}{E_{\text{cm}} z_b}\right) D^{(2,1)}(z_a, z_b, \mathcal{T}) \Big|_{Y=Y_1}^{Y=Y_2}. \end{aligned} \quad (6.11)$$

The dependence on $D^{(2,1)}$ exactly cancels in this expression. We can choose $D^{(2,1)}$ freely to obtain different forms of the Y -integrated result. The last term in eq. (6.11) is the boundary contribution, which vanishes as $Y_{1,2} \rightarrow \pm\infty$, i.e. only if one is fully inclusive in Y . They do in general contribute when placing acceptance cuts on Y .

We now work out explicitly the required integration by parts both at LL and NLL to bring our results into the integrated form as given in refs. [63, 70]. For concreteness, we focus on the $gg \rightarrow Hg$ channel. For the reasons mentioned earlier, we can only compare the results for the hadronic \mathcal{T} definition.

6.2.1 Comparison at LL

At LL, our results in eq. (5.16) simplify to

$$\begin{aligned}
 C_{f_g f_g}^{(2,1),\text{LL}}(z_a, z_b, \mathcal{T}) &= 4C_A \left[\frac{e^Y}{Q\rho} \ln \frac{\mathcal{T}\rho}{Qe^Y} + \frac{\rho}{Qe^Y} \ln \frac{\mathcal{T}e^Y}{Q\rho} \right] \delta(1-z_a)\delta(1-z_b), \\
 C_{f_g' f_g}^{(2,1),\text{LL}}(z_a, z_b, \mathcal{T}) &= -4C_A \frac{\rho}{Qe^Y} \ln \frac{\mathcal{T}e^Y}{Q\rho} \delta(1-z_a)\delta(1-z_b), \\
 C_{f_g f_g'}^{(2,1),\text{LL}}(z_a, z_b, \mathcal{T}) &= -4C_A \frac{e^Y}{Q\rho} \ln \frac{\mathcal{T}\rho}{Qe^Y} \delta(1-z_a)\delta(1-z_b).
 \end{aligned} \tag{6.12}$$

These agree with the earlier results obtained by a subset of the current authors in refs. [62, 64]. Note that for strict LL accuracy, one can also write the logarithms as $\ln(\mathcal{T}/Q) \pm \ln(\rho/e^Y)$ and only keep the $\ln(\mathcal{T}/Q)$ at LL, while including the $\pm \ln(\rho/e^Y)$ pieces in the NLL contributions. (This is the convention used in refs. [62, 64] and in section 7.) Here, we keep them as part of the LL result, as they are relevant for the comparison with ref. [70].

Up to a trivial change in notation, the LL result given in ref. [70] for hadronic \mathcal{T} is

$$\begin{aligned}
 \frac{d\sigma_{\text{LL}}^{\text{NLP [70]}}}{d\mathcal{T}^{\text{cm}}} &= \frac{\alpha_s C_A}{\pi} \int_0^1 d\tilde{x}_a d\tilde{x}_b 2\pi \delta(\tilde{x}_a \tilde{x}_b E_{\text{cm}}^2 - m_H^2) \frac{|\mathcal{M}_{gg \rightarrow H}^{\text{LO}}(m_H)|^2}{2\tilde{x}_a \tilde{x}_b E_{\text{cm}}^2} \\
 &\times \left[-\tilde{x}_a f_g'(\tilde{x}_a) f_g(\tilde{x}_b) \frac{\tilde{x}_a E_{\text{cm}}}{m_H^2} \ln \frac{\mathcal{T}^{\text{cm}}}{\tilde{x}_a E_{\text{cm}}} - \tilde{x}_b f_g(\tilde{x}_a) f_g'(\tilde{x}_b) \frac{\tilde{x}_b E_{\text{cm}}}{m_H^2} \ln \frac{\mathcal{T}^{\text{cm}}}{\tilde{x}_b E_{\text{cm}}} \right].
 \end{aligned} \tag{6.13}$$

As discussed before, the $\tilde{x}_{a,b}$ here are not equal to the Born variables $x_{a,b}$.

Inserting our LL result in eq. (6.12) with $\rho = 1$ into eq. (6.9), we have

$$\begin{aligned}
 \frac{d\sigma_{\text{LL}}^{(2,1)}}{d\mathcal{T}^{\text{cm}}} &= \frac{\alpha_s C_A}{\pi} \int_0^1 dx_a dx_b 2\pi \delta(x_a x_b E_{\text{cm}}^2 - m_H^2) \frac{|\mathcal{M}_{gg \rightarrow H}^{\text{LO}}(m_H)|^2}{2x_a x_b E_{\text{cm}}^2} \\
 &\times \left[f_g(x_a) f_g(x_b) \left(\frac{e^Y}{m_H} \ln \frac{\mathcal{T}^{\text{cm}} e^{-Y}}{m_H} + \frac{e^{-Y}}{m_H} \ln \frac{\mathcal{T}^{\text{cm}} e^Y}{m_H} \right) \right. \\
 &\quad \left. - x_a f_g'(x_a) f_g(x_b) \frac{e^{-Y}}{m_H} \ln \frac{\mathcal{T}^{\text{cm}} e^Y}{m_H} - x_b f_g(x_a) f_g'(x_b) \frac{e^Y}{m_H} \ln \frac{\mathcal{T}^{\text{cm}} e^{-Y}}{m_H} \right],
 \end{aligned} \tag{6.14}$$

where $e^Y = \sqrt{x_a/x_b}$. At the integrand level, the two results clearly have a different form, as was also remarked in refs. [64, 70].

To show explicitly that eqs. (6.13) and (6.14) do agree, we integrate by parts to move the $f_g f_g$ contribution in eq. (6.14) into the $f_g f_g'$ and $f_g' f_g$ terms. Using eq. (6.11), we can achieve this by choosing

$$D^{(2,1)}(z_a, z_b, \mathcal{T}^{\text{cm}}) = 4C_A \left(-\frac{e^Y}{m_H} \ln \frac{\mathcal{T}^{\text{cm}} e^{-Y}}{m_H} + \frac{e^{-Y}}{m_H} \ln \frac{\mathcal{T}^{\text{cm}} e^Y}{m_H} \right) \delta(1-z_a) \delta(1-z_b). \tag{6.15}$$

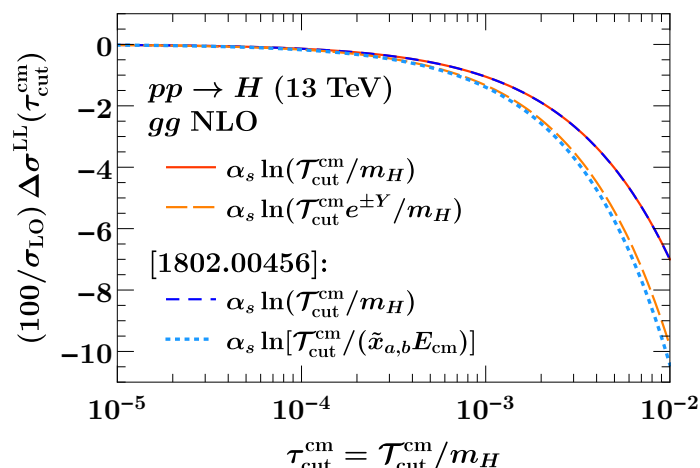


Figure 1. Comparison of the Y -integrated LL power correction for hadronic \mathcal{T} for $gg \rightarrow Hg$. The solid red and blue dashed curves show the LL results keeping only $\ln(\mathcal{T}/m_H)$. In the long-dashed orange and dotted light blue curves we keep all $\ln(\mathcal{T}e^{\pm Y}/m_H)$ or $\ln[\mathcal{T}/(\tilde{x}_{a,b}E_{\text{cm}})]$ terms. In both cases, our result in eq. (6.14) and the result of ref. [70] in eq. (6.13) agree. The small difference in the second case arises due to the fact that $e^{\pm Y}/m_H$ is not exactly the same as $\tilde{x}_{a,b}E_{\text{cm}}$.

Integrating over $Y_1 < Y < Y_2$ and using that $e^Y = \sqrt{x_a/x_b}$ and $m_H = \sqrt{x_a x_b} E_{\text{cm}}$, eq. (6.14) becomes

$$\begin{aligned}
 & \frac{d\sigma_{\text{LL}}^{(2,1)}(Y_1, Y_2)}{d\mathcal{T}^{\text{cm}}} & (6.16) \\
 &= \frac{\alpha_s C_A}{\pi} \int_0^1 dx_a dx_b 2\pi \delta(x_a x_b E_{\text{cm}}^2 - m_H^2) \frac{|\mathcal{M}_{gg \rightarrow H}^{\text{LO}}(m_H)|^2}{2x_a x_b E_{\text{cm}}^2} \\
 & \quad \times \left[-x_a f'_g(x_a) f_g(x_b) \frac{x_a E_{\text{cm}}}{m_H^2} \ln \frac{\mathcal{T}^{\text{cm}}}{x_a E_{\text{cm}}} - x_b f_g(x_a) f'_g(x_b) \frac{x_b E_{\text{cm}}}{m_H^2} \ln \frac{\mathcal{T}^{\text{cm}}}{x_b E_{\text{cm}}} \right] \\
 & + \frac{\alpha_s C_A}{\pi} \frac{2\pi |\mathcal{M}_{gg \rightarrow H}^{\text{LO}}(m_H)|^2}{2m_H^2 E_{\text{cm}}^2} f_g\left(\frac{m_H e^Y}{E_{\text{cm}}}\right) f_g\left(\frac{m_H e^{-Y}}{E_{\text{cm}}}\right) \\
 & \quad \times \left[\frac{e^Y}{m_H} \ln \frac{\mathcal{T}^{\text{cm}} e^{-Y}}{m_H} - \frac{e^{-Y}}{m_H} \ln \frac{\mathcal{T}^{\text{cm}} e^Y}{m_H} \right] \Big|_{Y_1}^{Y_2} \\
 & + \frac{\alpha_s C_A}{\pi} \int_0^1 dx_a dx_b 2\pi \delta(x_a x_b E_{\text{cm}}^2 - m_H^2) \frac{|\mathcal{M}_{gg \rightarrow H}^{\text{LO}}(m_H)|^2}{2x_a x_b E_{\text{cm}}^2} f_g(x_a) f_g(x_b) \frac{e^Y + e^{-Y}}{m_H}.
 \end{aligned}$$

The first two lines exactly reproduce eq. (6.13). The following two lines are the boundary term from integration by parts, which vanishes as $Y_{1,2} \rightarrow \pm\infty$. The last line is a NLL effect and can be neglected for the LL comparison. (It is induced by the integration by parts acting on the Y dependence kept inside the argument of the logarithms.) Therefore, the two expressions in eqs. (6.13) and (6.14) agree at LL and at integrated level if and only if one integrates over all rapidity.

To illustrate this numerically, the Y -integrated results are compared in figure 1. First note that the hadronic LL results in eq. (6.14) do not exactly correspond to those previously given in refs. [62, 64]. This is due to the formally NLL terms proportional to $\ln(\rho/e^Y)$,

discussed below eq. (6.12), which are dropped in the strict LL results in refs. [62, 64], but are kept in eq. (6.14). The analogous NLL terms proportional to $\ln(\tilde{x}_{a,b}E_{\text{cm}})$ are also kept in refs. [63, 70] and eq. (6.13). Dropping these NLL terms in eqs. (6.13) and (6.14), our and their LL results defined in terms of the same $\ln(\mathcal{T}/m_H)$ agree exactly, as shown by the solid red and blue dashed curves in figure 1.³ The long-dashed orange and dotted blue curves in figure 1 show the results when using instead $\ln(\mathcal{T}e^{\pm Y}/m_H)$ or $\ln[\mathcal{T}/(\tilde{x}_{a,b}E_{\text{cm}})]$ to multiply the LL coefficients. The observed difference to the solid red/dashed blue strict LL result has the size of a typical NLL contribution. There is also a very small difference between the long-dashed orange and dotted blue results due to the fact that $e^{\pm Y}/m_H$ is not exactly the same as $\tilde{x}_{a,b}E_{\text{cm}}$. This difference is exactly accounted for by the last line in eq. (6.16).

6.2.2 Comparison at NLL

We now extend our comparison of the Y -integrated results to NLL, focusing again only on the $gg \rightarrow Hg$ channel, which contains all possible complications. The full NLL result of ref. [70] can be written as

$$\begin{aligned} \frac{d\sigma^{\text{NLP [70]}}}{d\mathcal{T}^{\text{cm}}} &= \frac{\alpha_s C_A}{\pi} \int_0^1 d\tilde{x}_a d\tilde{x}_b 2\pi \delta(\tilde{x}_a \tilde{x}_b E_{\text{cm}}^2 - m_H^2) \frac{|\mathcal{M}_{gg \rightarrow H}^{\text{LO}}(m_H)|^2}{2\tilde{x}_a \tilde{x}_b E_{\text{cm}}^2} \int_{\tilde{x}_a}^1 \frac{dz_a}{z_a} \frac{\tilde{x}_a E_{\text{cm}}}{m_H^2} \\ &\times \left\{ f_g\left(\frac{\tilde{x}_a}{z_a}\right) f_g(\tilde{x}_b) \left[\left(\frac{(1-z_a+z_a^2)^2}{z_a^2} - 1 \right) \mathcal{L}_0(1-z_a) + \frac{3z_a^2+1-z_a+z_a^3}{z_a^2} \right] \right. \\ &\quad + \frac{\tilde{x}_a}{z_a} f'_g\left(\frac{\tilde{x}_a}{z_a}\right) f_g(\tilde{x}_b) \left[-\delta(1-z_a) \ln \frac{\mathcal{T}^{\text{cm}}}{\tilde{x}_a E_{\text{cm}}} + \frac{(1-z_a+z_a^2)^2}{z_a^2} \mathcal{L}_0(1-z_a) \right] \\ &\quad \left. - f_g\left(\frac{\tilde{x}_a}{z_a}\right) \tilde{x}_b f'_g(\tilde{x}_b) \delta(1-z_a) \right\} \\ &+ (a \leftrightarrow b). \end{aligned} \tag{6.17}$$

To bring our result into this same form, we need to integrate by parts twice, first with respect to Y as shown in eq. (6.11), and then with respect to z_a . The details of this calculation are given in appendix B. The final result is shown in eq. (B.5) and is given by the result of ref. [70] in eq. (6.17) plus an extra contribution,

$$\begin{aligned} \frac{d\sigma^{(2,1)}}{d\mathcal{T}^{\text{cm}}} &= \frac{d\sigma^{\text{NLP [70]}}}{d\mathcal{T}^{\text{cm}}} \\ &+ 2 \frac{\alpha_s C_A}{\pi} \int_0^1 dx_a dx_b 2\pi \delta(x_a x_b E_{\text{cm}}^2 - m_H^2) \frac{|\mathcal{M}_{gg \rightarrow H}^{\text{LO}}(m_H)|^2}{2x_a x_b E_{\text{cm}}^2} f_g(x_a) f_g(x_b) \frac{e^Y + e^{-Y}}{m_H}. \end{aligned} \tag{6.18}$$

The two results should agree exactly upon integration, and we have not been able to find a source for this discrepancy. As discussed in more detail in section 7, the numerical comparison with MCFM provides a strong confirmation of our result. The numerical extraction of the integrated NLL coefficient yields -0.460 ± 0.026 , which agrees well with

³In the first version of ref. [70] an analogous numerical comparison showed a disagreement between their integrated LL results and our corresponding result from ref. [64]. This was only due to an incorrect comparison. We thank the authors of ref. [70] for confirming this.

our analytic predicted value of -0.466 (see table 2 below). Dropping the term in the final line of eq. (6.18) would instead predict the value -1.669 .⁴

7 Numerical results

In this section we study our results numerically, including the size of the power corrections and the rapidity dependence. We also compare our analytic results for the $\mathcal{O}(\alpha_s)$ NLP power corrections with the full nonsingular spectrum obtained numerically from the LO V +jet and H +jet calculations in MCFM8 [27, 73–75]. In refs. [62, 64], the NLP corrections were extracted numerically by using a fit of the known form of their logarithmic structure to the nonsingular spectrum from MCFM8. In refs. [62, 64], these fits were carried out for the leptonic definition. Here, we have in addition performed the fits also for the hadronic definition. We find excellent agreement between the analytically predicted values and the numerically extracted values for all coefficients, i.e., for the LL and NLL coefficients in all partonic channels for both the leptonic and hadronic definition. This provides a strong and independent cross check for the correctness of the analytic NLL results obtained here. By comparing the complete nonsingular spectrum with our NLP result, we can also assess the importance of power corrections beyond NLP.

The NLO power corrections for each partonic channel are extracted from the nonsingular spectrum by using the fit function

$$F_{\text{NLO}}(\tau) = \frac{d}{d \ln \tau} \left\{ \tau [(a_1 + b_1 \tau + c_1 \tau^2) \ln \tau + a_0 + b_0 \tau + c_0 \tau^2] \right\}, \quad (7.1)$$

with $\tau \equiv \mathcal{T}_0/m_Z$ for Z production and $\tau \equiv \mathcal{T}_0/m_H$ for Higgs production. Details of the fitting procedure have been described already in refs. [62, 64], so we do not repeat them here. A key point is that in order to obtain a precise and unbiased fit result for the to-be extracted a_i coefficients, it is crucial to include the higher-power b_i and c_i terms in eq. (7.1), and to carefully choose the fit range and verify the stability of the fit, as was done in refs. [62, 64]. At the level of precision the a_i are extracted, this is essential since the full nonsingular cross section includes the complete set of power corrections and if the b_i and c_i terms were neglected, these higher-power corrections would be absorbed by the a_i terms in the fit, rendering their numerically extracted values meaningless. To obtain a precise extraction of the NLL coefficient a_0 , we fix the LL coefficient a_1 in the fit to its analytic result.

The relevant coefficients for our NLP comparison at NLO are the LL coefficient a_1 and the NLL coefficient a_0 . For leptonic \mathcal{T} they were extracted for Drell-Yan in ref. [62] and for gluon-fusion Higgs in ref. [64] and for the hadronic \mathcal{T} we have obtained them here. Depending on the partonic channel, the uncertainties on the fitted coefficients range from 0.08% to 2.3% for leptonic \mathcal{T} and from 0.6% to 5.7% for hadronic \mathcal{T} . The latter has larger uncertainties because its power corrections are larger, requiring the fit to be restricted to smaller \mathcal{T} values where the uncertainties in the nonsingular data are larger.

⁴We recently received confirmation from the authors of ref. [70] that after rechecking their calculation they identified a missing term, and now agree with our result for $d\sigma^{(2,1)}/d\mathcal{T}^{\text{cm}}$.

NLO $\mathcal{T}_0^{\text{lep}} q\bar{q} \rightarrow Zg$	a_1	a_0
fitted [62]	$+0.25366 \pm 0.00131$	$+0.13738 \pm 0.00057$
analytic	$+0.25509$	$+0.13708$
NLO $\mathcal{T}_0^{\text{lep}} qg + gq \rightarrow Zq$	a_1	a_0
fitted [62]	-0.27697 ± 0.00113	-0.40062 ± 0.00052
analytic	-0.27720	-0.40105
NLO $\mathcal{T}_0^{\text{cm}} q\bar{q} \rightarrow Zg$	a_1	a_0
fitted	$+1.4188 \pm 0.0614$	-2.4808 ± 0.0176
analytic	$+1.3935$	-2.4806
NLO $\mathcal{T}_0^{\text{cm}} qg + gq \rightarrow Zq$	a_1	a_0
fitted	-2.2981 ± 0.0442	$+4.0991 \pm 0.0132$
analytic	-2.3224	$+4.0965$

Table 1. Comparison between our analytic predictions and the fitted results for the LL a_1 and NLL a_0 coefficients in Drell-Yan production. These fitted values for a_1 and a_0 with the leptonic definition and the analytic results for a_1 were already given in ref. [62].

7.1 Drell-Yan production

We first consider Drell-Yan production, taking $pp \rightarrow Z/\gamma^*$ at $E_{\text{cm}} = 13 \text{ TeV}$. We use the MMHT2014 NNLO PDFs [87] with fixed scales $\mu_r = \mu_f = m_Z$, and $\alpha_s(m_Z) = 0.118$. We fix $Q = m_Z$, integrate over the vector-boson rapidity, and work in the narrow-width approximation for the Z -boson. The NLP corrections for the leptonic \mathcal{T} definition were numerically extracted in ref. [62]. The results for both the leptonic and hadronic definitions for all partonic channels are collected and compared to our analytic predictions in table 1. We find excellent agreement within the fit uncertainties in all cases.

In figure 2 we show the complete NLO nonsingular contributions as black dots, as well as a fit to their form with the solid red curve. Given the agreement in table 1 between our analytic a_0 and the earlier fit result for a_0 , we have fixed a_0 to the analytic result, and redone the fit using eq. (7.1) to obtain this red curve. The red curve from this fit is fully consistent with the earlier fit result from ref. [62]. The dashed orange curve in figure 2 is the extension of the fit function beyond its fit range. In dotted green and dashed blue we show our analytic predictions. We see that with the inclusion of the NLL power corrections, we obtain an excellent description of the full nonsingular cross section up to nearly $\mathcal{T}_0 \sim 1 \text{ GeV}$. This is quite remarkable, and shows that additional higher-order power correction terms are truly suppressed.

In figure 3 we show a plot of the corresponding residual power corrections for the cumulant, $\Delta\sigma(\tau_{\text{cut}})$, on both a linear scale (left) and logarithm scale (right). The solid red curve shows the full power corrections, the solid green curves show the remaining power corrections after including a_1 in the subtractions, and the solid blue curve those after including a_1 and a_0 in the subtractions. We see that with the inclusion of the full NLL power corrections, we achieve more than a factor of 100 reduction in the residual power

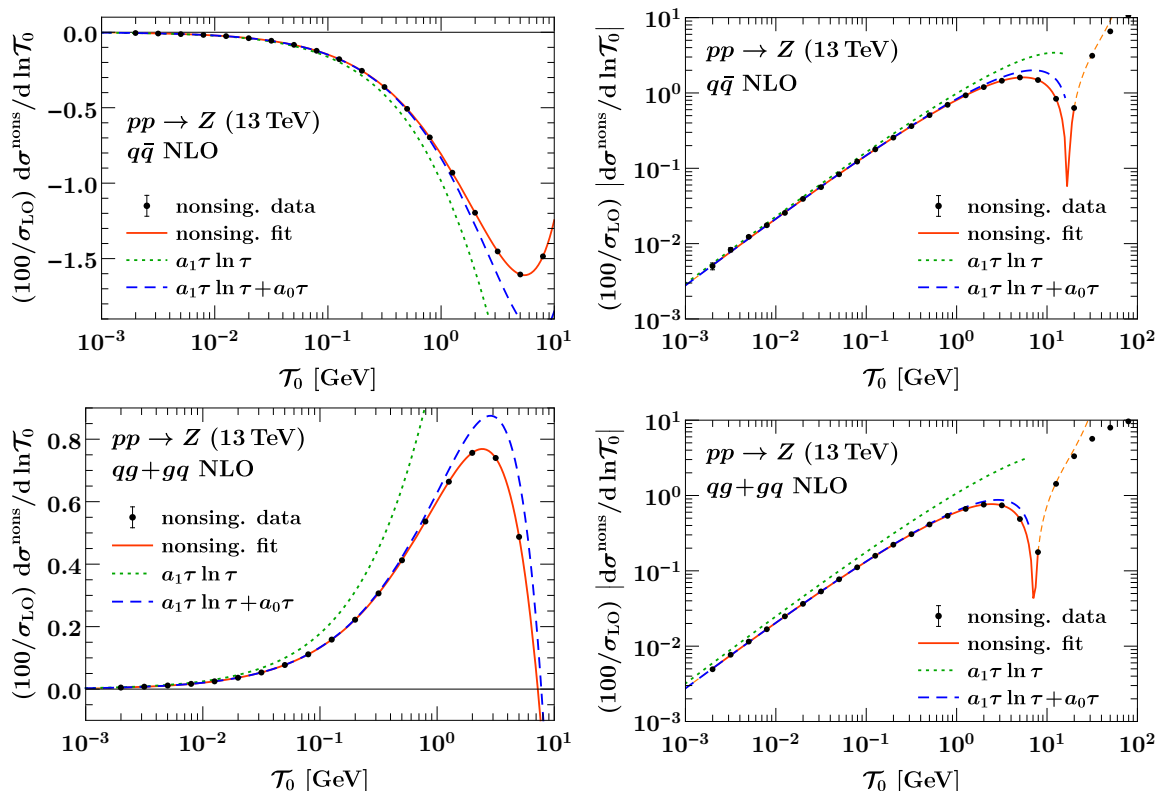


Figure 2. The $\mathcal{O}(\alpha_s)$ nonsingular corrections for Z production for the $q\bar{q}$ channel (top row) and the $qg + gq$ channel (bottom row). A fit to the nonsingular data is shown by the solid red curve. The LL and NLL results are shown by green dotted and blue dashed curves, respectively. In all cases, the NLL approximation provides an excellent approximation to the complete nonsingular cross section.

corrections as compared with the leading-power result at NLO. Both partonic channels have similarly sized power corrections and show a fast convergence of the power expansion. The fact that the blue curve in the logarithmic plot exhibits a steeper slope than the red and green curves is due to its $\mathcal{O}(\tau_{\text{cut}}^2)$ scaling corresponding to a next-to-next-to-leading power correction. This provides a nice visualization that our results correctly capture the complete NLP contribution.

The analogous results for the fitted nonsingular spectrum and the residual power corrections $\Delta\sigma(\tau_{\text{cut}}^{\text{cm}})$ for the hadronic \mathcal{T} definition are shown in figures 4 and 5. As expected, the power corrections are substantially larger for \mathcal{T}^{cm} than for the leptonic definition. To obtain similarly sized power corrections, one has to go to about an order of magnitude smaller values of \mathcal{T}^{cm} . Apart from the overall enhancement, the qualitative behavior of the LL and NLL contributions and the different partonic channels is the same. This is expected from our analytic results, which show that the coefficients for both definitions have essentially the same structure and primarily differ in the overall factors of $e^{\pm Y}$ leading to the rapidity enhancement for the hadronic definition already observed in refs. [62, 64].

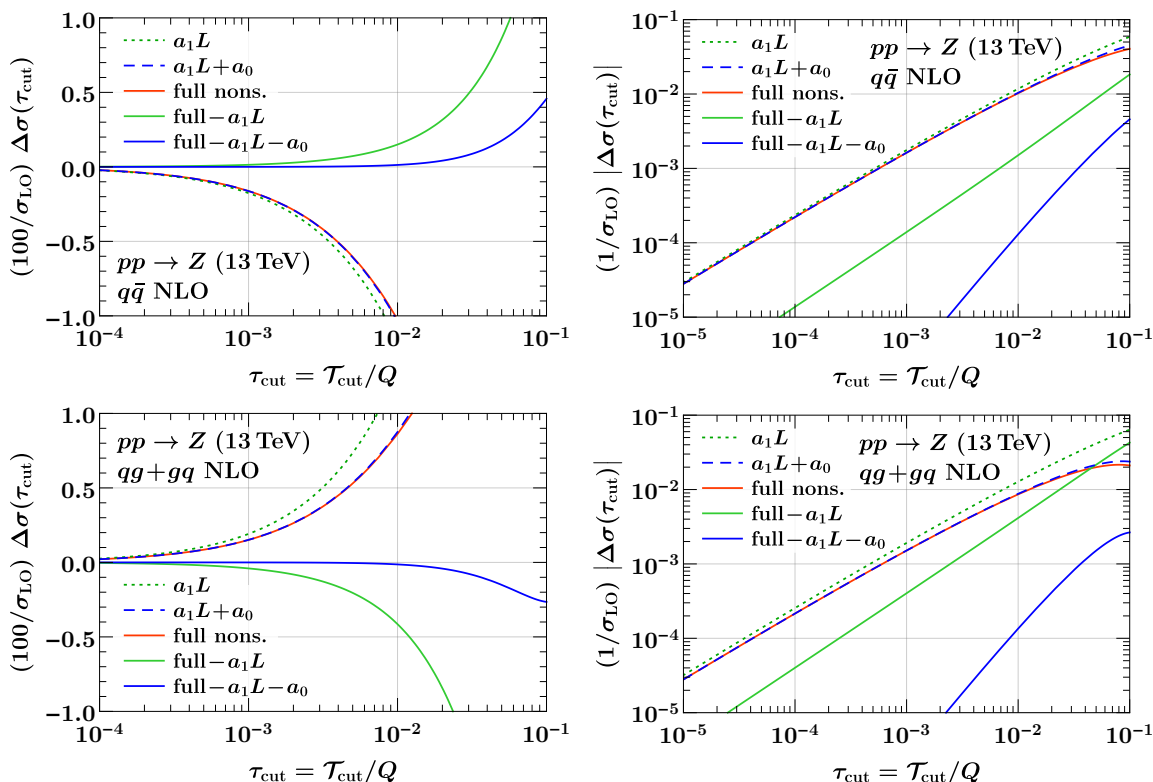


Figure 3. The power corrections for the cumulative $\Delta\sigma(\tau_{\text{cut}})$ at $\mathcal{O}(\alpha_s)$ for Z production in the $q\bar{q}$ channel (top row) and $qg + gq$ channel (bottom row). In both cases, after the inclusion of the NLL power corrections, $\Delta\sigma(\tau_{\text{cut}})$ is reduced by a factor of 100 or more for $\tau_{\text{cut}} < 10^{-2}$.

In figure 6 we show the rapidity dependence of the NLP corrections at fixed $\tau_{\text{cut}} = 10^{-3}$ for both leptonic and hadronic \mathcal{T} normalized to the LO rapidity spectrum. We can clearly see the exponential enhancement for the hadronic definition at large $|Y|$. For the qg channel, the asymmetric behavior in rapidity is expected from its analytic result. The result for the gq channel corresponds to taking $Y \rightarrow -Y$, such that their sum is symmetric in rapidity. While the leptonic definition does not suffer from the exponential enhancement of the hadronic definition, it still exhibits a substantial increase at large positive Y in the qg channel, as well as a suppression at large negative Y . This is due to the substantially different x -dependence of the quark-gluon luminosity (and its derivative) compared to the $q\bar{q}$ luminosity in the LO result to which we normalize. Knowing the NLL contribution to the power corrections differential in rapidity enables one to explicitly account for this effect in the subtractions.

7.2 Gluon-fusion Higgs production

Next, we consider gluon-fusion Higgs production. We take $pp \rightarrow H$ at $E_{\text{cm}} = 13$ TeV with an on-shell, stable Higgs boson with $m_H = 125$ GeV, integrated over all Y . We use the MMHT2014 NNLO PDFs [87], with fixed scales $\mu_r = \mu_f = m_H$, and $\alpha_s(m_H) = 0.1126428$. The NLP power corrections for this configuration for the leptonic \mathcal{T} definition were ex-

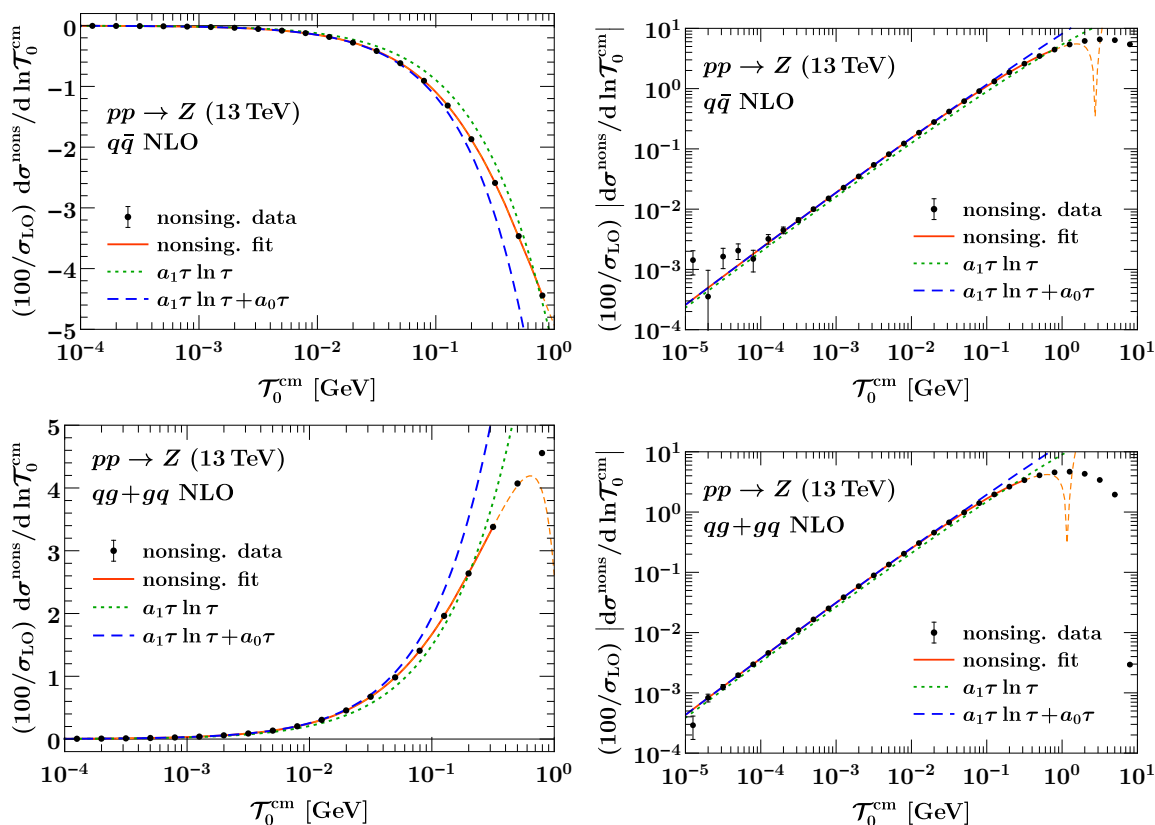


Figure 4. Same as figure 2 for the hadronic \mathcal{T} definition.

tracted numerically in ref. [64]. The results for both leptonic and hadronic definitions for all partonic channels are collected and compared to our analytic predictions in table 2. In all cases, excellent agreement is observed within the fit uncertainties.

In figure 7 we show as the solid red curve a fit to the full nonsingular result at NLO (black points), which is compared with the LL and NLL predictions in dashed green and dashed blue, respectively. Once again this solid red fit curve is obtained using the form in eq. (7.1) with a_1 and a_0 fixed by the analytic result in table 2, and agrees very well with the corresponding result obtained in ref. [64] where a_0 was a parameter in the fit. In all cases, we find that the NLL result provides a good description of the full nonsingular cross section. This is expected since the NLL results includes all NLP terms in the NLO cross section. We see, however, that particularly for the $gq + qg$ channel, the NLL result for a_0 is required to get a good description, and the LL power correction a_1 alone is not sufficient. Thus the $gq + qg$ channel provides an example where simply looking at the size of the residual nonsingular result after subtracting the a_1 term does not suffice to validate the value of this coefficient.

In figure 8, we show a plot of the corresponding power corrections for the cumulant, $\Delta\sigma(\tau_{\text{cut}})$, on both a linear scale (left) and logarithm scale (right). Here we more easily see that the inclusion of the NLL power corrections significantly reduces the residual power corrections for the subtractions. For the dominant $gg \rightarrow Hg$ channel at a typical value of $\tau_{\text{cut}} \sim 10^{-3}$ approximately one order of magnitude is gained at each logarithmic order

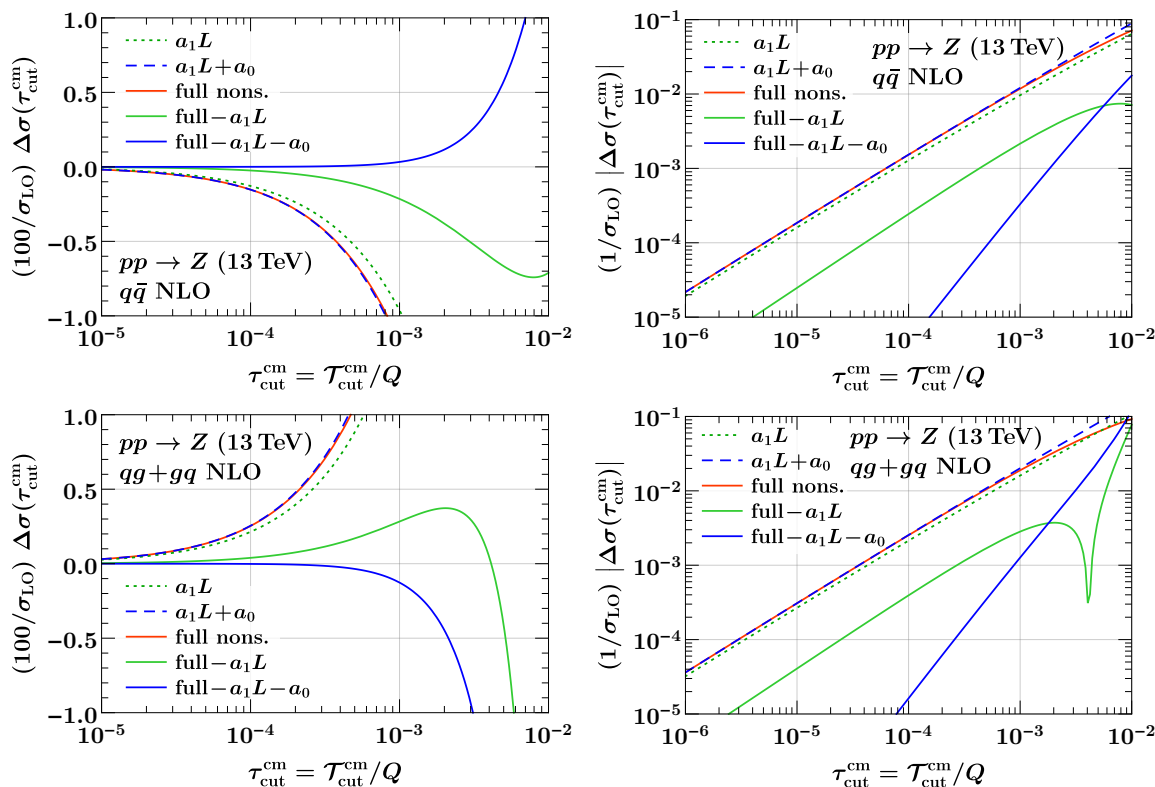


Figure 5. Same as figure 3 for the hadronic \mathcal{T} definition.

that the power corrections are computed. From table 2, we see that for the $gq + qq \rightarrow Hq$ channel, the LL coefficient is numerically suppressed, while in contrast its NLL coefficient is quite larger. Due to this unusual behavior, the NLL result is required to consistently reduce the power corrections as compared with the leading-power result. In the $q\bar{q}$ channel there is no a_1 term, and significant improvement is apparent from including a_0 .

The analogous results for the fitted nonsingular spectrum and the residual power corrections $\Delta\sigma(\tau_{\text{cut}}^{\text{cm}})$ for the hadronic \mathcal{T} definition are shown in figures 9 and 10. The power corrections are noticeably larger, though the effect of the rapidity enhancement is not as pronounced as for Drell-Yan, since here the PDFs suppress the cross section contributions at larger rapidities. For the dominant $gg \rightarrow Hg$ channel there are also numerical cancellations in the NLL coefficient. More precisely the value for a_0 in table 2 arises as $a_0 = 2.356 + (-2.822) = -0.466$, where the first term corresponds to the rapidity-enhanced version of the leptonic a_0 while the second term is the NLL contribution arising from the additional rapidity dependence in the argument of the leading logarithm discussed below eq. (6.12). As a result of this cancellation, including only a_1 in the subtractions leads to slightly smaller power correction above $\tau_{\text{cut}} > 10^{-3}$ than subtracting both a_1 and a_0 (compare the green and blue solid lines in the top row of figure 10). If the second NLL contribution were included as part of the LL result, the latter would provide a much poorer approximation and including the remaining NLL contribution would provide a substantial improvement. Either way, the remaining power corrections after subtracting the full NLL

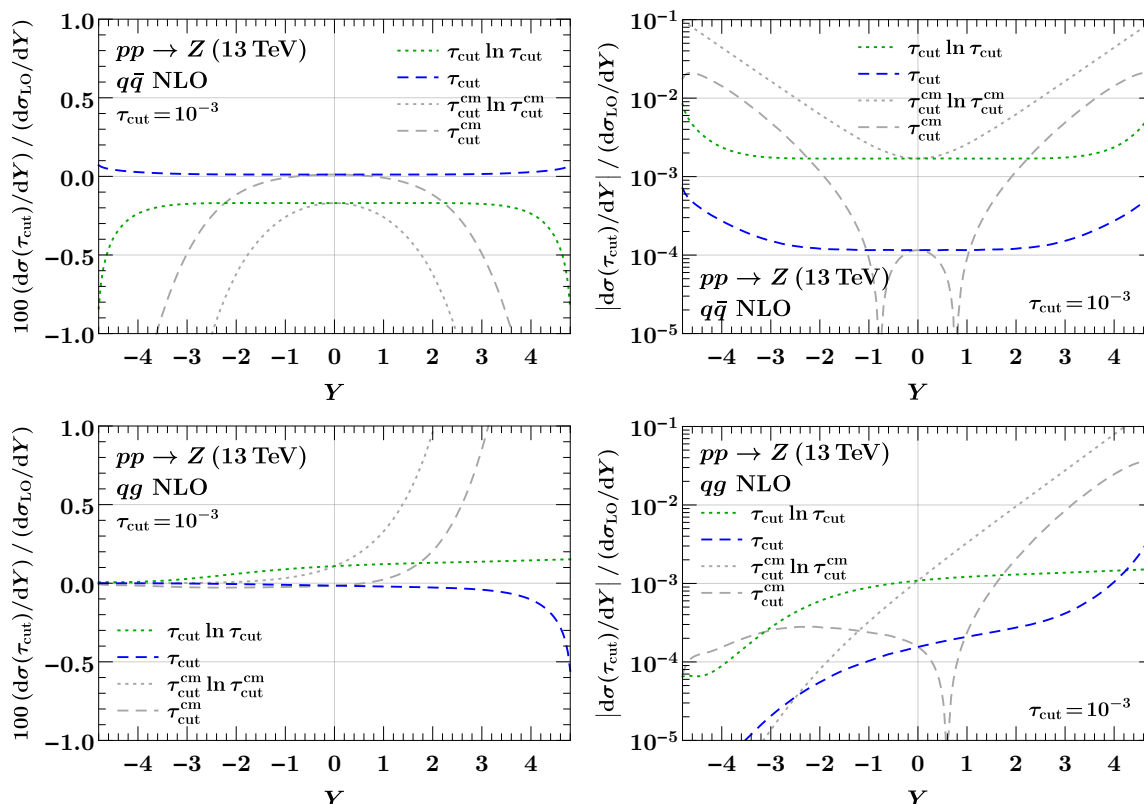


Figure 6. The NLO NLP corrections as a function of rapidity at fixed $\tau_{\text{cut}} = 10^{-3}$ for Z production for the $q\bar{q}$ channel (top row) and the qg channel (bottom row). The LL and NLL coefficients for leptonic \mathcal{T} are shown by the green dotted and blue dashed curves and for hadronic \mathcal{T} by the dotted and dashed gray curves.

result shows a much steeper slope, which is as expected from its $\mathcal{O}(\tau_{\text{cut}}^2)$ scaling. This provides another example where considering only the overall size of the improvement can be potentially misleading. The $gq + qg \rightarrow Hq$ channel shows a similarly unusual behavior as for the leptonic definition.

In figure 11 we show the rapidity dependence of the NLP corrections at fixed $\tau_{\text{cut}} = 10^{-3}$ for both leptonic and hadronic \mathcal{T} normalized to the LO rapidity spectrum. The exponential enhancement for the hadronic definition at large $|Y|$ is again apparent in the LL results. The NLL coefficients again exhibit an enhancement already for the leptonic definition at large Y . This is again due to the different x dependence of the quark PDF and the PDF derivatives compared to the LO gg luminosity to which we normalize. The quark PDF contributions are also the main reason why the NLL term for the gq channel (a_0 in table 2) is much larger than the LL contribution. For the hadronic definition, the $e^{\pm Y}$ factors from the observable definition turn out to partially compensate these PDF effects. This is best visible in the gq channel, where the PDF enhanced terms at negative (LL) or positive (NLL) Y get reduced by a $e^{\pm Y}$ factor from the observable definition. The same effect is also present in the gg channel at NLL. This is the reason why the a_0 term for the hadronic definition in the gq channel turns out to be even slightly smaller than for the leptonic definition.

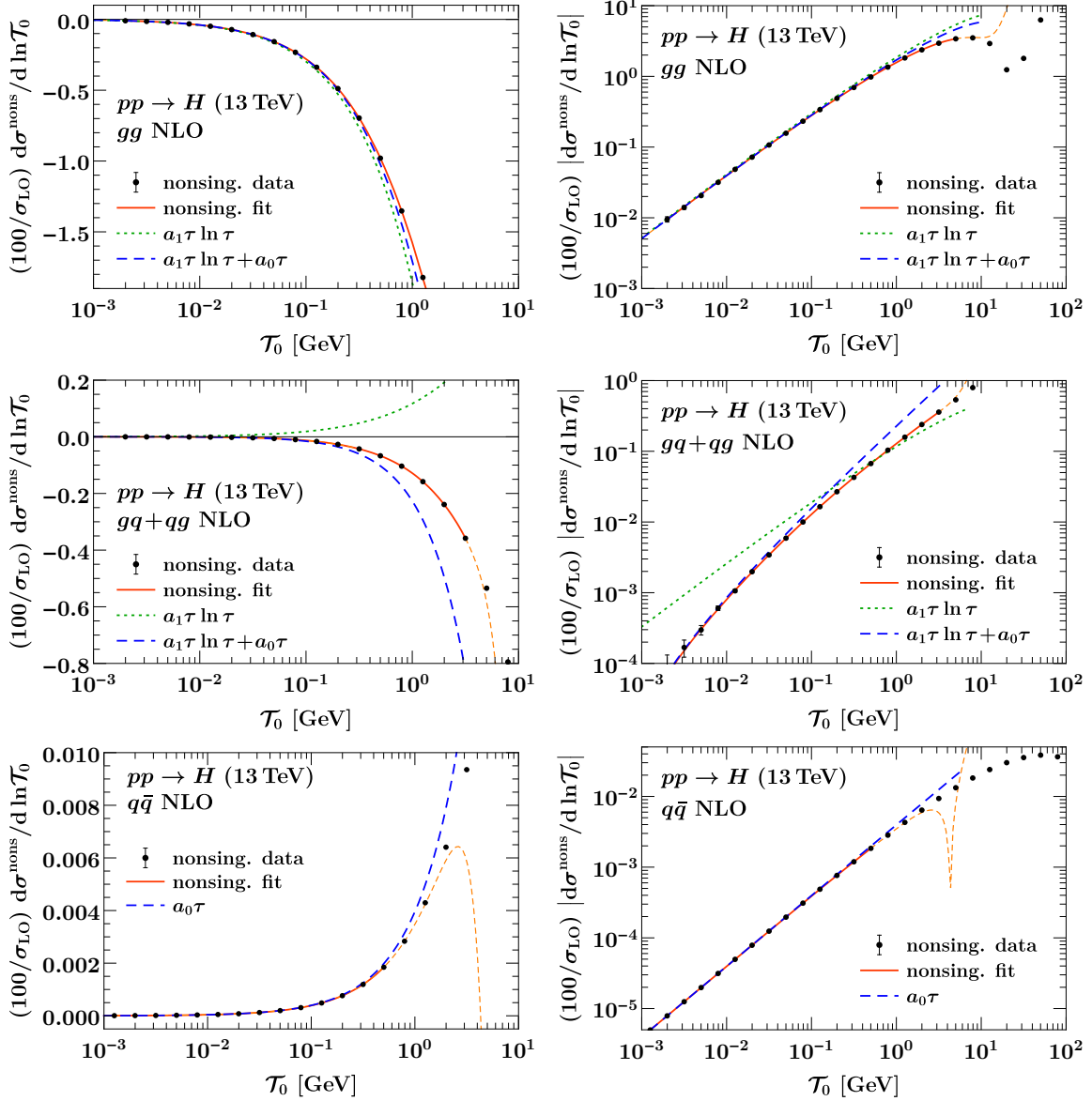


Figure 7. The $\mathcal{O}(\alpha_s)$ nonsingular corrections for Higgs production for the gg channel (top row), $gg+qg$ channel (middle row), and $q\bar{q}$ channel (bottom row). A fit to the nonsingular data (black dots) is shown by the solid red curve. The LL and NLL results are shown by green dotted and blue dashed curves, respectively. In all cases, the NLL approximation provides an excellent approximation to the complete nonsingular cross section for sufficiently small \mathcal{T}_0 .

NLO $\mathcal{T}_0^{\text{lep}} gg \rightarrow Hg$	a_1	a_0
fitted [64]	$+0.60936 \pm 0.00600$	$+0.18241 \pm 0.00425$
analytic	$+0.60400$	$+0.18627$
NLO $\mathcal{T}_0^{\text{lep}} gq + qg \rightarrow Hq$	a_1	a_0
fitted [64]	-0.03733 ± 0.00066	-0.42552 ± 0.00032
analytic	-0.03807	-0.42576
NLO $\mathcal{T}_0^{\text{lep}} q\bar{q} \rightarrow Hg$	a_1	$10^3 a_0$
fitted [64]	–	$+4.90060 \pm 0.00013$
analytic	–	$+4.90047$
NLO $\mathcal{T}_0^{\text{cm}} gg \rightarrow Hg$	a_1	a_0
fitted	$+1.5436 \pm 0.0585$	-0.45954 ± 0.02606
analytic	$+1.5225$	-0.46646
NLO $\mathcal{T}_0^{\text{cm}} gq + qg \rightarrow Hq$	a_1	a_0
fitted	-0.06606 ± 0.00161	-0.33932 ± 0.00194
analytic	-0.06498	-0.34068
NLO $\mathcal{T}_0^{\text{cm}} q\bar{q} \rightarrow Hg$	a_1	$10^3 a_0$
fitted	–	$+6.13445 \pm 0.00015$
analytic	–	$+6.13448$

Table 2. Comparison between our analytic predictions and the fitted results for the LL a_1 and NLL a_0 coefficients in Higgs production. These fitted values for a_1 and a_0 with the leptonic definition and the analytic results for a_1 were already given in ref. [64].

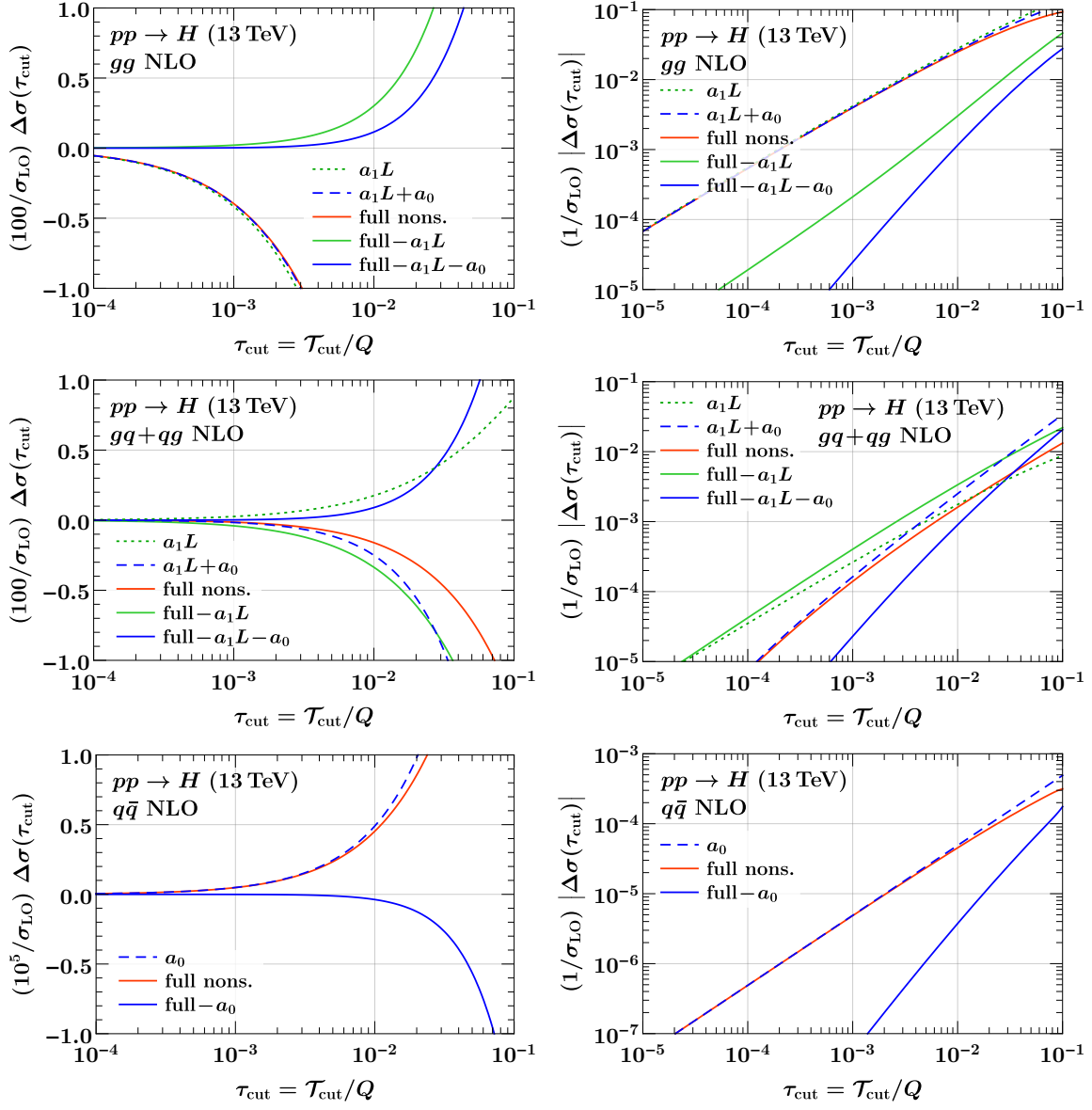


Figure 8. The power corrections for the cumulant $\Delta\sigma(\tau_{\text{cut}})$ at $\mathcal{O}(\alpha_s)$ for Higgs production in the gg channel (top row), $qq + gg$ channel (middle row), $q\bar{q}$ channel (bottom row).

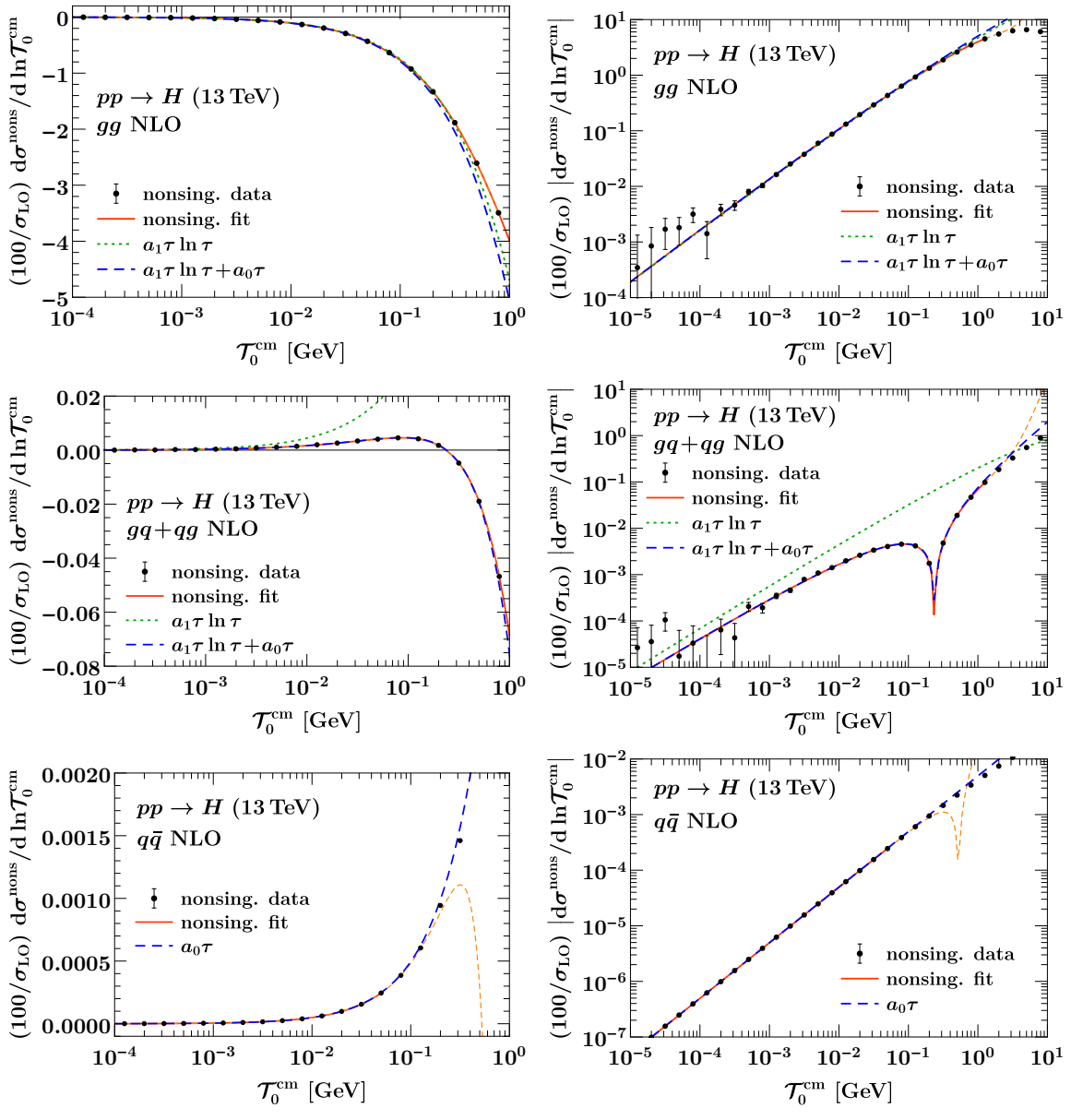


Figure 9. Same as figure 7 for the hadronic \mathcal{T} definition.

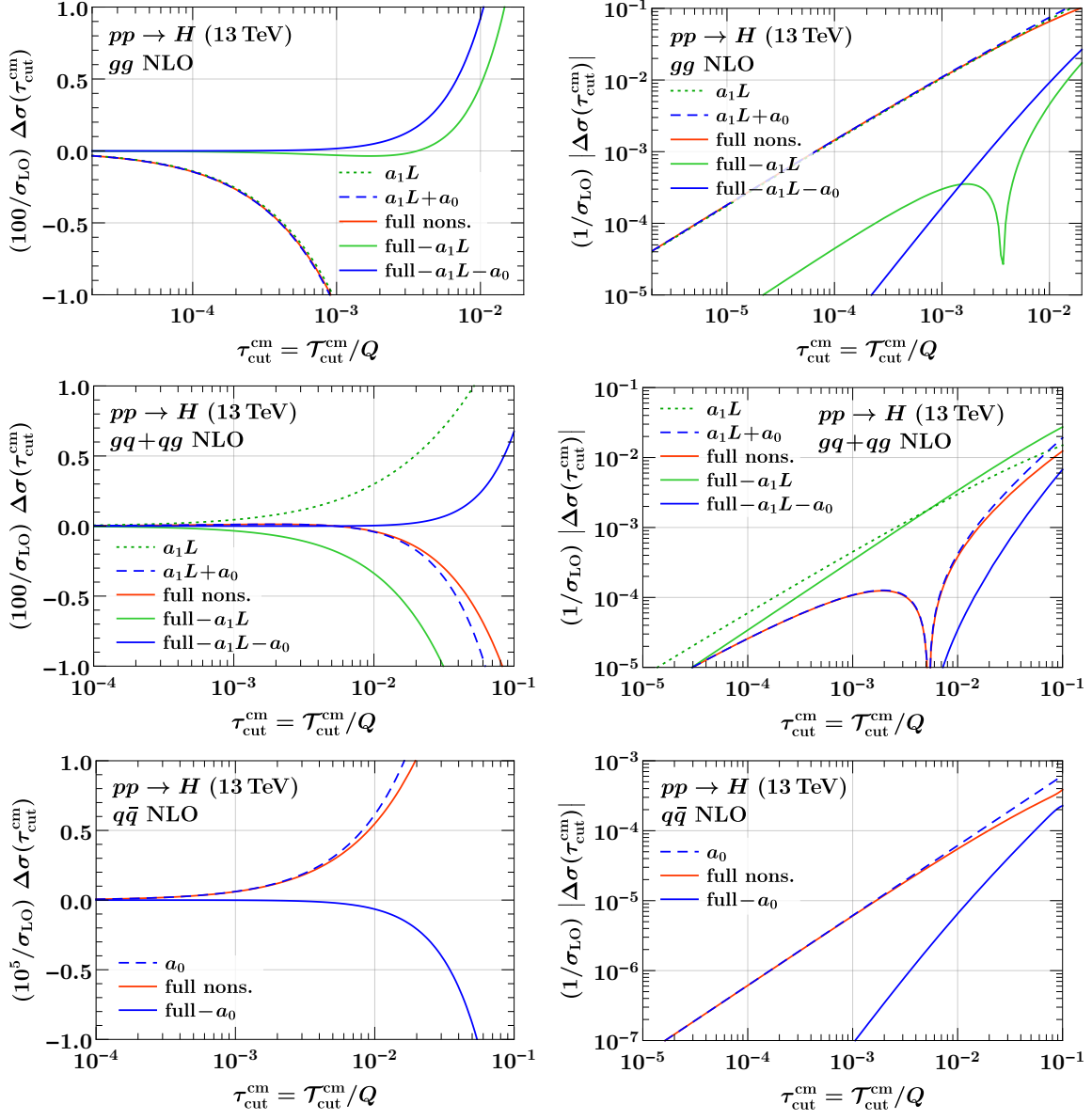


Figure 10. Same as figure 8 for the hadronic \mathcal{T} definition.

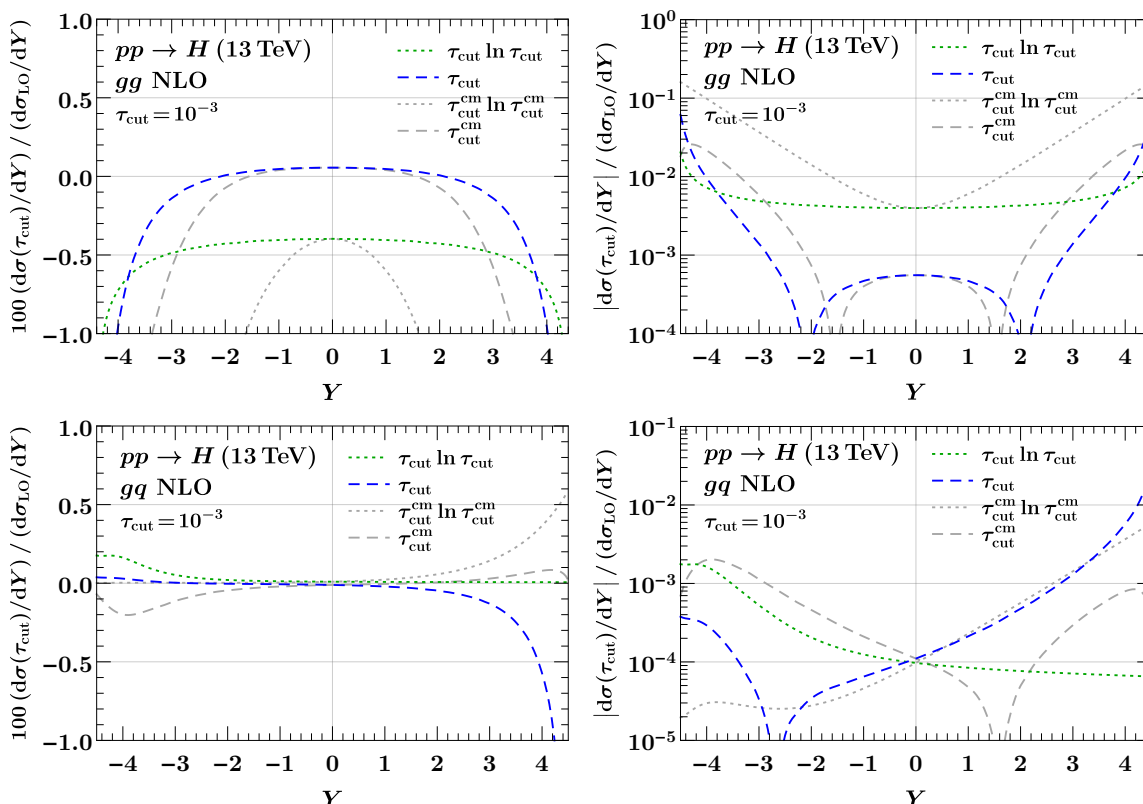


Figure 11. The NLO NLP corrections as a function of rapidity at fixed $\tau_{\text{cut}} = 10^{-3}$ for Higgs production for the gg channel (top row) and the gq channel (bottom row). The LL and NLL coefficients for leptonic \mathcal{T} are shown by the green dotted and blue dashed curves and for hadronic \mathcal{T} by the dotted and dashed gray curves.

8 Conclusions

In this paper, we have computed the next-to-leading power corrections in the N -jettiness resolution variable for Drell-Yan and gluon-fusion Higgs production at NLO. This builds on our previous work by computing the non-logarithmically enhanced terms at this order. These results enable the performance of the N -jettiness subtraction method to be improved, and provide important information on the structure of subleading power corrections beyond the leading logarithms. Our calculation is based on a master formula applicable to SCET_I observables, and highlights a large degree of universality of these power corrections.

We explained in detail the issue of the treatment of Born measurements at subleading power. We have shown that an apparent disagreement in the literature arises due to the fact that the representation used to obtain the power corrections in refs. [63, 70] is only valid when integrated over all rapidities, and therefore cannot be directly compared with the results of refs. [62, 64] and those in the present paper, which are differential in rapidity. We show that after integration over rapidity the LL results agree. Further details can be found in section 6.

We find that the rapidity dependence of the NLL terms is quite sizeable and is therefore important to know to be able to improve the subtractions. One reason for this effect is

the different x -dependence of parton luminosities or derivatives of PDFs appearing in the power corrections as compared to the Born-level parton luminosity. Hence, one can expect this to be a generic feature of subleading power corrections.

We also compared our analytic NLL results for gluon fusion Higgs production and Drell-Yan to numerical predictions for these NLO power corrections obtained from a fit to data from MCFM. In all cases, excellent agreement was found. In addition we studied the extent to which the inclusion of the NLL power corrections improves the subtraction. At NLO, the inclusion of the NLL power corrections completely captures the $\mathcal{O}(\tau)$ terms. Numerically, summing over production channels, the inclusion of these results reduces the size of the power corrections by two orders of magnitude in Higgs production and three orders of magnitude in Drell-Yan production.

There are a number of directions for future work. It will be interesting to extend the calculation of the NLL power corrections to NNLO. Generically we expect up to an order of magnitude improvement could also be obtained by extending the known LL power corrections at this order to NLL. Beyond fixed order, the derivation of subleading power renormalization group evolution equations at NLL would allow for the all-orders prediction of the NLL terms. Finally, while we have focused here on color-singlet production, our results provide an important step toward the calculation of the NLP corrections at higher orders and for more complicated processes.

Acknowledgments

We thank Radja Boughezal, Andrea Isgro, Xiaohui Liu, and Frank Petriello for discussions regarding the results of refs. [63, 70]. This work was supported in part by the Office of Nuclear Physics of the U.S. Department of Energy under Contract No. DE-SC0011090, by the Office of High Energy Physics of the U.S. Department of Energy under Contract No. DE-AC02-05CH11231, and the Simons Foundation Investigator Grant No. 327942. We thank the Aspen Center for Theoretical Physics, which is supported by National Science Foundation grant PHY-1607611, for hospitality while portions of this work were completed. We also thank DESY and MIT for hospitality.

A Derivation of NLO leading power results

At leading power the singular terms for N -jettiness are most easily obtained from known factorization formulas [23, 24], which describe the singular behavior of the observable to all orders. The fixed order approach of this paper is therefore most useful when such factorization formula are not available, or well understood, such as at subleading power. However, it can also be applied to reproduce the LP results. In this appendix we illustrate this at NLO, by reproducing the one-loop beam and soft functions for beam thrust.

To relate the beam and soft functions as defined in SCET to our calculation in this work, recall the LP factorization formula for beam thrust [23],

$$\frac{d\sigma^{(0)}}{dQ^2 dY d\mathcal{T}} = \hat{\sigma}^{\text{LO}}(Q, Y) H_{ab}(Q, \mu) \int dt_a dt_b B_a(t_a, x_a, \mu) B_b(t_b, x_b, \mu) S\left(\mathcal{T} - \frac{t_a}{Q} - \frac{t_b}{Q}, \mu\right), \quad (\text{A.1})$$

where the superscript ⁽⁰⁾ refers to LP, and as before $x_{a,b} = \frac{Q}{E_{\text{cm}}} e^{\pm Y}$. The hard function H_{ab} describes virtual corrections to the hard process $ab \rightarrow L$, $B_{a,b}$ are the two beam functions and S is the soft function. The beam functions can be further matched onto normal PDFs,

$$B_i(t, x, \mu) = \sum_j \int_x^1 \frac{dz}{z} \mathcal{I}_{ij}(t, z, \mu) f_j\left(\frac{x}{z}, \mu\right). \quad (\text{A.2})$$

All of these functions have definitions as field theory matrix elements in the EFT. Their fixed order definitions give rise to UV divergences, which are as usual removed by a renormalization procedure, which in turn gives rise to RGEs that can be used to resum large logarithms of \mathcal{T} . In the approach presented in this paper, the same divergences appear as $1/\epsilon$ IR divergences in the soft and collinear limits of QCD amplitudes.

At LO, we have

$$H_{ij}^{\text{LO}}(Q^2, \mu) = 1, \quad \mathcal{I}_{ij}^{\text{LO}}(t, x, \mu) = \delta_{ij} \delta(t), \quad S^{\text{LO}}(\mathcal{T}, \mu) = \delta(\mathcal{T}). \quad (\text{A.3})$$

At one loop, the convolution structure thus becomes trivial. Working with hard, beam, soft, and PDFs in the bare factorization theorem we have

$$\begin{aligned} \frac{d\sigma^{(0,1)}}{dQ^2 dY d\mathcal{T}} &= \hat{\sigma}^{\text{LO}} H_{ab}^{\text{NLO}}(Q^2, \epsilon) \delta(\mathcal{T}) f_a(x_a, \epsilon) f_b(x_b, \epsilon) \\ &+ \hat{\sigma}^{\text{LO}} \sum_{a'} \int_{x_a}^1 \frac{dz_a}{z_a} Q \mathcal{I}_{aa'}^{\text{NLO}}(Q\mathcal{T}, z_a, \epsilon) f_{a'}(x_a/z_a, \epsilon) f_b(x_b, \epsilon) \\ &+ \hat{\sigma}^{\text{LO}} \sum_{b'} \int_{x_b}^1 \frac{dz_b}{z_b} Q \mathcal{I}_{bb'}^{\text{NLO}}(Q\mathcal{T}, z_b, \epsilon) f_a(x_a, \epsilon) f_{b'}(x_b/z_b, \epsilon) \\ &+ \hat{\sigma}^{\text{LO}} f_a(x_a, \epsilon) f_b(x_b, \epsilon) S^{\text{NLO}}(\mathcal{T}, \epsilon). \end{aligned} \quad (\text{A.4})$$

Note the extra factor of Q in the beam contributions, arising from $t_{a,b}$ and \mathcal{T} having different mass dimensions. We have written eq. (A.4) in a form similar to our master formulas, such that we can easily read off the one-loop beam function kernels and soft function. The ϵ arguments in eq. (A.4) all refer to ultraviolet divergences and can be removed by SCET counterterms to obtain the renormalized factorization theorem. To obtain this it is important to include virtual graphs in the various sectors as well as zero-bin subtractions for the beam functions.

A.1 Leading-power expansion of matrix elements

The leading-power behavior of real emission matrix elements in the soft and collinear limits is universal, see e.g. [7], and has already been used in section 4.4. Here, we briefly review the relevant formulas, and give the relevant one-loop expressions.

Given the Born process

$$\kappa_a(q_a) + \kappa_b(q_b) \rightarrow L(q_a + q_b), \quad (\text{A.5})$$

where the incoming momenta are given by

$$q_a^\mu = Q e^Y \frac{n^\mu}{2}, \quad q_b^\mu = Q e^{-Y} \frac{\bar{n}^\mu}{2}, \quad (\text{A.6})$$

and we write the one-emission process as

$$\kappa'_a(q'_a) + \kappa'_b(q'_b) \rightarrow L(q'_a + q'_b - k) + \kappa_1(k). \quad (\text{A.7})$$

In the soft limit $k^\mu \ll q_a^\mu, q_b^\mu$, the squared matrix element obeys the LP relation

$$A_{a'b' \rightarrow Lk}^{(0)}(Q, Y; \{k\}) = \frac{16\pi\alpha_s\mu_{\text{MS}}^{2\epsilon}\mathbf{C}}{k^+k^-} \times \delta_{aa'}\delta_{bb'} A_{ab \rightarrow L}^{\text{LO}}(Q, Y), \quad (\text{A.8})$$

where we made explicit that a soft emission can not change the incoming flavors. $\mathbf{C} = C_F, C_A$ is the Casimir constant for $ab = q\bar{q}, gg$.

In the LP n -collinear limit, the particle k arises from the splitting $\kappa'_a \rightarrow \kappa_a + \kappa_1$. If this splitting is allowed, at LP we have (in the notation of section 4) $q'_a = q_a/z_a$ and $q'_b = q_b$, and the LP limit of the matrix element is given by

$$A_{a'b' \rightarrow Lk}^{(0)}(Q, Y, \{k\}) = \frac{8\pi\alpha_s\mu_{\text{MS}}^{2\epsilon}}{Qe^Y k^+} P_{aa'}(z_a, \epsilon) \times \delta_{bb'} A_{ab \rightarrow L}^{\text{LO}}(Q, Y). \quad (\text{A.9})$$

Similarly, in the \bar{n} -collinear limit arising from $\kappa'_b \rightarrow \kappa_b + \kappa_1$, at LP we get $q'_a = q_a, q'_b = q_b/z_b$,

$$A_{a'b' \rightarrow Lk}^{(0)}(Q, Y, \{k\}) = \frac{8\pi\alpha_s\mu_{\text{MS}}^{2\epsilon}}{Qe^{-Y} k^-} P_{bb'}(z_b, \epsilon) \times \delta_{aa'} A_{ab \rightarrow L}^{\text{LO}}(Q, Y). \quad (\text{A.10})$$

The one-loop splitting functions in $d = 4 - 2\epsilon$ dimensions are given by [7]

$$\begin{aligned} P_{qq}(z, \epsilon) &= C_F \left[\frac{1+z^2}{1-z} - \epsilon(1-z) \right], \\ P_{gq}(z, \epsilon) &= C_F \left[\frac{1+(1-z)^2}{z} - \epsilon z \right], \\ P_{qg}(z, \epsilon) &= T_F \left[1 - \frac{2z(1-z)}{1-\epsilon} \right], \\ P_{gg}(z, \epsilon) &= 2C_A \left[\frac{z}{1-z} + \frac{1-z}{z} + z(1-z) \right]. \end{aligned} \quad (\text{A.11})$$

Note that we flipped the notation of qg and gq relative to [7], following the standard convention.

A.2 NLO soft function

The NLO LP soft function follows from combining eq. (4.12) with eq. (A.8) using the same steps as in section 4.3,

$$\begin{aligned} \frac{d\sigma_s^{(0,1)}}{dQ^2 dY d\mathcal{T}} &= \int_0^\infty \frac{dk^+ dk^-}{(k^+ k^-)^\epsilon} \frac{f_a(x_a) f_b(x_b)}{(4\pi)^2 2x_a x_b E_{\text{cm}}^4} \frac{(4\pi)^\epsilon}{\Gamma(1-\epsilon)} A^{(0)}(Q, Y; \{k\}) \delta[\mathcal{T} - \hat{\mathcal{T}}(\{k\})] \\ &= \frac{A^{\text{LO}}(Q, Y)}{2x_a x_b E_{\text{cm}}^4} \frac{\alpha_s \mathbf{C}}{\pi} f_a(x_a) f_b(x_b) \times \frac{e^{\epsilon\gamma_E} \mu^{2\epsilon}}{\Gamma(1-\epsilon)} \int_0^\infty \frac{dk^+ dk^-}{(k^+ k^-)^{\epsilon+1}} \delta[\mathcal{T} - \hat{\mathcal{T}}(\{k\})] \\ &= \hat{\sigma}^{\text{LO}}(Q, Y) \frac{\alpha_s \mathbf{C}}{\pi} f_a(x_a) f_b(x_b) \frac{e^{\epsilon\gamma_E}}{\Gamma(1-\epsilon)} \frac{2}{\epsilon} \frac{1}{\mu} (\mathcal{T}/\mu)^{-1-2\epsilon} \\ &= \hat{\sigma}^{\text{LO}}(Q, Y) \frac{\alpha_s \mathbf{C}}{4\pi} f_a(x_a) f_b(x_b) \left[-\frac{4}{\epsilon^2} \delta(\mathcal{T}) + \frac{8}{\epsilon} \frac{1}{\mu} \mathcal{L}_0(\mathcal{T}/\mu) \right. \\ &\quad \left. - \frac{16}{\mu} \mathcal{L}_1(\mathcal{T}/\mu) + \frac{\pi^2}{3} \delta(\mathcal{T}) + \mathcal{O}(\epsilon) \right]. \end{aligned} \quad (\text{A.12})$$

The $\mathcal{L}_n(x)$ are the standard one-dimensional plus distributions, see e.g. [88] for details. Note that there, the precise definition of the $\overline{\text{MS}}$ scheme is important. We use

$$\mu^2 \equiv \mu_{\overline{\text{MS}}}^2 = \frac{4\pi}{e^{\gamma_E}} \mu_{\overline{\text{MS}}}^2. \quad (\text{A.13})$$

If one were to use $\mu^{2\epsilon} = \frac{(4\pi)^\epsilon}{\Gamma(1-\epsilon)} \mu_{\overline{\text{MS}}}^{2\epsilon}$, one would miss the $\pi^2/3$ term. For the NLP results presented in the main text, both definitions yield identical results.

Taking eq. (A.12) and adding the virtual soft diagram, and then comparing to eq. (A.4), the one-loop bare soft function can be read off as

$$S^{\text{NLO}}(\mathcal{T}, \epsilon) = \frac{\alpha_s \mathbf{C}}{4\pi} \left[-\frac{4}{\epsilon^2} \delta(\mathcal{T}) + \frac{8}{\epsilon} \frac{1}{\mu} \mathcal{L}_0(\mathcal{T}/\mu) - \frac{16}{\mu} \mathcal{L}_1(\mathcal{T}/\mu) + \frac{\pi^2}{3} \delta(\mathcal{T}) \right]. \quad (\text{A.14})$$

The finite terms precisely yield the renormalized one-loop soft function [23].

A.3 NLO beam function

Applying the LP master formula eq. (4.12) to the n -collinear case and following the same steps as in section 4.2 gives

$$\begin{aligned} \frac{d\sigma_n^{(0,1)}}{dQ^2 dY d\mathcal{T}} &= \int_{x_a}^1 \frac{dz_a}{z_a} \frac{f_{a'}(x_a/z_a) f_b(x_b)}{2x_a x_b E_{\text{cm}}^4} \frac{Q e^Y}{\rho} \left(\frac{Q\mathcal{T} e^Y}{\rho} \right)^{-\epsilon} \frac{z_a^\epsilon}{(1-z_a)^\epsilon} \frac{(4\pi)^\epsilon}{(4\pi)^2 \Gamma(1-\epsilon)} \\ &\quad \times A(Q, Y; \{k\}). \end{aligned} \quad (\text{A.15})$$

Using the universal n -collinear limit eq. (A.9), we obtain

$$\frac{d\sigma_n^{(0,1)}}{dQ^2 dY d\mathcal{T}} = \hat{\sigma}^{\text{LO}}(Q, Y) \int_{x_a}^1 \frac{dz_a}{z_a} f_{a'}\left(\frac{x_a}{z_a}\right) f_b(x_b) \frac{\alpha_s}{2\pi} \frac{e^{\epsilon\gamma_E}}{\Gamma(1-\epsilon)} \frac{1}{\mathcal{T}} \left(\frac{Q\mathcal{T} e^Y}{\mu^2 \rho} \right)^{-\epsilon} \frac{z_a^\epsilon P_{aa'}(z_a, \epsilon)}{(1-z_a)^\epsilon}, \quad (\text{A.16})$$

where $P_{aa'}(z)$ is the standard ϵ -dependent splitting kernel at NLO. Comparing to eq. (A.4), we can read off a result that will enable us to obtain the real radiation bare NLO beam function kernel,

$$\mathcal{I}_{ij}^{(1)\text{real}}(t, z, \epsilon) = \frac{\alpha_s}{2\pi} \left[\frac{e^Y}{\rho} \frac{e^{\epsilon\gamma_E}}{\Gamma(1-\epsilon)} \frac{1}{\mu^2} \left(\frac{t e^Y}{\mu^2 \rho} \right)^{-1-\epsilon} \frac{z^\epsilon P_{ij}(z, \epsilon)}{(1-z)^\epsilon} \right]. \quad (\text{A.17})$$

The splitting function $P_{ij}(z)$ may contain divergences as $z \rightarrow 1$, which are regulated by the overall $(1-z)^{-\epsilon}$. All divergences thus arise from the two expansions

$$\frac{1}{\mu_\rho^2} \left(\frac{t}{\mu_\rho^2} \right)^{-\epsilon-1} = -\frac{\delta(t)}{\epsilon} + \frac{1}{\mu_\rho^2} \mathcal{L}_0(t/\mu_\rho^2) - \epsilon \frac{1}{\mu_\rho^2} \mathcal{L}_1(t/\mu_\rho^2) + \mathcal{O}(\epsilon^2), \quad (\text{A.18})$$

$$(1-z)^{-1-\epsilon} = -\frac{1}{\epsilon} \delta(1-z) + \mathcal{L}_0(1-z) - \epsilon \mathcal{L}_1(1-z) + \mathcal{O}(\epsilon^2), \quad (\text{A.19})$$

where we defined $\mu_\rho^2 = \mu^2 \frac{\rho}{e^Y}$ for ease of notation. As written eq. (A.17) does not yet contain the corresponding collinear virtual and zero-bin contributions.

Example: qq kernel. From eq. (A.11), we obtain

$$\begin{aligned} \frac{z^\epsilon P_{qq}(z, \epsilon)}{(1-z)^\epsilon} &= C_F \frac{z^\epsilon}{(1-z)^\epsilon} \left[\frac{1+z^2}{1-z} - \epsilon(1-z) \right] \\ &= P_{qq}(z) + C_F \left\{ -\frac{2}{\epsilon} \delta(1-z) - \frac{3}{2} \delta(1-z) \right. \\ &\quad \left. + \epsilon \left[(z-1) - (1+z^2) \mathcal{L}_1(1-z) + (1+z^2) \ln(z) \mathcal{L}_0(1-z) \right] \right\} + \mathcal{O}(\epsilon^2), \end{aligned} \quad (\text{A.20})$$

where the LO quark splitting function is given by

$$P_{qq}(z) = C_F \left[\Theta(1-z) \frac{1+z^2}{1-z} \right]_+ = (1+z^2) \mathcal{L}_0(1-z) + \frac{3}{2} \delta(1-z). \quad (\text{A.21})$$

Adding the corresponding virtual collinear and zero-bin contributions, eq. (A.17) yields

$$\begin{aligned} \mathcal{I}_{qq}^{(1)}(t, z, \epsilon) &= \frac{\alpha_s C_F}{2\pi} \left\{ \frac{2}{\epsilon^2} \delta(t) \delta(1-z) + \frac{\delta(1-z)}{\epsilon} \left[\frac{3}{2} \delta(t) - 2 \frac{1}{\mu_\rho^2} \mathcal{L}_0(t/\mu_\rho^2) \right] - \frac{\delta(t)}{\epsilon} \frac{P_{qq}(z)}{C_F} \right. \\ &\quad \left. + 2\delta(1-z) \frac{1}{\mu_\rho^2} \mathcal{L}_1(t/\mu_\rho^2) + \frac{1}{\mu_\rho^2} \mathcal{L}_0(t/\mu_\rho^2) \left[P_{qq}(z) - \frac{3}{2} \delta(1-z) \right] \right. \\ &\quad \left. + \delta(t) \left[(1+z^2) \mathcal{L}_1(1-z) - \frac{1+z^2}{1-z} \ln(z) + (1-z) - \frac{\pi^2}{6} \delta(1-z) \right] \right\}. \end{aligned} \quad (\text{A.22})$$

Note that all divergences are proportional to $\delta(1-z)$, such that they cancel after adding the soft, \bar{n} collinear and the virtual hard contribution from $H_{ab}^{\text{NLO}}(Q^2, \epsilon)$, as the latter also has the universal structure (for Drell-Yan)

$$\frac{d\sigma_{\text{virt}}^{(0,1)}}{dQ^2 dY d\mathcal{T}} = \hat{\sigma}^{\text{LO}}(Q, Y) f_a(x_a) f_b(x_b) \delta(\mathcal{T}) \frac{\alpha_s C_F}{\pi} \left[-\frac{1}{\epsilon^2} - \frac{1}{\epsilon} \left(\frac{3}{2} - \ln \frac{Q^2}{\mu^2} \right) + \mathcal{O}(\epsilon) \right]. \quad (\text{A.23})$$

The cancellation of the $1/\epsilon^2$ and the remaining $3/(2\epsilon)$ pieces is obvious from comparing to eqs. (A.22) and (A.14). The $P_{qq}(z)/\epsilon$ term cancels with the ultraviolet divergence from the bare quark PDF. The remaining $\ln(Q^2/\mu^2)/\epsilon$ term cancels when combining the $\mathcal{L}_0(\mathcal{T}/\mu)/\epsilon$ and $\mathcal{L}_0(t/\mu^2)/\epsilon$ distribution terms. The remaining $\mathcal{O}(\epsilon^0)$ piece in eq. (A.22) gives the renormalized beam function and agrees with the result in ref. [42].

Example: qg kernel. For the full LP correction to Drell-Yan production, $q\bar{q} \rightarrow Z$, we also require the quark-gluon kernel. Here we only need

$$\begin{aligned} \frac{z^\epsilon P_{qg}(z, \epsilon)}{(1-z)^\epsilon} &= \frac{z^\epsilon}{(1-z)^\epsilon} T_F \left[1 - \frac{2z(1-z)}{1-\epsilon} \right] \\ &= P_{qg}(z) \left[1 + \epsilon \left(\ln \frac{z}{1-z} + 1 \right) \right] - \epsilon T_F + \mathcal{O}(\epsilon^2), \end{aligned} \quad (\text{A.24})$$

where the finite quark-gluon splitting function is defined as

$$P_{qg}(z) = T_F [(1-z)^2 + z^2]. \quad (\text{A.25})$$

Equation (A.17) thus yields

$$\mathcal{I}_{qg}^{(1)}(t, z, \mu) = \frac{\alpha_s T_F}{2\pi} \left\{ -\frac{\delta(t)}{\epsilon} \frac{P_{qg}(z)}{T_F} + \frac{1}{\mu_\rho^2} \mathcal{L}_0(t/\mu_\rho^2) P_{qg}(z) + \delta(t) \left[P_{qg}(z) \left(\ln \frac{1-z}{z} - 1 \right) + 1 \right] \right\}. \quad (\text{A.26})$$

Again the $P_{qg}(z)/\epsilon$ divergence cancels against the same mixing term from the bare gluon PDF. The remaining $\mathcal{O}(\epsilon^0)$ terms give the mixing term in the one-loop quark beam function, agreeing with the result in [42].

B Comparison of NLP contributions for $gg \rightarrow Hg$ at NLO

Here, we give the explicit calculation to obtain our full NLP result for hadronic \mathcal{T} in the $gg \rightarrow Hg$ channel in the form of eq. (6.18). Our result prior to integration by parts is obtained by inserting eq. (5.16) with $\rho = 1$ into eq. (6.9),

$$\begin{aligned} \frac{d\sigma^{(2,1)}}{d\mathcal{T}^{\text{cm}}} &= \frac{\alpha_s C_A}{\pi} \int_0^1 dx_a dx_b 2\pi \delta(x_a x_b E_{\text{cm}}^2 - m_H^2) \frac{|\mathcal{M}_{gg \rightarrow H}^{\text{LO}}(m_H)|^2}{2x_a x_b E_{\text{cm}}^2} \int_{x_a}^1 \frac{dz_a}{z_a} \frac{e^Y}{m_H} \\ &\times \left\{ f_g \left(\frac{x_a}{z_a} \right) f_g(x_b) \left[\left(\ln \frac{\mathcal{T}^{\text{cm}}}{m_H e^Y} + 1 \right) \delta(1 - z_a) \right. \right. \\ &\quad \left. \left. - \mathcal{L}_0(1 - z_a) + \frac{1 - z_a + 9z_a^2 - 5z_a^3 + 7z_a^4 - 3z_a^5}{2z_a^2} \right] \right. \\ &\quad + \frac{x_a}{z_a} f_g' \left(\frac{x_a}{z_a} \right) f_g(x_b) \frac{(1 - z_a + z_a^2)^2}{2z_a} \\ &\quad + f_g \left(\frac{x_a}{z_a} \right) x_b f_g'(x_b) \left[\left(-\ln \frac{\mathcal{T}^{\text{cm}}}{m_H e^Y} - 1 \right) \delta(1 - z_a) \right. \\ &\quad \left. \left. + \frac{(1 + z_a)(1 - z_a + z_a^2)^2}{2z_a^2} \mathcal{L}_0(1 - z_a) \right] \right\} \\ &+ (a \leftrightarrow b, e^Y \leftrightarrow e^{-Y}). \end{aligned} \quad (\text{B.1})$$

Here, we also separated the pure $\mathcal{L}_0(1 - z_a)$ term from terms regular as $z_a \rightarrow 1$.

We now apply integration by parts to the $f_g f_g'$ piece, except for its $-\delta(1 - z_a)$ term. In the notation of eq. (6.11), this is achieved by choosing

$$D^{(2,1)}(z_a, z_b, \mathcal{T}^{\text{cm}}) = 4C_A \frac{e^Y}{m_H} \left[-\ln \frac{\mathcal{T}^{\text{cm}}}{m_H e^Y} \delta(1 - z_a) \right. \\ \left. + \frac{(1 + z_a)(1 - z_a + z_a^2)^2}{2z_a^2} \mathcal{L}_0(1 - z_a) \right] \delta(1 - z_b). \quad (\text{B.2})$$

Here, we only consider being inclusive in Y , so we do not write down the boundary term.

Eq. (B.1) becomes

$$\begin{aligned}
\frac{d\sigma^{(2,1)}}{d\mathcal{T}^{\text{cm}}} &= \frac{\alpha_s C_A}{\pi} \int_0^1 dx_a dx_b 2\pi\delta(x_a x_b E_{\text{cm}}^2 - m_H^2) \frac{|\mathcal{M}_{gg\rightarrow H}^{\text{LO}}(m_H)|^2}{2x_a x_b E_{\text{cm}}^2} \int_{x_a}^1 \frac{dz_a}{z_a} \frac{e^Y}{m_H} \\
&\times \left\{ f_g\left(\frac{x_a}{z_a}\right) f_g(x_b) \left[2\delta(1-z_a) + \left(\frac{(1+z_a)(1-z_a+z_a^2)^2}{2z_a^2} - 1 \right) \mathcal{L}_0(1-z_a) \right. \right. \\
&\quad \left. \left. + \frac{1-z_a+9z_a^2-5z_a^3+7z_a^4-3z_a^5}{2z_a^2} \right] \right. \\
&\quad \left. + \frac{x_a}{z_a} f_g'\left(\frac{x_a}{z_a}\right) f_g(x_b) \left[-\delta(1-z_a) \ln \frac{\mathcal{T}^{\text{cm}}}{m_H e^Y} + \frac{(1-z_a+z_a^2)^2}{z_a^2} \mathcal{L}_0(1-z_a) \right. \right. \\
&\quad \left. \left. - \frac{(1-z_a)(1-z_a+z_a^2)^2}{2z_a^2} \right] \right. \\
&\quad \left. - f_g\left(\frac{x_a}{z_a}\right) x_b f_g'(x_b) \delta(1-z_a) \right\} \\
&+ (a \leftrightarrow b, e^Y \leftrightarrow e^{-Y}), \tag{B.3}
\end{aligned}$$

where as usual, $e^Y = \sqrt{x_a/x_b}$. Next, we apply the following integration by parts:

$$\begin{aligned}
&\int_{x_a}^1 \frac{dz_a}{z_a} \frac{x_a}{z_a} f_g'\left(\frac{x_a}{z_a}\right) f_g(x_b) \left[-\frac{(1-z_a)(1-z_a+z_a^2)^2}{2z_a^2} \right] \\
&= \int_{x_a}^1 \frac{dz_a}{z_a} f_g\left(\frac{x_a}{z_a}\right) f_g(x_b) \frac{2-3z_a+5z_a^3-6z_a^4+3z_a^5}{2z_a^2}. \tag{B.4}
\end{aligned}$$

Putting this back into eq. (B.3), we can rewrite it in a form close to eq. (6.17),

$$\begin{aligned}
\frac{d\sigma^{(2,1)}}{d\mathcal{T}^{\text{cm}}} &= \frac{\alpha_s C_A}{\pi} \int_0^1 dx_a dx_b 2\pi\delta(x_a x_b E_{\text{cm}}^2 - m_H^2) \frac{|\mathcal{M}_{gg\rightarrow H}^{\text{LO}}(m_H)|^2}{2x_a x_b E_{\text{cm}}^2} \int_{x_a}^1 \frac{dz_a}{z_a} \frac{e^Y}{m_H} \\
&\times \left\{ f_g\left(\frac{x_a}{z_a}\right) f_g(x_b) \left[2\delta(1-z_a) + \left(\frac{(1-z_a+z_a^2)^2}{z_a^2} - 1 \right) \mathcal{L}_0(1-z_a) \right. \right. \\
&\quad \left. \left. + \frac{3z_a^2+1-z_a+z_a^3}{z_a^2} \right] \right. \\
&\quad \left. + \frac{x_a}{z_a} f_g'\left(\frac{x_a}{z_a}\right) f_g(x_b) \left[-\delta(1-z_a) \ln \frac{\mathcal{T}^{\text{cm}}}{m_H e^Y} + \frac{(1-z_a+z_a^2)^2}{z_a^2} \mathcal{L}_0(1-z_a) \right] \right. \\
&\quad \left. - f_g\left(\frac{x_a}{z_a}\right) x_b f_g'(x_b) \delta(1-z_a) \right\} \\
&+ (a \leftrightarrow b, e^Y \leftrightarrow e^{-Y}). \tag{B.5}
\end{aligned}$$

To compare this result to eq. (6.17), use the relations

$$\frac{e^Y}{m_H} = \frac{x_a E_{\text{cm}}}{m_H^2}, \quad \ln \frac{\mathcal{T}^{\text{cm}}}{m_H e^Y} = \ln \frac{\mathcal{T}^{\text{cm}}}{x_a E_{\text{cm}}}. \tag{B.6}$$

Open Access. This article is distributed under the terms of the Creative Commons Attribution License ([CC-BY 4.0](https://creativecommons.org/licenses/by/4.0/)), which permits any use, distribution and reproduction in any medium, provided the original author(s) and source are credited.

References

- [1] C. Anastasiou, L.J. Dixon, K. Melnikov and F. Petriello, *High precision QCD at hadron colliders: Electroweak gauge boson rapidity distributions at NNLO*, *Phys. Rev. D* **69** (2004) 094008 [[hep-ph/0312266](#)] [[INSPIRE](#)].
- [2] F. Dulat, S. Lionetti, B. Mistlberger, A. Pelloni and C. Specchia, *Higgs-differential cross section at NNLO in dimensional regularisation*, *JHEP* **07** (2017) 017 [[arXiv:1704.08220](#)] [[INSPIRE](#)].
- [3] B. Mistlberger, *Higgs boson production at hadron colliders at N^3 LO in QCD*, *JHEP* **05** (2018) 028 [[arXiv:1802.00833](#)] [[INSPIRE](#)].
- [4] S. Frixione, Z. Kunszt and A. Signer, *Three jet cross-sections to next-to-leading order*, *Nucl. Phys. B* **467** (1996) 399 [[hep-ph/9512328](#)] [[INSPIRE](#)].
- [5] S. Frixione, *A General approach to jet cross-sections in QCD*, *Nucl. Phys. B* **507** (1997) 295 [[hep-ph/9706545](#)] [[INSPIRE](#)].
- [6] S. Catani and M.H. Seymour, *The Dipole formalism for the calculation of QCD jet cross-sections at next-to-leading order*, *Phys. Lett. B* **378** (1996) 287 [[hep-ph/9602277](#)] [[INSPIRE](#)].
- [7] S. Catani and M.H. Seymour, *A General algorithm for calculating jet cross-sections in NLO QCD*, *Nucl. Phys. B* **485** (1997) 291 [*Erratum ibid.* **B 510** (1998) 503] [[hep-ph/9605323](#)] [[INSPIRE](#)].
- [8] S. Catani, S. Dittmaier, M.H. Seymour and Z. Trócsányi, *The Dipole formalism for next-to-leading order QCD calculations with massive partons*, *Nucl. Phys. B* **627** (2002) 189 [[hep-ph/0201036](#)] [[INSPIRE](#)].
- [9] S. Catani and M. Grazzini, *An NNLO subtraction formalism in hadron collisions and its application to Higgs boson production at the LHC*, *Phys. Rev. Lett.* **98** (2007) 222002 [[hep-ph/0703012](#)] [[INSPIRE](#)].
- [10] F. Caola, K. Melnikov and R. Röntsch, *Nested soft-collinear subtractions in NNLO QCD computations*, *Eur. Phys. J. C* **77** (2017) 248 [[arXiv:1702.01352](#)] [[INSPIRE](#)].
- [11] F. Herzog, *Geometric IR subtraction for final state real radiation*, *JHEP* **08** (2018) 006 [[arXiv:1804.07949](#)] [[INSPIRE](#)].
- [12] L. Magnea, E. Maina, G. Pelliccioli, C. Signorile-Signorile, P. Torrielli and S. Uccirati, *Local Analytic Sector Subtraction at NNLO*, [arXiv:1806.09570](#) [[INSPIRE](#)].
- [13] V. Del Duca, C. Duhr, A. Kardos, G. Somogyi and Z. Trócsányi, *Three-Jet Production in Electron-Positron Collisions at Next-to-Next-to-Leading Order Accuracy*, *Phys. Rev. Lett.* **117** (2016) 152004 [[arXiv:1603.08927](#)] [[INSPIRE](#)].
- [14] V. Del Duca et al., *Jet production in the CoLoRFulNNLO method: event shapes in electron-positron collisions*, *Phys. Rev. D* **94** (2016) 074019 [[arXiv:1606.03453](#)] [[INSPIRE](#)].
- [15] A. Kardos, G. Bevilacqua, G. Somogyi, Z. Trócsányi and Z. Tulipánt, *CoLoRFulNNLO for LHC processes*, *PoS(LL2018)074* (2018) [[arXiv:1807.04976](#)] [[INSPIRE](#)].
- [16] A. Gehrmann-De Ridder, T. Gehrmann and E.W.N. Glover, *Antenna subtraction at NNLO*, *JHEP* **09** (2005) 056 [[hep-ph/0505111](#)] [[INSPIRE](#)].
- [17] M. Czakon, *A novel subtraction scheme for double-real radiation at NNLO*, *Phys. Lett. B* **693** (2010) 259 [[arXiv:1005.0274](#)] [[INSPIRE](#)].

- [18] R. Boughezal, K. Melnikov and F. Petriello, *A subtraction scheme for NNLO computations*, *Phys. Rev. D* **85** (2012) 034025 [[arXiv:1111.7041](#)] [[INSPIRE](#)].
- [19] M. Czakon and D. Heymes, *Four-dimensional formulation of the sector-improved residue subtraction scheme*, *Nucl. Phys. B* **890** (2014) 152 [[arXiv:1408.2500](#)] [[INSPIRE](#)].
- [20] R. Boughezal, C. Focke, X. Liu and F. Petriello, *W-boson production in association with a jet at next-to-next-to-leading order in perturbative QCD*, *Phys. Rev. Lett.* **115** (2015) 062002 [[arXiv:1504.02131](#)] [[INSPIRE](#)].
- [21] R. Boughezal, C. Focke, W. Giele, X. Liu and F. Petriello, *Higgs boson production in association with a jet at NNLO using jettiness subtraction*, *Phys. Lett. B* **748** (2015) 5 [[arXiv:1505.03893](#)] [[INSPIRE](#)].
- [22] J. Gaunt, M. Stahlhofen, F.J. Tackmann and J.R. Walsh, *N-jettiness Subtractions for NNLO QCD Calculations*, *JHEP* **09** (2015) 058 [[arXiv:1505.04794](#)] [[INSPIRE](#)].
- [23] I.W. Stewart, F.J. Tackmann and W.J. Waalewijn, *Factorization at the LHC: From PDFs to Initial State Jets*, *Phys. Rev. D* **81** (2010) 094035 [[arXiv:0910.0467](#)] [[INSPIRE](#)].
- [24] I.W. Stewart, F.J. Tackmann and W.J. Waalewijn, *N-Jettiness: An Inclusive Event Shape to Veto Jets*, *Phys. Rev. Lett.* **105** (2010) 092002 [[arXiv:1004.2489](#)] [[INSPIRE](#)].
- [25] J.M. Campbell, R.K. Ellis and C. Williams, *Associated production of a Higgs boson at NNLO*, *JHEP* **06** (2016) 179 [[arXiv:1601.00658](#)] [[INSPIRE](#)].
- [26] J.M. Campbell, R.K. Ellis, Y. Li and C. Williams, *Predictions for diphoton production at the LHC through NNLO in QCD*, *JHEP* **07** (2016) 148 [[arXiv:1603.02663](#)] [[INSPIRE](#)].
- [27] R. Boughezal et al., *Color singlet production at NNLO in MCFM*, *Eur. Phys. J. C* **77** (2017) 7 [[arXiv:1605.08011](#)] [[INSPIRE](#)].
- [28] J.M. Campbell, T. Neumann and C. Williams, *Z γ Production at NNLO Including Anomalous Couplings*, *JHEP* **11** (2017) 150 [[arXiv:1708.02925](#)] [[INSPIRE](#)].
- [29] G. Heinrich, S. Jahn, S.P. Jones, M. Kerner and J. Pires, *NNLO predictions for Z-boson pair production at the LHC*, *JHEP* **03** (2018) 142 [[arXiv:1710.06294](#)] [[INSPIRE](#)].
- [30] R. Boughezal et al., *Z-boson production in association with a jet at next-to-next-to-leading order in perturbative QCD*, *Phys. Rev. Lett.* **116** (2016) 152001 [[arXiv:1512.01291](#)] [[INSPIRE](#)].
- [31] R. Boughezal, X. Liu and F. Petriello, *W-boson plus jet differential distributions at NNLO in QCD*, *Phys. Rev. D* **94** (2016) 113009 [[arXiv:1602.06965](#)] [[INSPIRE](#)].
- [32] J.M. Campbell, R.K. Ellis and C. Williams, *Driving missing data at the LHC: NNLO predictions for the ratio of $\gamma + j$ and $Z + j$* , *Phys. Rev. D* **96** (2017) 014037 [[arXiv:1703.10109](#)] [[INSPIRE](#)].
- [33] G. Abelof, R. Boughezal, X. Liu and F. Petriello, *Single-inclusive jet production in electron-nucleon collisions through next-to-next-to-leading order in perturbative QCD*, *Phys. Lett. B* **763** (2016) 52 [[arXiv:1607.04921](#)] [[INSPIRE](#)].
- [34] S. Alioli et al., *Combining Higher-Order Resummation with Multiple NLO Calculations and Parton Showers in GENEVA*, *JHEP* **09** (2013) 120 [[arXiv:1211.7049](#)] [[INSPIRE](#)].
- [35] S. Alioli, C.W. Bauer, C. Berggren, F.J. Tackmann and J.R. Walsh, *Drell-Yan production at NNLL' + NNLO matched to parton showers*, *Phys. Rev. D* **92** (2015) 094020 [[arXiv:1508.01475](#)] [[INSPIRE](#)].

- [36] C.W. Bauer, S. Fleming and M.E. Luke, *Summing Sudakov logarithms in $B \rightarrow X_s \gamma$ in effective field theory*, *Phys. Rev. D* **63** (2000) 014006 [[hep-ph/0005275](#)] [[INSPIRE](#)].
- [37] C.W. Bauer, S. Fleming, D. Pirjol and I.W. Stewart, *An Effective field theory for collinear and soft gluons: Heavy to light decays*, *Phys. Rev. D* **63** (2001) 114020 [[hep-ph/0011336](#)] [[INSPIRE](#)].
- [38] C.W. Bauer and I.W. Stewart, *Invariant operators in collinear effective theory*, *Phys. Lett. B* **516** (2001) 134 [[hep-ph/0107001](#)] [[INSPIRE](#)].
- [39] C.W. Bauer, D. Pirjol and I.W. Stewart, *Soft collinear factorization in effective field theory*, *Phys. Rev. D* **65** (2002) 054022 [[hep-ph/0109045](#)] [[INSPIRE](#)].
- [40] C.W. Bauer, S. Fleming, D. Pirjol, I.Z. Rothstein and I.W. Stewart, *Hard scattering factorization from effective field theory*, *Phys. Rev. D* **66** (2002) 014017 [[hep-ph/0202088](#)] [[INSPIRE](#)].
- [41] T. Becher and M. Neubert, *Toward a NNLO calculation of the $\bar{B} \rightarrow X_s \gamma$ decay rate with a cut on photon energy. II. Two-loop result for the jet function*, *Phys. Lett. B* **637** (2006) 251 [[hep-ph/0603140](#)] [[INSPIRE](#)].
- [42] I.W. Stewart, F.J. Tackmann and W.J. Waalewijn, *The Quark Beam Function at NNLL*, *JHEP* **09** (2010) 005 [[arXiv:1002.2213](#)] [[INSPIRE](#)].
- [43] T. Becher and G. Bell, *The gluon jet function at two-loop order*, *Phys. Lett. B* **695** (2011) 252 [[arXiv:1008.1936](#)] [[INSPIRE](#)].
- [44] C.F. Berger, C. Marcantonini, I.W. Stewart, F.J. Tackmann and W.J. Waalewijn, *Higgs Production with a Central Jet Veto at NNLL+NNLO*, *JHEP* **04** (2011) 092 [[arXiv:1012.4480](#)] [[INSPIRE](#)].
- [45] T.T. Jouttenus, I.W. Stewart, F.J. Tackmann and W.J. Waalewijn, *The Soft Function for Exclusive N-Jet Production at Hadron Colliders*, *Phys. Rev. D* **83** (2011) 114030 [[arXiv:1102.4344](#)] [[INSPIRE](#)].
- [46] R. Kelley, M.D. Schwartz, R.M. Schabinger and H.X. Zhu, *The two-loop hemisphere soft function*, *Phys. Rev. D* **84** (2011) 045022 [[arXiv:1105.3676](#)] [[INSPIRE](#)].
- [47] P.F. Monni, T. Gehrmann and G. Luisoni, *Two-Loop Soft Corrections and Resummation of the Thrust Distribution in the Dijet Region*, *JHEP* **08** (2011) 010 [[arXiv:1105.4560](#)] [[INSPIRE](#)].
- [48] A. Hornig, C. Lee, I.W. Stewart, J.R. Walsh and S. Zuberi, *Non-global Structure of the $O(\alpha_s^2)$ Dijet Soft Function*, *JHEP* **08** (2011) 054 [Erratum *ibid.* **10** (2017) 101] [[arXiv:1105.4628](#)] [[INSPIRE](#)].
- [49] D. Kang, O.Z. Labun and C. Lee, *Equality of hemisphere soft functions for e^+e^- , DIS and pp collisions at $O(\alpha_s^2)$* , *Phys. Lett. B* **748** (2015) 45 [[arXiv:1504.04006](#)] [[INSPIRE](#)].
- [50] J.R. Gaunt, M. Stahlhofen and F.J. Tackmann, *The Quark Beam Function at Two Loops*, *JHEP* **04** (2014) 113 [[arXiv:1401.5478](#)] [[INSPIRE](#)].
- [51] J. Gaunt, M. Stahlhofen and F.J. Tackmann, *The Gluon Beam Function at Two Loops*, *JHEP* **08** (2014) 020 [[arXiv:1405.1044](#)] [[INSPIRE](#)].
- [52] R. Boughezal, X. Liu and F. Petriello, *N-jettiness soft function at next-to-next-to-leading order*, *Phys. Rev. D* **91** (2015) 094035 [[arXiv:1504.02540](#)] [[INSPIRE](#)].

- [53] H.T. Li and J. Wang, *Next-to-Next-to-Leading Order N -Jettiness Soft Function for One Massive Colored Particle Production at Hadron Colliders*, *JHEP* **02** (2017) 002 [[arXiv:1611.02749](#)] [[INSPIRE](#)].
- [54] R. Boughezal, F. Petriello, U. Schubert and H. Xing, *Spin-dependent quark beam function at NNLO*, *Phys. Rev. D* **96** (2017) 034001 [[arXiv:1704.05457](#)] [[INSPIRE](#)].
- [55] J.M. Campbell, R.K. Ellis, R. Mondini and C. Williams, *The NNLO QCD soft function for 1-jettiness*, *Eur. Phys. J. C* **78** (2018) 234 [[arXiv:1711.09984](#)] [[INSPIRE](#)].
- [56] E. Laenen, L. Magnea and G. Stavenga, *On next-to-eikonal corrections to threshold resummation for the Drell-Yan and DIS cross sections*, *Phys. Lett. B* **669** (2008) 173 [[arXiv:0807.4412](#)] [[INSPIRE](#)].
- [57] E. Laenen, L. Magnea, G. Stavenga and C.D. White, *Next-to-eikonal corrections to soft gluon radiation: a diagrammatic approach*, *JHEP* **01** (2011) 141 [[arXiv:1010.1860](#)] [[INSPIRE](#)].
- [58] D. Bonocore, E. Laenen, L. Magnea, L. Vernazza and C.D. White, *The method of regions and next-to-soft corrections in Drell-Yan production*, *Phys. Lett. B* **742** (2015) 375 [[arXiv:1410.6406](#)] [[INSPIRE](#)].
- [59] D. Bonocore, E. Laenen, L. Magnea, S. Melville, L. Vernazza and C.D. White, *A factorization approach to next-to-leading-power threshold logarithms*, *JHEP* **06** (2015) 008 [[arXiv:1503.05156](#)] [[INSPIRE](#)].
- [60] D.W. Kolodrubetz, I. Moulton and I.W. Stewart, *Building Blocks for Subleading Helicity Operators*, *JHEP* **05** (2016) 139 [[arXiv:1601.02607](#)] [[INSPIRE](#)].
- [61] D. Bonocore, E. Laenen, L. Magnea, L. Vernazza and C.D. White, *Non-abelian factorisation for next-to-leading-power threshold logarithms*, *JHEP* **12** (2016) 121 [[arXiv:1610.06842](#)] [[INSPIRE](#)].
- [62] I. Moulton, L. Rothen, I.W. Stewart, F.J. Tackmann and H.X. Zhu, *Subleading Power Corrections for N -Jettiness Subtractions*, *Phys. Rev. D* **95** (2017) 074023 [[arXiv:1612.00450](#)] [[INSPIRE](#)].
- [63] R. Boughezal, X. Liu and F. Petriello, *Power Corrections in the N -jettiness Subtraction Scheme*, *JHEP* **03** (2017) 160 [[arXiv:1612.02911](#)] [[INSPIRE](#)].
- [64] I. Moulton, L. Rothen, I.W. Stewart, F.J. Tackmann and H.X. Zhu, *N -jettiness subtractions for $gg \rightarrow H$ at subleading power*, *Phys. Rev. D* **97** (2018) 014013 [[arXiv:1710.03227](#)] [[INSPIRE](#)].
- [65] I. Moulton, I.W. Stewart and G. Vita, *A subleading operator basis and matching for $gg \rightarrow H$* , *JHEP* **07** (2017) 067 [[arXiv:1703.03408](#)] [[INSPIRE](#)].
- [66] I. Feige, D.W. Kolodrubetz, I. Moulton and I.W. Stewart, *A Complete Basis of Helicity Operators for Subleading Factorization*, *JHEP* **11** (2017) 142 [[arXiv:1703.03411](#)] [[INSPIRE](#)].
- [67] V. Del Duca, E. Laenen, L. Magnea, L. Vernazza and C.D. White, *Universality of next-to-leading power threshold effects for colourless final states in hadronic collisions*, *JHEP* **11** (2017) 057 [[arXiv:1706.04018](#)] [[INSPIRE](#)].
- [68] C.-H. Chang, I.W. Stewart and G. Vita, *A Subleading Power Operator Basis for the Scalar Quark Current*, *JHEP* **04** (2018) 041 [[arXiv:1712.04343](#)] [[INSPIRE](#)].
- [69] M. Beneke, M. Garny, R. Szafron and J. Wang, *Anomalous dimension of subleading-power N -jet operators*, *JHEP* **03** (2018) 001 [[arXiv:1712.04416](#)] [[INSPIRE](#)].

- [70] R. Boughezal, A. Isgro and F. Petriello, *Next-to-leading-logarithmic power corrections for N -jettiness subtraction in color-singlet production*, *Phys. Rev. D* **97** (2018) 076006 [[arXiv:1802.00456](#)] [[INSPIRE](#)].
- [71] N. Bahjat-Abbas, J. Sinninghe Damsté, L. Vernazza and C.D. White, *On next-to-leading power threshold corrections in Drell-Yan production at N^3 LO*, *JHEP* **10** (2018) 144 [[arXiv:1807.09246](#)] [[INSPIRE](#)].
- [72] I. Moulst, I.W. Stewart, G. Vita and H.X. Zhu, *First Subleading Power Resummation for Event Shapes*, *JHEP* **08** (2018) 013 [[arXiv:1804.04665](#)] [[INSPIRE](#)].
- [73] J.M. Campbell and R.K. Ellis, *An Update on vector boson pair production at hadron colliders*, *Phys. Rev. D* **60** (1999) 113006 [[hep-ph/9905386](#)] [[INSPIRE](#)].
- [74] J.M. Campbell and R.K. Ellis, *MCFM for the Tevatron and the LHC*, *Nucl. Phys. Proc. Suppl.* **205-206** (2010) 10 [[arXiv:1007.3492](#)] [[INSPIRE](#)].
- [75] J.M. Campbell, R.K. Ellis and W.T. Giele, *A Multi-Threaded Version of MCFM*, *Eur. Phys. J. C* **75** (2015) 246 [[arXiv:1503.06182](#)] [[INSPIRE](#)].
- [76] I.W. Stewart, F.J. Tackmann and W.J. Waalewijn, *The Beam Thrust Cross Section for Drell-Yan at NNLL Order*, *Phys. Rev. Lett.* **106** (2011) 032001 [[arXiv:1005.4060](#)] [[INSPIRE](#)].
- [77] A.V. Manohar and I.W. Stewart, *The Zero-Bin and Mode Factorization in Quantum Field Theory*, *Phys. Rev. D* **76** (2007) 074002 [[hep-ph/0605001](#)] [[INSPIRE](#)].
- [78] D. Nandan, J. Plefka and W. Wormsbecher, *Collinear limits beyond the leading order from the scattering equations*, *JHEP* **02** (2017) 038 [[arXiv:1608.04730](#)] [[INSPIRE](#)].
- [79] F. Cachazo, S. He and E.Y. Yuan, *Scattering of Massless Particles in Arbitrary Dimensions*, *Phys. Rev. Lett.* **113** (2014) 171601 [[arXiv:1307.2199](#)] [[INSPIRE](#)].
- [80] F. Cachazo, S. He and E.Y. Yuan, *Scattering of Massless Particles: Scalars, Gluons and Gravitons*, *JHEP* **07** (2014) 033 [[arXiv:1309.0885](#)] [[INSPIRE](#)].
- [81] F.E. Low, *Bremsstrahlung of very low-energy quanta in elementary particle collisions*, *Phys. Rev.* **110** (1958) 974 [[INSPIRE](#)].
- [82] T.H. Burnett and N.M. Kroll, *Extension of the low soft photon theorem*, *Phys. Rev. Lett.* **20** (1968) 86 [[INSPIRE](#)].
- [83] V. Del Duca, *High-energy Bremsstrahlung Theorems for Soft Photons*, *Nucl. Phys. B* **345** (1990) 369 [[INSPIRE](#)].
- [84] S. Dawson, *Radiative corrections to Higgs boson production*, *Nucl. Phys. B* **359** (1991) 283 [[INSPIRE](#)].
- [85] A. Djouadi, M. Spira and P.M. Zerwas, *Production of Higgs bosons in proton colliders: QCD corrections*, *Phys. Lett. B* **264** (1991) 440.
- [86] R.J. Gonsalves, J. Pawłowski and C.-F. Wai, *QCD Radiative Corrections to Electroweak Boson Production at Large Transverse Momentum in Hadron Collisions*, *Phys. Rev. D* **40** (1989) 2245 [[INSPIRE](#)].
- [87] L.A. Harland-Lang, A.D. Martin, P. Motylinski and R.S. Thorne, *Parton distributions in the LHC era: MMHT 2014 PDFs*, *Eur. Phys. J. C* **75** (2015) 204 [[arXiv:1412.3989](#)] [[INSPIRE](#)].
- [88] Z. Ligeti, I.W. Stewart and F.J. Tackmann, *Treating the b quark distribution function with reliable uncertainties*, *Phys. Rev. D* **78** (2008) 114014 [[arXiv:0807.1926](#)] [[INSPIRE](#)].